International Graduate School in Molecular Medicine Ulm

GR actions in stromal cells suppress inflammatory arthritis by induction of anti-inflammatory macrophages

Dissertation submitted in partial fulfilment of the requirements for the degree of „Doctor rerum naturalium" (Dr. rer. nat.) of the International Graduate School in Molecular Medicine Ulm

Submitted by

Mascha Koenen

Heidelberg, Germany

2018

Institute of Comparative Molecular Endocrinology

Head: Prof. Dr. Jan Tuckermann

1. Current dean / chairman of the Graduate School: Prof. Dr. Thomas Wirth / Prof Dr. Michael Kühl

2. Thesis Advisory Committee:
   - First supervisor: Prof. Dr. Jan Peter Tuckermann
   - Second supervisor: Prof. Dr. Hans-Jörg Fehling
   - Third supervisor: Prof. Dr. Andrea Vortkamp

3. External reviewer: Prof. Dr. Aline Bozec

4. Day doctorate awarded: 24.10.2018

Results gained in my thesis have previously been published in the following publications:

Koenen M., Culemann S., Vettorazzi S., Caratti G., Frappart L., Baum W., Krönke G., Baschant U.†, Tuckermann J.P.† (2018) The glucocorticoid receptor in stromal cells is essential for glucocorticoid-mediated resolution of inflammation in arthritis *Ann. Rheum. Dis* 77, 1610-1618, doi: 10.1136/annrheumdis-2017-212762

† UB and JT contribute equally.

CC BY-NC 4.0 License, https://creativecommons.org/licenses/by-nc/4.0/deed.de

Table of contents

ABBREVIATIONS 7

1. INTRODUCTION 13

1.1. Rheumatoid Arthritis 13

1.1.1. Disease pathology 14

1.1.2. Mouse models of Arthritis 15

1.1.3. The serum transfer-induced arthritis model (STIA) 16

1.1.4. Treatment Strategies 18

1.2. Glucocorticoid Signaling 19

1.2.1. Glucocorticoid receptor (GR) biology 20

1.2.2. GR dimer dependent regulation of inflammation 23

1.2.3. Potential GC-target cells and pathways in arthritis 25

1.3. Bone biology and osteophytes development 27

1.3.1. Bone biology 27

1.3.2. Adverse effects of GCs on bone growth 28

1.3.3. Osteophytes 29

1.4. Aims of the thesis 31

2. MATERIAL AND METHODS 32

2.1. Materials 32

2.1.1. General chemicals 32

2.1.2. Common buffers and solutions 32

2.1.3. Primers 32

2.1.4. Antibodies 34

2.1.5. Histology and microscopy materials 36

2.1.6. Molecular biology materials 36

2.1.7. Cell culture materials 37

2.1.8. Laboratory Equipment 39

2.1.9. Software 40

2.2. Methods 42

2.2.1. Mouse strains and facilities 42

2.2.2. Serum transfer-induced arthritis (STIA) 42

2.2.3. Mouse genotyping 43

2.2.4. RNA isolation, cDNA Synthesis and qRT-PCR 45

2.2.5. Histology 45

2.2.6. Hematoxylin Eosin staining 46
2.2.7. Safranin-O staining 46
2.2.8. Immunohistochemistry 46
2.2.9. Micro Computed Tomography (µCT) 47
2.2.10. Flow cytometry 47
2.2.11. Multiplex cytokine profiling 48
2.2.12. iTRAQ proteomics protocol 48
2.2.13. BCA protein assay 49
2.2.14. FLS isolation 49
2.2.15. Isolation of bone marrow-derived macrophages 49
2.2.16. Efferocytosis assay 50
2.2.17. RNA-Sequencing 50
2.2.18. Statistical analysis 51

3. RESULTS 52

3.1. GR dimerization, but not in immune cells, is a general necessity for GC-mediated suppression of arthritis 52

3.1.1. Mice with a complete impaired GR dimerization are refractory to DEX treatment in STIA 52
3.1.2. Non-immune cells mediate the GR dimer-dependent anti-inflammatory effects of DEX in STIA 56
3.1.3. GC-mediated cytokine suppression is insufficient to suppress progression of STIA 59
3.1.4. Induction of anti-inflammatory macrophages by GCs depend on GR dimerization in non-immune cells 62
3.1.5. Anti-inflammatory macrophage marker genes, associated with phagocytosis activity are increased in a GR dimer-dependent manner 67
3.1.6. Proteomics analysis revealed several potential dimerization-depended, DEX-regulated target proteins 71
3.1.7. Metallothionein-1 and -2-deficiency does not affect the outcome of DEX treatment in STIA 73
3.1.8. CD163-deficiency does not affect DEX-mediated suppression of STIA 74

3.2. Cell type-specific deletion of the GR in fibroblast-like synoviocytes results in delayed anti-inflammatory actions of GC treatment in STIA 77

3.2.1. GR in endothelial cells does not mediate the anti-inflammatory effects of DEX treatment in STIA 77
3.2.2. GR-deficiency in chondrocytes is not important for exogenous GC-treatment in STIA 79
3.2.3. GR deletion in neurons of the peripheral or the central nervous system do not influence DEX-mediated suppression of STIA 80
3.2.4. GR-deficiency in FLS attenuates DEX-mediated suppression of STIA 83
3.2.5. Diminished GR expression in FLS does not prevent DEX-mediated cytokine suppression 87
3.2.6. GR in FLS influences the ratio of non-classical macrophages 88
3.2.7. GR dimer-dependent induction of efferocytosis and associated factors in FLS *in vitro* 92

3.2.8. RNA sequencing revealed a distinct expression pattern with specifically enriched pathways in GR^{dim} FLS compared to wt FLS treated with IL1β and DEX 94

3.2.9. GR dimer-dependent suppression of secreted pro-inflammatory chemokines associated with macrophage biology 98

4. DISCUSSION 100

4.1. A dual role for GR dimerization in immune and stromal cells to suppress inflammation and osteophyte development 101

4.2. Cytokine suppression is not sufficient to suppress STIA 102

4.3. GR dimer-dependent induction of non-classical macrophages suppresses STIA 104

4.4. GR in FLS, but not other non-immune cells, mediate the anti-inflammatory effects in STIA 111

4.5. Working model and relevance for future direction in research and therapy 116

5. SUMMARY 119

6. REFERENCES 120

7. LIST OF PUBLICATIONS 150

Abbreviations

°C	Degree Celsius
11β-HSD	11β-hydroxysteroid dehydrogenase
3D	Tree-dimensional
ACPA	Anti-citrullinated peptide antibody
ACR20	20% improvement in American college of rheumatology criteria
ADAM10	A disintegrin and metalloproteinase domain-containing protein 10
AF-1	Activation function
AIA	Antigen-induced arthritis
AnxA1	Annexin A1
AP-1	Activator protein 1
ARE	Antioxidant response element
AUC	Area under the curve
Axl	AXL receptor tyrosin kinase
BCA	Bicinchoninic acid
Bcl	B-cell lymphoma
BGI	Beijing genomics institute
BMDM	Bone marrow-derived macrophages
Bmp	Bone morphogenetic protein
BSA	Bovine serum albumin
C/EBPβ	CCAAT/enhancer-binding protein β
CAMKII	Ca^{2+}/calmodulin-dependent protein kinase 2
CD	Cluster of differentiation
Cdh-11	Cadherin-11
CIA	Collagen-induced arthritis
Col1α2	Collagen type 1 alpha 2
Col2α1	Collagen type 2 alpha 1
Cre	Cre-Recombinase
d	Day

DAB	3,3'Diaminobenzidine
DBD	DNA-binding domain
DEX	Dexamethasone
DMARD	Disease modifying anti-rheumatic drug
DMEM	Dulbecco's Modified Eagle's Medium
DNA	Deoxyribonucleic acid
dNTPs	Desoxynucleotides (dATP, dCTP, dGTP,dTTP)
Dusp-1	Dual-specificity phosphatase 1
EDTA	Ethylenediaminetetraacitic acid
EtOH	Ethanol
FACS	Fluorescence-activated cell sorting
FBS	Fetal bovine serum
FCS	Fetal calf serum
Fcγ	Fragment, crystallizable receptor gamma
FGCZ	Functional Genomics Center Zürich
FKBP	FK506-binding protein
FLI	Fritz-Leibniz-Institute
FLS	Fibroblast-like synoviocytes
g	Gram
G6IP	Glucose-6-phosphate isomerase
Gas6	Growth arrest-specific 6
GC	Glucocorticoid
Gilz	Glucocorticoid-induced leucine zipper
GR	Glucocorticoid receptor
GR^{dim}	Glucocorticoid receptor dimerization-impaired mouse line
GRE	Glucocorticoid response element
GR^{flox}	Mouse with a GR flanked by two LoxP sites
GSTA2	Glutathione S-transferase alpha 2
Gy	Gray
h	hour
H&E	Hematoxylin and eosin

H_2O_2	Hydrogenperoxide
HDAC	Histone Deacetylase
HEPES	4-(2-Hydroxyethyl)-1-piperazineethanesulfonic acid
HLA	Human leukocyte antigen
HPA axis	Hypotalamic-pituitary-adrenal axis
HRP	Horseradish peroxidase
Hsp	Heat-shock protein
hTNFα	Human tumor necrosis factor α-overexpressing mouse model
i.p.	Intra peritoneal
i.v.	Intra venous
ICAM-1	Intercellular adhesion molecule-1
IFNγ	Interferon γ
IgG	Immunoglobulin G
Il-16C	Interleukin-16C
Il-17	Interleukin-17
Il-1β	Interleukin-1β
Il-6	Interleukin-6
iTRAQ	Isobaric tags for relative and absolute quantification
JNK	c-Jun N-terminal kinase
K/BxN	F1 generation of NOD x KRN mice producing STIA serum
kg	Kilogram
KRN	T-cell receptor transgenic mouse
LBD	Ligand-binding domain
LFA-1	Lymphocyte function-associated antigen-1
LPS	Lipopolysaccharide
Ly6	Lymphocyte antigen 6
M	Molar
M-CSF	Macrophage colony-stimulating factor
MAPK	Mitogen activated protein kinase
MC	Monocyte
MCP-1	Monocyte chemotactic protein 1

Mer^{kd}	mice with a truncated signaling tyrosine kinase domain of MerTK
MerTK	Tyrosine-protein kinase MER
mg	Milligram
MHCII	Major histocompatibility locus II
MIF	Macrophage migration inhibitory factor
min	Minute
Mip	Macrophage inflammatory protein
miR	Micro RNA
ml	Milliliter
mm	Millimeter
Mmp	Matrix metalloproteinases
Mø	Macrophage
MSC	Mesenchymal stem cell
Msk-1	Mitogen- and stress-activated protein kinase 1
Mt	Metallothionein
n.s.	Not significant
NCoR	Nuclear receptor co-repressor
neg	Negative
NET	Neutrophil extracellular traps
NFκB	Nuclear factor ‘kappa-light-chain-enhancer’ of activated B-cells
nm	Nanometer
NOD	Non-obese diabetic mouse
Nr3c1	Nuclear receptor subfamily 3, group C, member 1 (gene name of the GR)
Nrf2	Nuclear factor E2-related factor-2
OA	Osteoarthritis
PADI	Peptidyl arginase deiminase
PBS	Phosphate buffered saline
PCR	Polymerase chain reaction
PFA	Paraformaldehyde
pg	Picogram

PI3K	Phospoinositide 3 kinase
PMA	Phorbol-12-myristate-13-acetate
Pol	Polymerase
pos	Positive
Pros1	Protein S
PTHr/-P	Parathyroid hormone-related protein
PTPN22	Protein tyrosin phosphatase, non-receptor type two
Pu.1	Transcription factor Pu.1
qRT-PCR	Quantitative reverse transcriptase PCR
RA	Rheumatoid arthritis
RANKL	Receptor activator of NFκB Ligand
Rcf	Relative centrifugal force
RF	Rheumatoid factor
RNA	Ribonucleic acid
ROI	Region of interest
RPL	L ribosomal protein
Rpm	Rounds per minute
RPMI	Roswell Park Memorial Institute medium
RT	Room temperature
S1P	Sphingosine-1-phosphate
S1PR	S1P receptor
SCR-1	Steroid receptor co-activator 1
siRNA	Small interfering RNA
SIRT1	Sirtuin-1
SMRT	Silencing mediator for retinoid or thyroid-hormone receptor
SNP	Single-nucleotide polymorphism
Sphk-1	Sphingosine kinase 1
STIA	Serum transfer-induced arthritis
TAM	Tyro3, Axl, MerTK receptors
TFZ	Tierforschungszentrum
TGFβ	Transforming growth factor β
TH-17	T-helper 17 cells

TIF2	Translation initiation factor eIF4A
TNFα	Tumor necrosis factor α
TRAF6	TNF receptor associated factor 6
Tyro3	Protein tyrosine kinase 3
U	Unit
VCAM-1	Vascular cell adhesion molecule
Wnt	Wingless-type
wt	Wild type
Wt→GR^{dim}	Bone marrow chimeric mice with GR^{dim} recipients and wt bone marrow donors
Wt→wt	Bone marrow chimeric mice with wt recipients and wt bone marrow donors
x g	G-force
µCT	Micro computed tomography
µg	Microgram
µl	Microliter
µm	Micrometer

1. Introduction

1.1. Rheumatoid Arthritis

Rheumatoid arthritis (RA) is an inflammatory autoimmune disease affecting approximately 1% of the world population (Tsokos et al., 2000). Although disease development is still incompletely understood there is a clear association to several genetic (Weyand et al., 1992; Fonseca et al., 2007; Stahl et al., 2010) and environmental factors (Afridi et al., 2014; Symmons et al., 1997). The most important genetic risk factors in RA development are variations in the class II major histocompability (MHC) locus (HLA-DR4 and DR1) (Nepom et al., 1989; Weyand et al., 1992). MHCII-variants are detected in 90% of RA patients (Weyand et al., 1992) leading to a higher binding-efficiency to citrullinated proteins and enhanced presentation to T-cells (Hill et al., 2003). This, subsequently give rise to increased cytokine and chemokine expression and more importantly, production of anti-citrullinated peptide antibodies (ACPAs) detected in 80-90% of all patients. In addition, most RA patients produce autoantibodies directed against the Fc region of immunoglobulin G (IgG) antibodies, known as rheumatoid factors (RF) (Rose et al., 1948). Remarkable, both ACPAs and RF appear in the blood of patients long before clinical symptoms emerge (de Hair et al., 2014). Interestingly, their presence does not induce arthritis development when subjected to healthy mice, but aggravate existing arthritis progression (Kuhn et al., 2006). Other genetic factors involved are polymorphisms in cytokines and their receptors (e.g. Interleukin-1β (Il-1β), tumor necrosis factor α (TNFα) (Fonseca et al., 2007; Lagha et al., 2015), single-nucleotide polymorphisms (SNPs) in T-cell signaling (PTPN22 - protein tyrosine phosphatase, non-receptor type two) and citrullination enzymes (PADI - peptidyl arginase deiminase) (Stahl et al., 2010).

Besides genetic factors, epigenetic features play an emerging role, as demonstrated by the low chance of monozygotic twins (12-15%) and first-degree relatives (1%) to develop RA (Firestein and McInnes, 2017). Especially, methylation of fibroblast-like synoviocytes (FLS) was suggested to contribute to RA (Nakano et al., 2013). Studies, in this regard, have shown that methylation and composition of transcriptomes differ between FLS isolated from RA knee and hip

of the same patient (Ai et al., 2016), which could explain differences in therapeutic outcome for various joints of the same patient. Interestingly, FLS methylation in RA involves genes associated with focal adhesion and cell recruitment (Nakano et al., 2013).

In addition, environmental factors like smoking, dietary changes and the microbiome can influence the probability of RA development (Firestein and McInnes, 2017) as well. Smoking, for example, increases the citrullination of bronchoalveolar lavage of healthy smokers compared to healthy non-smokers by induction of citrulinating enzymes (Makrygiannakis et al., 2008). As a result increased citrullination of peptides might enhance the risk to develop ACPAs and support disease initiation. Moreover, changes in diet and environment can influence the composition of the microbiota. In microbiota of RA patients and arthritic mice the genus of *Lactobacillus* was identified to be more abundant than in healthy controls (Liu et al., 2013, 2016). In addition, colonizing germ-free arthritic mice with the microbiota of arthritic mice led to a higher incidence and an increased severity of arthritis compared to colonization with control microbiota, presumably due to the induction of interleukin-17 and TH17 cells (Liu et al., 2016). Furthermore, several bacterial peptidoglycanes of bacterial cell walls were able to induce arthritis in rats (Šimelyte et al., 2003).

Thus, present research indicates that not a single cause but multiple genetic and environmental factors influences the risk for RA development.

1.1.1. Disease pathology

Development of rheumatoid arthritis (RA) is characterized by autoimmune activation, cell infiltration and subsequent activation of stromal cells and cartilage and bone destruction. Pre-clinical RA is characterized by the appearance of ACPAs and RF but lack changes in immune cell content in the joints (de Hair et al., 2014). After disease onset, increasing amounts of immune cells become activated, leading to a massive infiltration of various innate and adaptive immune

cells into joints of the body (mostly affected are hand, knee and hip). These infiltrating cells, including neutrophils and macrophages, produce a number of inflammatory stimuli, like cytokines (e.g. Il-1β, TNFα) and matrix degrading enzymes (matrix metalloproteinases), inducing the activation of the synovium (McInnes and Schett, 2007). The healthy synovium consists of a non-vascularized layer with a thickness of two to three cells consistent of lining FLS and scattered tissue-resident macrophages. During disease progression, however, FLS are activated, hyper-proliferate and form a pannus-like structure, which invades into cartilage and bone, resulting in massive destruction. The damage of cartilage and bone might generate additional novel auto-antigens and neovascularization of the synovium facilitates on-going recruitment of immune cells stabilizing the maintenance of an inflammatory circuit.

Thus, RA can be defined as a highly complex disease caused and maintained by a sophisticated interplay of immune cells with non-immune stromal cells, like FLS (Bartok and Firestein, 2010; McInnes and Schett, 2011).

1.1.2. Mouse models of Arthritis

Several arthritic mouse models were generated to mimic the complex pathology of inflammatory arthritis, with each mouse line presenting different aspects of the human pathology. One of the most commonly used mouse models for rheumatoid arthritis is the collagen-induced arthritis (CIA). CIA mimics the autoantibody production of patients, and is induced by native type two collagen extracts in combination with incomplete Freud's adjuvants (Trentham et al., 1977). CIA mice develop a strong synovial infiltration and hyperplasia combined with cartilage and bone destruction in several joints. One drawback of the CIA model is its dependency on the DBA/1 genetic background, which complicates the usage of most transgenic mouse lines substantially (Pan et al., 2004). The human TNFα-overexpressing transgenic mouse model (hTNFα) of arthritis is another chronic, polyarthritic model characterized by immune infiltration, synovial hyperplasia, pannus formation and severe articular cartilage and bone erosion (Keffer et al., 1991). In contrast to the CIA model, the hTNFα model is independent of

autoimmunity and arthritis develops spontaneously (Li and Schwarz, 2003). This is different from antigen-induced arthritis (AIA) characterized as a T-cell dependent and antigen specific model of arthritis, suitable for various mouse-lines. Like CIA, AIA is induced by immunization with Freud's adjuvant in combination of methylated bovine serum albumin (BSA) and Bordetella pertussis vaccination (Brackertz et al., 1977). However, the AIA model is an inducible, acute model that selectively affects a single knee joint and, thus, does not reflect the polyarthritic inflammation of several joints seen in RA patients. The serum transfer-induced arthritis (STIA) represents a reasonable compromise between all available arthritic mouse models.

1.1.3. The serum transfer-induced arthritis model (STIA)

In 1996 Kouskoff et al. first described STIA (also called K/BxN arthritis) as a spontaneously developing arthritis in the F1 generation (K/BxN) of T-cell receptor transgenic (KRN) and autoimmune-prone non-obese diabetic (NOD) mice (Kouskoff et al., 1996). Later it was shown that transfer of serum of arthritic K/BxN mice is sufficient to develop robust arthritis in a number of mouse strains (Ji et al., 2001). Due to this feature, STIA can be used as an inducible arthritis model in several transgenic mouse lines. Although, STIA mainly reflects the effector phase of arthritis, it yields a strong and stable polyarthritis that can become chronic by repeated serum administration (Korganow et al., 1999). The initiation phase of STIA is characterized by autoantibodies against the ubiquitously expressed glucose-6-phospate isomerase (G6PI), which in turn is increasingly expressed within the joint after disease onset (Matsumoto et al., 2002). Interestingly, van Gaalen et al. (2004) demonstrated that the production of autoantibodies directed again G6PI is associated with an extra articular manifestation of the disease in RA patients (van Gaalen et al., 2004). Compared to control IgGs, purified anti-G6PI antibodies are efficiently redirected into joint tissue after intra venous injections (Wipke et al., 2002) and crucially need to build anti-G6PI/G6PI-immune complexes to initiate RA (Maccioni et al., 2002). Nevertheless, it remains illusive, why G6PI antibodies specifically target joint tissue, although G6PI is ubiquitously expressed.

In the blood, G6PI-immune complexes bind to Fcγ Receptors (FcγR) on neutrophils, leading to the release of vasoactive mediators increasing the local vascular permeability (Christensen et al., 2016) and enabling translocation into the joints. The lack of FcyRIII specifically on immune cells completely blocks STIA (Corr and Crain, 2002) through disruption of trans-localization of G6PI-immune complexes into the joints (Wipke et al., 2004). In the joints, G6PI-immune complex binds to the FcγR on mast cells and thus, lack of mast cells also prevents trans-localization of G6PI-immune complexes to the joint (Wipke et al., 2004). Upon activation by FcγR binding, mast cells secrete interleukin-1 and thereby essentially support STIA development (Nigrovic et al., 2007). Mice lacking mast cells or mice with interleukin1-deficient mast cells fail to develop STIA (Corr and Crain, 2002; Lee et al., 2002; Nigrovic et al., 2007). In addition, a complete depletion of neutrophils blocks STIA development (Wipke and Allen, 2001) while depletion of interleukin-1 in neutrophils reduces disease severity. Interestingly, a lack of interleukin-1 receptor on neutrophils has no effect on STIA progression (Monach et al., 2010). Furthermore, ligation of neutrophil-specific Ly6G showed the dependence of neutrophil recruitment and endothelial transmigration in STIA on a β2-integrine dependent mechanism (Wang et al., 2012). Neutrophil extravasation, on the other hand, required the expression of the adhesion molecule lymphocyte function-associated antigen 1 (LFA-1), which binds to intercellular adhesion molecule-1 (ICAM-1) and LFA-1-deficiency prevents STIA development (Monach et al., 2010). Finally, macrophage depletion completely inhibits STIA development (Solomon et al., 2005) but depletion of macrophages and subsequent reconstitution with Ly6C-negative monocytes rescues STIA development suggesting that Ly6C-negative monocytes are the driving force for STIA development (Misharin et al., 2014). Likewise, pro-inflammatory cytokines Il-1β and TNFα (Ji et al., 2002) and the complement system (Monach et al., 2007) essentially contribute to the development of STIA. Finally, FLS, activated by the inflammatory environment, hyper proliferate (Henderson and Pettipher, 1985), produce cytokines and chemokines and increased level of adhesion molecules like VCAM and ICAM to interact with the infiltrating immune cells (Bombara et al., 1993; Noss and Brenner, 2008). This specific aspect of STIA is supported by human studies showing that G6PI-immune complexes promote proliferation and reduction of apoptosis of FLS in patients (Zong et al., 2015). In this regard, the

importance of FLS in STIA development was demonstrated by a 50% reduction of ankle swelling and reduced cell infiltration in STIA mice after disruption of FLS specific cell-cell contact by cadherin-11-deletion (Lee et al., 2007). Similarly, the study showed a reduction in bone and cartilage destruction in cadherin-11 deficient mice, indicating that FLS essentially contribute to bone destruction (Lee et al., 2007).

Most important for our studies is the capability to transfer STIA to various transgenic mouse lines.

1.1.4. Treatment Strategies

More than 60 years rheumatoid arthritis is treated with Glucocorticoids (GCs) (Philip S. Hench, 1950; van Everdingen et al., 2002) and today GCs are still among the most frequently prescribed and effective therapeutics in RA (Bijlsma and Jacobs, 2014; Buttgereit and Bijlsma, 2017; Gaujoux-Viala and Gossec, 2014). GCs have strong immune suppressive effects, however, long-term treatment necessary in RA therapy is frequently accompanied by adverse side effects, like osteoporosis, insulin resistance and GC-resistance (Ogawa et al., 1992; O'Brien et al., 2004; Canalis et al., 2007; Hartmann et al., 2016). A recent study reported that RA patients treated with GCs developed an elevated risk for diabetes, osteoporosis, thrombotic stroke or myocardial infarction, serious infections and death compared to non-RA patients treated with GCs (Wilson et al., 2018). Worthwhile to mention, duration and median cumulative dose were higher in RA-patients (1650mg for 284 days) then in non-RA patients (500mg for 55 days) (Wilson et al., 2018). The median average daily dose of GCs, however, was lower in RA patients (5,5mg) then in non-RA patients (8,7mg) (Wilson et al., 2018). Although GC treatment of RA patients increased the risk for osteoporosis; the risk for fracture as well as the risk for glaucoma was unchanged (Wilson et al., 2018). Despite these comorbidities, GCs are presently used in a broad range in clinical practice (Buttgereit and Bijlsma, 2017), and risk minimization is continually adjusted by changes in dose and application (Emkey et al., 1996; Wassenberg et al., 2005; Weitoft et al., 2005; Jafari et al., 2016; Quan et al., 2016). Especially, the

usage of specifically packed GCs, that influences drug kinetics and cell or joint-specific delivery are in favor to reduce comorbidities (Jafari et al., 2016; Quan et al., 2016; Lühder and Reichardt, 2017). Other means to circumvent these comorbidities are combination-therapies with disease modifying anti-rheumatic drugs (DMARDs) like methotrexate (Bakker et al., 2012) or biologics like antibodies against TNFα (e.g. Adalimumab), interleukin-6 (Tocilizumab) or CD80/86 (Apatacept). While in some patients biologics have a great effectiveness, others display strong varying effects that correlate with the specific synovial phenotype of these patients (Dennis et al., 2014).

GC treatment provides strong anti-inflammatory actions and therapy is improved for long-term treatment by low-doses or by patient-specific applications. Understanding of the underlying cellular processes and the interplay of the involved cells is of utmost importance to further optimize individual treatment and to overcome adverse side effects.

1.2. Glucocorticoid Signaling

Endogenous glucocorticoids (GCs), cortisone in humans and corticosterone in rodents, are steroid hormones secreted in a circadian and ultradian rhythm playing a crucial role in metabolism, inflammation and stress responses. Their synthesis and secretion is controlled by a tight feedback loop of the hypothalamic-pituitary-adrenal (HPA) axis. Within the HPA axis, the hypothalamic corticotropin-releasing factor induces the secretion of adrenocorticotropic hormone from the anterior pituitary gland (Papadimitriou and Priftis, 2009), leading to the production of key molecules (e.g. progesterone) for GC synthesis. Secreted GCs that circulate through the bloodstream are bound to the transport protein transcortin and finally enter cells as lipophilic steroid hormones. Within the cell endogenous GCs are regulated by specific enzymes 11β-hydroxysteroid dehydrogenase 1 and -2 (11β-HSD-1, -2) where, 11β-HSD-1 transforms the inactive form of cortisone to its active form cortisol and 11β-HSD-2 directs the reverse reaction from cortisol to cortisone (Hardy et al., 2014). Interestingly, 11β-HSD1-deficient mice show an enhanced infiltration of cells and a slightly increased ankle swelling in STIA, while

11β-HSD2-deficiency does not affect disease progression (Coutinho et al., 2012). It should be noted that synthetic GCs like dexamethasone (DEX) used in this study are mostly protected from inactivation by 11β-HSD-2 (Weinstein, 2012). Other GCs used in RA patients include prednisolone, triamcinolone, methylprednisolone and the most often prescribed GC: prednisone (reuhmatoidarthritis.org). Finally, activated GCs bind to the glucocorticoid receptor (GR), a ligand-induced transcription factor, and initiate cell type specific genomic as well as non-genomic changes.

1.2.1. Glucocorticoid receptor (GR) biology

The ubiquitously expressed GR (encoded by the *Nr3c1* gene) belongs to the nuclear receptor superfamily and is, if not bound to GCs, located in the cytoplasm. In the cytoplasm the GR is associated to a chaperon complex of several proteins (including Hsp90, Hsp70 and FKBP51), which upon GC binding to the receptor changes its composition (FKBP51 is replaced by FKBP52) with the consequence that GR translocates into the nucleus acting as ligand-induced transcription factor that both induce and suppress gene expression (Figure 1.1). Although, non-genomic effects have been reported, the majority of therapeutic effects are mediated by nuclear actions. Some of the non-genomic reports show a mitochondrial effect of GCs resulting in apoptosis (Sionov et al., 2006); others report the direct interaction of cytosolic GR (Löwenberg et al., 2005) or membrane bound GR (Strehl et al., 2011) with kinases of signal transduction pathways like Phospoinositide-3 kinase (PI3K) (Limbourg et al., 2002) and c-jun N-terminal kinase (JNK) (Caelles et al., 1997; Bruna et al., 2003). The GR structure is composed of five different domains; the N-terminal located transactivation domain, or activation function-1 (AF-1), the DNA-binding domain (DBD), the hinge region, the ligand-binding domain (LBD) and the C-terminal ligand-dependent AF-2 domain (Hollenberg and Evans, 1988; Danielian et al., 1992). Ligand binding to the GR results in a conformational change within the AF-2 domain that enables interaction of helix 12 with co-activators such as TIF2 or SCR1(Danielian et al., 1992; Oñate et al., 1995; Kucera et al., 2002; Frego and Davidson, 2006). This interaction is facilitated by multiple LXXLL motifs of the co-activator with residues

from helix 12 of the GR (Darimont et al., 1998). Interestingly, co-repressors, like NCoR (Schulz et al., 2002) are thought to share binding sites with co-activators (Nagy et al., 1999; Frego and Davidson, 2006). The DBD mediates binding of the receptor to full or half-sides of so called GC response elements (GRE) (Payvar et al., 1981) which are palindromic motives (Strähle et al., 1987) located all over the genome; the hinge domain is necessary for the proper translocation of GR to the nucleus and links the DBD to the LBD that equally binds endogenous or synthetic GCs. Importantly, the LBD also contains several dimerization interfaces, vital for the homo-dimerization of GR (Bledsoe et al., 2002). As a monomeric molecule, GR can interact with other transcription factors like NFκB and AP1, a so called tethering mechanism to suppress gene expression, or directly bind to half-side GRE motifs (Schiller et al., 2014) resulting in repression as well as activation of gene expression. Recently, it was reported that monomeric GR also binds to a GRE half-site within the AP-1 response elements on the DNA even in the absence of AP-1 questioning the mechanism of tethering for the suppression of, at least, AP-1 (Weikum et al., 2017). In a second mechanism GR can form a homo-dimer, which binds to full size “classical” GREs to induce gene expression (Figure 1.1). Interestingly, positive “classical” GREs, consisting of an imperfect palindromic DNA sequence with two hexameric half-sites that are separated by three nucleotides (Strähle et al., 1987; Beato, 1989) were reported as well as negative GREs consistent of a palindromic sequence separated by only two nucleotides (Surjit et al., 2011). The negative GREs recruit co-repressors like nuclear receptor co-repressor (NCoR) and silencing mediator for retinoid and thyroid receptors (SMRT), which interact with histone deacetylase-3 (HDAC3) resulting in repression of gene expression (Surjit et al., 2011). Furthermore, SMRT and NCoR repressor complexes also binds to monomeric GR and affect tethered trans-repression, which in both cases depend on the SUMOylation of GR (Hua et al., 2016a, 2016b). However, both activities, monomeric GR and dimeric GR essentially require the presence of an open chromatin structure. To this extent GRs are thought to rely mainly on the interaction with other transcription factors that function as pioneering factors shaping the landscape for GR accessibility to chromatin (e.g. Pu.1 for macrophages (Uhlenhaut et al., 2013) or C/EBP-β in the liver (Grøntved et al., 2013). This also explains the enormous variety of GR actions in different cell types and tissues. Moreover, there are only few spots on

the genome where GR itself acts as a *de novo* pioneering factor (John et al., 2011). However, if a GR molecule once binds to chromatin it enhances the accessibility for additional GRs or other transcription factors, a mechanism called assisted loading (Swinstead et al., 2016). Interestingly, Lim et al. (2015) reported that monomeric GRs show a stronger association to lineage-determining transcription factors then GR dimer, indicating that an assisted loading mechanism is required for GR monomers to efficiently bind to half-site GRE motifs due to the lack of stabilizing forces present in GR dimers (Lim et al., 2015). Furthermore, beside the monomeric and dimeric state of action of GR, Presman at al. (2016) recently described GR tetramers as an additional configuration of GR action (Presman et al., 2016), however, the physiological relevance of GR tetramer complexes still needs to be validated.

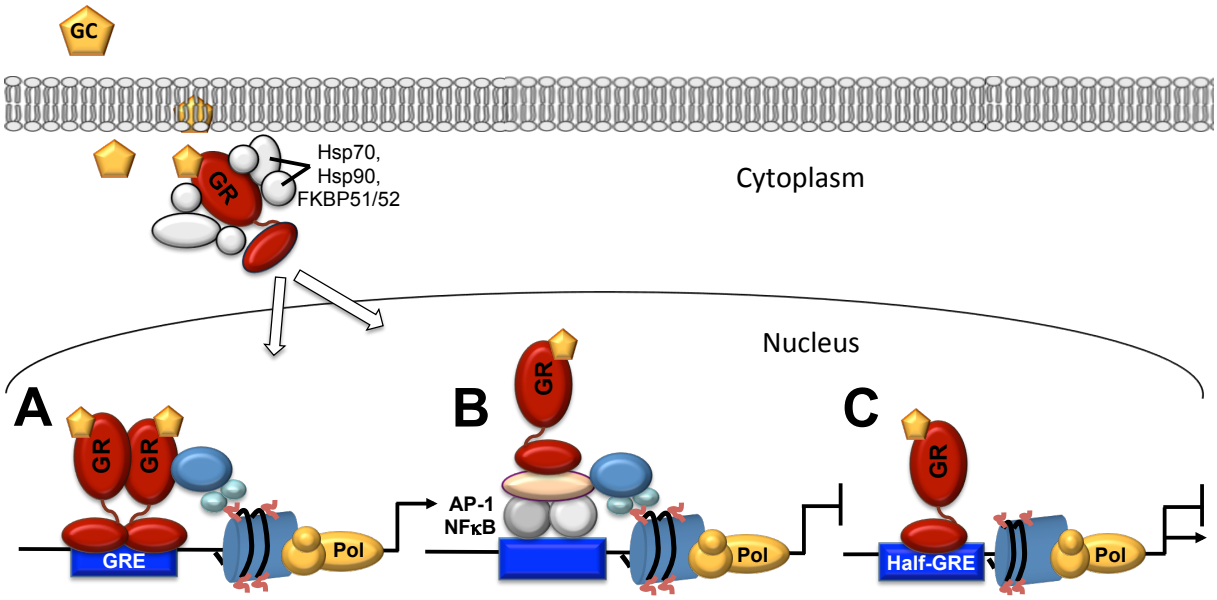

Figure 1.1 Schematic transcriptional mechanisms of the GR within a cell

After ligand binding the cytosolic GR chaperone complex changes and GR is relocated into the nucleus obtaining the ability to facilitate three modes of action: (A) GR homo-dimer bind to GRE, mainly inducing gene expression, (B) as monomeric GR that interacts with other transcription factors (e.g. AP-1, NFκB) to suppress gene expression and (C) as monomeric GR binding to half-site GREs. GC=Glucocorticoid, GR=Glucocorticoid receptor, Hsp=Heat-shock protein, FKBP=FK506 binding protein, Pol=Polymerase, GRE=Glucocorticoid response element, AP-1=Activator protein-1, NFκB=Nuclear factor kappa-light-chain-enhancer of activated B-cell.

A very interesting effect after GC treatment is a strong GR redistribution on the chromatin, reported by Lim et al. (2015). They could show that prednisolone treatment for 24h leads to an increase of GR dimer binding to the classical

palindromic motifs of the genome that is accompanied by a simultaneously reduction of binding of GR monomers to genomic DNA. This effect was mostly abolished in GR^{dim} mice (Lim et al., 2015) carrying an amino acid knock-in mutation at position 465 (GR-A465T) within the zinc finger domain of the DBD that abolish GR dimerization (Reichardt et al., 1998). However, recent *in vitro* studies have shown that a residual dimerization activity remained after overexpression (Jewell et al., 2012); yet, *in vivo* analysis displayed only little to no dimeric GR occupancy in liver of GR^{dim} mice (Lim et al., 2015).

1.2.2. GR dimer dependent regulation of inflammation

As mentioned above, upon ligand binding, the GR can form homo-dimers that directly bind to specific DNA motives, so called GREs, resulting in activation of gene expression. Of utmost importance in the understanding of the impact of this GR dimerization in inflammatory diseases was the generation of mice with an impaired GR dimerization (GR^{dim}) (Reichardt et al., 1998). The usage of GR^{dim} mice revealed an important contribution of GR transactivation in several inflammatory diseases (Tuckermann et al., 2007; Baschant et al., 2011; Vandevyver et al., 2012; Vettorazzi et al., 2015). For instance in AIA, GR^{dim} mice were resistant to GC-treatment and suppression of the pro-inflammatory cytokines interleukin-6, Interferon γ (IFNγ) and interleukin-17 were completely dependent of GR dimerization (Baschant et al., 2011). It should be noted that impaired GR dimerization strongly attenuates GC-treatment in the acute phase of G6IP-induced arthritis (Schubert et al., 2004; Baschant et al., 2011). In other diseases than arthritis, GR dimerization was also proven to play a pivotal role. For example, in a model of acute lung injury, GR dimerization was necessary together with inflammatory stimuli to induce sphingosine kinase-1 (Sphk1), which in turn increased sphingosine-1-phosphate (S1P) leading to a reduced vascular leakage of the endothelial cell barrier of the lung (Vettorazzi et al., 2015). Vascular leakage is also involved in arthritis development; however, Sphk-1-deficiencient mice have a strong attenuated arthritis score and synovial inflammation in the hTNFα model (Baker et al., 2010) point to a pro-inflammatory effect of Sphk1 in arthritis. Furthermore, Kitano et al. (2006) showed that S1P increases the proliferation and

expression of pro-inflammatory mediators in FLS isolated from RA patients (Kitano et al., 2006). Similarly, the receptor for S1P, $S1P_1$ was significantly increased in FLS derived from RA patients compared to FLS of osteoarthritic patients (Kitano et al., 2006) and knock down of Sphk-1 inhibits migration and invasion of RA FLS (Yuan et al., 2014). Whereas GR dimerization mediated the suppressive effects of GCs in AIA via a T-cell dependent mechanism, in acute lung injury and in contact allergy anti-inflammatory effects were mediated by macrophages (Tuckermann et al., 2007; Vettorazzi et al., 2015) and neutrophils (Tuckermann et al., 2007). In contact allergy impaired GR dimerization resulted in an ongoing infiltration of macrophages and neutrophils to the site of inflammation (Tuckermann et al., 2007). This was accompanied with the resistance of suppression of TNFα, Il-1β, and of the chemokines, monocyte chemoattractant protein-1 (MCP-1) and macrophage inflammatory protein-2 (Mip-2) in isolated bone marrow cells (Tuckermann et al., 2007). As a consequence, injection of one of these factors resulted in the worsening of contact allergy despite GC-treatment (Tuckermann et al., 2007). Finally, GR dimerization was essential for survival in TNFα-induced lethal inflammation (Vandevyver et al., 2012) by the induction of Dual-specificity phosphatase-1 (Dusp-1). Dusp-1 is a classical GR dimer-dependent GC target gene, that is important for the de-phosphorylation of mitogen activated protein kinases (MAPK) like p38 and JNK (Clark and Lasa, 2003). The interaction of GR with MAPK-signaling, specifically with p38 and Msk-1, was also involved in the suppression of acute lung injury (Vettorazzi et al., 2015). In TNFα-induced lethal inflammation, however, anti-inflammatory effects of GCs were mediated by the de-phosphorylation of JNK2 (Vandevyver et al., 2012) suggesting a role in the inhibition of pro-apoptotic pathways.

Together these studies reveal a strong association of GR dimer function in different cell types with protective effects in several inflammatory diseases. It remains uncertain, which of these pathways and cell types are involved in arthritis (except of the role of GR dimer in AIA; (Baschant et al., 2011)), specifically in STIA and how these pathways affect the cross talk of cells in the joint?

1.2.3. Potential GC-target cells and pathways in arthritis

The most important inflammatory cell types in the STIA arthritis model are neutrophils and macrophages. Neutrophils are the first responder to inflammatory stimuli and subsequently migrate from the blood stream into the injured tissue. This migration is suppressed by GCs through glucocorticoid-induced leucine zipper (GILZ) and AnnexinA1 (Ricci et al., 2017). Within the injured tissue, neutrophils raise their anti-inflammatory properties by phagocytosis of pathogens, secretion of anti-microbial proteins and the release of extracellular traps a mechanism called NETosis. The impact of dexamethasone treatment on NETosis is variable, as it shows no effect on PMA or TNFα-induced NETosis (Lapponi et al., 2013) but reduces bacterial-induced NETosis (Wan et al., 2017). Macrophages are the immediate responders to invading neutrophils and various subsets of macrophages arise from either infiltrating monocyte-derived macrophages or tissue-resident macrophages which both can differentiate/polarize into classical, pro-inflammatory or non-classical, anti-inflammatory subsets playing a role in inflammatory arthritis (Murray, 2017). Misharin and colleagues (2014), demonstrated the importance of infiltrating macrophages for the development of STIA, surprisingly however, after onset of STIA the same macrophages switch their gene expression patterns towards a non-classical, anti-inflammatory phenotype, crucial for the resolution of STIA (Misharin et al., 2014). These anti-inflammatory macrophages are also thought to play an essential role in clearance of apoptotic cells in inflammation, a process called efferocytosis. Genes associated to efferocytosis include the TAM receptors (MerTK, Axl and Tyro3), CD36 and AnnexinA1. The deficiency in TAM receptors or Anxa1 results in an impaired clearance of apoptotic cell infiltrate (Maderna et al., 2005; Seitz et al., 2007), leading to accelerated arthritis (Yang et al., 2004; Waterborg et al., 2017). Interestingly, neutrophils and macrophages are major sources of AnnexinA1, an anti-inflammatory protein regulated by endogenous GCs in a GR dimer dependent mechanism (Kovacic et al., 1991). Accordingly, high dose AnnexinA1 injections protect against STIA and AnnexinA1-deficient mice are resistant to GC treatment in STIA (Patel et al., 2012). In addition, AnnexinA1-deficiency is associated with

increased levels of IL-1β, TNFα, IL-6 and MIF and accelerated histological scores in antigen-induced arthritis (Yang et al., 2004). Some cytokines have been shown to play a pivotal role in arthritis development and progression and their suppression by GCs might affect treatment outcome. However, deficiency of interleukin-6 does not influence STIA development (Ji et al., 2002) while disruption of TNFα-signaling resulted in inconclusive effects (Ji et al., 2002; Kyburz et al., 2000). This is different for interleukin-1β, which is absolutely necessary for STIA development (Ji et al., 2002) and similarly important in CIA but not in AIA arthritis (Wooley et al., 1993). The fact that GCs strongly suppress Interleukin-1β transcription and mRNA stability (Lee et al., 1988) makes Interleukin-1β a potent GC target in arthritis therapy. In addition, our group demonstrated that interleukin-17 is of critical importance in GC-therapy of AIA since its deficiency results in GC resistant in the AIA model (Baschant et al., 2011).

Otherwise, cytokines are produced not solely by immune cells but also by non-immune cells, particularly FLS that generally contribute to the inflammatory processes in arthritis (Hardy et al., 2013; Bartok and Firestein, 2010; Bottini and Firestein, 2013). In this regard, specific targeting of FLS by liposomal encapsulated prednisolone leads to a strong suppression in AIA (Vanniasinghe et al., 2014). In STIA, disruption of FLS tissue integrity by deletion of FLS-specific cadherin-11 reduces disease progression by about 50% (Lee et al., 2007). Furthermore, FLS exhibit a strong inflammatory phenotype in STIA but remain responsive to GC treatment, underlining their potential therapeutic relevance in GC-therapy (Hardy et al., 2013). In addition, *in vitro* treatment of human FLS with the synthetic GC, dexamethasone (DEX) prevents TNFα-mediated interleukin-1β induction essentially required for STIA development (Gossye et al., 2009). Besides its role in neutrophil migration, GC-induced expression of GR dimer-dependent GILZ (Baschant et al., 2011) also affects cytokine expression. Correspondingly, depletion of endogenous GILZ by siRNA treatment worsened CIA arthritis and increased TNFα and IL-1β in the joints (Beaulieu et al., 2010) while adenoviral injections of GILZ into knee joints of CIA mice leads to a significant reduction of arthritis severity (Ngo et al., 2013). Deletion of GILZ, in contrast, has no influence on the clinical outcome of AIA arthritis (Ngo et al., 2013). Other GR dimer-dependent anti-inflammatory genes possibly involved in GC-mediated suppression

of arthritis are metallothionine-1 and -2 (Karin and Herschman, 1979), which when injected into CIA mice, strongly suppress arthritis (YOUN et al., 2002) and the above-mentioned DUSP-1, of which deletion results in an accelerated onset and increased incidence and severity in CIA mice (Vattakuzhi et al., 2012).

Taken together, several anti-inflammatory mediators of arthritis (GILZ, DUSP-1, AnnexinA1, Sphk-1 and Metallothionein) are dimer-dependent regulated and affect different cell types and most often involve cytokine suppression. However the exact cell type and the effect on surrounding cells, specifically stromal cells, is most often not addressed. Thus, further investigations are required to understand the cellular processes and interactions mediating suppression of arthritis and affecting detrimental side effects on bone.

1.3. Bone biology and osteophytes development

Bone is a mineralized stable connective tissue, which protects soft tissue, enables locomotion and is used as calcium and phosphate storage. Despite its rigid appearance it is a highly active tissue, which is constantly remodeled throughout our lives. GCs affect bone growth and remodeling on different levels and, dependent on dosing and inflammatory environment, result in beneficial or detrimental effects (Hartmann et al., 2016).

1.3.1. Bone biology

In healthy individuals bone is constantly rebuild and resorbed by bone forming osteoblasts and bone resorbing osteoclasts. If this homeostasis is disrupted, as it occurs in elderly people, bone strength is impaired and osteoporosis and fracture risk are increased. Inflammatory conditions present in arthritis also influence bone homeostasis, by the inhibition of osteoblast differentiation and induction of bone resorption by osteoclasts (Shaw and Gravallese, 2016). In addition, GCs affect growth of long bones by affecting endochondral ossification (Hartmann et al., 2016) a complex process that mainly comprises mesenchymal stem cells (MSCs),

chondrocytes and osteoblasts. MSC-derived chondrocytes are lined up in the growth plate at the diaphyseal ends of the developing bones and subsequently build a cartilaginous matrix. Finally, mature chondrocytes mineralize the matrix and undergo apoptosis and osteoblasts subsequently infiltrate the residual matrix lacunas and build the final bone matrix. Until the beginning of sexual maturation the growth plate is mostly replaced by bone, and longitudinal growth will be completed (Burdan et al., 2009). GCs interfere with the process of endochondral ossification on several levels (Hartmann et al., 2016) and in pathological conditions, endochondral ossification can be observed at ectopic sites of bones, leading to the formation of bone spurs called osteophytes, often-observed in arthritic diseases.

1.3.2. Adverse effects of GCs on bone growth

Long-term treatment of RA patients is associated with an increased risk for osteoporosis (Wilson et al., 2018) and GC treatment during juvenile arthritis impairs longitudinal bone growth (Bechtold et al., 2009) and affects endochondral ossification (Hartmann et al., 2016). GCs suppress self-renewing of chondrocyte-progenitors and the proliferation of chondrocytes through inhibition of growth factors (Jux et al., 1998). Further, GCs induce apoptosis of chondrocytes by increased expression of caspases-3, -8 and -9 (Chrysis et al., 2005) and reduction of anti-apoptotic Bcl-2 and -X (Chrysis et al., 2003). Finally, in rats, dexamethasone treatment also results in the inhibition of maturation of chondrocytes (Annefeld, 1992). Interestingly, withdrawal of GCs results in a so-called “catch-up” growth in children, describing the increased proliferation of self-renewing chondrocytes resulting in a normal bone length (Schrier et al., 2006). Besides the effects of GCs on chondrocytes, they also interfere strongly with the differentiation of osteoblast precursors (Rauch et al., 2010) by affecting Wnt- and BMP-signaling (Luppen et al., 2003; Hayashi et al., 2009; Butler et al., 2010; Baron and Kneissel, 2013). Furthermore, GCs inhibit osteoblast proliferation and stimulate apoptosis of osteoblasts (Chang et al., 2009) as well as of terminally differentiated osteoblasts, called osteocytes (Plotkin et al., 2007). Finally, GC treatment leads to a rapid but transient enhancement of bone resorption (Dovio et

al., 2004) associated with an increased number and activity of osteoclasts. Furthermore, GCs induce the expression of RANKL in cells of the osteoblast lineage, which induce osteoclast differentiation and antibody neutralizing of RANKL prevents GC-induced bone loss (Hofbauer et al., 2009). This combination of effects on bone cells results in the most common secondary form of osteoporosis, the GC-induced osteoporosis, which affects up to 25% of all cases of osteoporosis (Eastell et al., 1998).

1.3.3. Osteophytes

Osteophytes are ectopically grown bony spurs in the joints of patients with inflammatory arthritis (e.g. spondyloarthritis) and osteoarthritis. They can be differentiated into three classes, the traction spur, the inflammatory spur (syndesmophyte) and the genuine osteophytes (van der Kraan and van den Berg, 2007). Traction spurs and inflammatory spurs occur at the site of ligaments and tendons to bone, whereas genuine osteophytes arise in the periosteum, a cellular layer at the junction between cartilage and bone (van der Kraan and van den Berg, 2007). Osteophytes can cause pain, stiffness and loss of function in the joint due to nerve compression and reduced mobility.

Osteoblast, chondrocytes but also periosteal and synovial MSCs (Sandell and Aigner, 2001) as well as synovial macrophages are involved in osteophyte development (Blom et al., 2004). After induction, by a yet not understood mechanism, cells in the periosteum start to proliferate and undergo chondrogenic differentiation within the osteophyte. The inner chondrocytes become hypertrophic and undergo endochondral ossification, bone deposition and bone marrow cavity formation (Dodds et al., 1994; van der Kraan and van den Berg, 2007). So far only few pathways were identified that are involved in osteophyte formation, TGFβ, BMP- and hedgehog- and PTHr-/P-signaling (Scharstuhl et al., 2002; Huch et al., 2003; Ruiz-Heiland et al., 2012).

Remarkable, it was shown that the STIA mouse model also develops strong osteophytes (Ruiz-Heiland et al., 2012) whose formation is suppressed by dexamethasone in experimental osteoarthritis (Bajpayee et al., 2017) independent of cytokine suppression (Finzel et al., 2013).

Thus, GC treatment has bilateral effects on bone in arthritis. On the one hand, GCs mediate negative side effects through suppression of osteoblast differentiation and weakening bone strength but on the other hand mediate clearly favorable effects through suppression of osteophyte formation.

Strikingly, most studies regarding osteophyte development and more importantly the suppression of osteophyte formation by dexamethasone are descriptive and do not reveal molecular mechanisms. Due to a lack of *in vitro* culture systems mimicking osteophyte formation, a functional proof of the suggested pathways and cross talk of certain cells is difficult to analyze. We will address these question by using mice with a disrupted GR function in different cellular compartments, to define whether the suppressive effects of DEX on osteophytes are caused by none-immune cells like osteoblasts or by immune cells like macrophages. And further, we will define the effects of impaired GR dimerization on osteophyte development to narrow down possible target genes affected by GC-suppression of osteophyte formation.

1.4. Aims of the thesis

Rheumatoid arthritis is affecting 1% of the world's population and GCs are among the most frequently prescribed immune-suppressive drugs to treat RA (Buttgereit and Bijlsma, 2017). Long-term treatment needed in RA, is accompanied with negative side effects, like osteoporosis and diabetes (Wilson et al., 2018). To improve therapy outcome it is necessary to understand the underlying cellular and molecular processes favoring the anti-inflammatory effects. Previous studies have shown the importance of GR dimerization in suppression of several inflammatory models by different cell types (Baschant et al., 2011; Vettorazzi et al., 2015). In order to understand how GCs affect different cell types to suppress inflammation in STIA and if GCs influence the interplay of these ell types we address the following questions:

1. **What are the direct effects of GCs on the immune and the non-immune compartment in STIA and how do GCs affect the interplay of these compartments during STIA?**

In detail:

   a. What is the role for immune and non-immune cells in GC-mediated suppression of STIA and which transcriptional mechanism of the GR is important?
   b. Is cytokine suppression the main outcome of GC treatment and is this sufficient to prohibit disease progression?
   c. How does GC treatment affect the cell composition in joints of STIA and what is their effect on cellular cross talk in STIA?

2. **Which cell type is mediating the anti-inflammatory effects of GC treatment in STIA and which molecular, potentially anti-inflammatory pathways are affected by GCs in STIA?**

2. Material and Methods

2.1. Materials

2.1.1. General chemicals

General chemicals (acids, standard organic salts, solvents, anorganic chemicals, etc.) were purchased from Sigma-Aldrich (Taufkirch), Roth (Karlsruhe), Merck (Darmstadt) and Applichem (Darmstadt).

2.1.2. Common buffers and solutions

10X PBS: 81 mM Na_2HPO, 15mM KH_2PO_4, 1370 mM NaCl, 27 mM KCl, pH 7.2

10X TBS-T: 200 mM Tris, 1370 mM Glycine, 1% Tween-20, dH_2O, pH 7.6

TAE buffer: 40 mM Tris, 20 mM acetic acid, 1 mM EDTA

NID buffer: 50 mM KCl, 10 mM Tris-HCl pH 8.3, 1 mM $MgCl_2$, 0.1 g/ml Gelatine, 0.45% NP40, 0.45% Tween-20, H_2O

4% Paraformaldehyde (PFA): 20 g PFA, 500 ml PBS, 100 µl 10M NaOH, 75 µl 37% HCl, pH 7.0-7.2

15% EDTA: 750 g EDTA, 100 g 10M NaOH, 40 ml 37% HCl, upto 5 L dH_2O, pH 7.0-7.2

Eosin: 5g eosin Y, 250 ml dH_2O, 250 ml 100% ethanol

FACS Buffer: 10%FCS, 1%EDTA in PBS

2.1.3. Primers

Primers for genotyping (Tabel 2.1) and for qRT-PCR (Tabel 2.2.) were purchased from Sigma-Aldrich (Taufkirch) or Eurofins Scientific (Luxembourg).

Table 2.1 Genotyping PCR primer sequences

Transgene	Forward 5' → 3'	Reverse 5' → 3'
GR^{dim}	TTCTCATGTGACAGGCAGACAG	TGTGTCTTGATGATAGTCTGCTC
GR^{flox}	GGCATGCACATTACTGGCCTTCT and CCTTCTCATTCCATGTCAGCATGT	GTGTAGCAGCCAGCTTACAGGA
General Cre	ACCTGAAGATGTTCGCGATTATCT	ACCGTCAGTACGTGAGATATCTT
Col2a1-Cre	GAGTGATGAGGTTCGCAAGA	CTACACCAGAGACGG
CAMKII-Cre ERT2	GGTTCTCCGTTTGCACTCAGGA and CTGCATCGGGACAGCTCT	GCTTGCAGGTACAGGAGGTAGT

Table 2.2 qRT-PCR primer sequences

Target gene	Forward 5' → 3'	Reverse 5' → 3'
CD163	TCAGCAAAGATCACGCTTCT	ACAGTTATGCTTGCCCCATC
CD36	TGGCAAAGAACAGCAGCAAA	CACAGTGTGGTCCTCGGG
MerTK	GCTGGCATTTCATGGTGGAA	CATTGTCTGAGCGCTGCAC

Axl	AGCCTTCCTGTGCCCCTA	GAGGTGGGGGTTCACTCA
AnxA1	AAGGTGTGGATGAAGCAACC	AGGGCTTTCCATTCTCCTGT
RPL	CCTGCTGCTCTCAAGGTT	TGGCTGTCACTGCCTGGTACTT
GR	GGCCGCTCAGTGTTTTCTAA	GCAGAGTTTGGGAGGTGGT
Tyro3	TGGAGCCATCCTAGAGTTCC	GAGGGGCCTGACTTCCTG
Mt-1	CACCAGATCTCGGAATGG	GTTCGTCACATCAGGCACA
Mt-2	CTTGTCGGAAGCCTCTTTGC	CGCCTGCAAATGCAAACAATG
Gas6	TGTGGCAAACTATCTCCGTG	CAGCTACCGCGATCTTCATT

2.1.4. Antibodies

Table 2.3 Antibodies used for immunohistochemistry

Antibody	**Company**	**Catalog number**	**Dilution**
Monoclonal rabbit anti-GR (D8H2) XP	Cell signaling	#3660	1:200
Polyclonal rabbit anti-Cdh11	Invitrogen	#71-7600	1:200
VECTASTAIN ABC HRP Kit (Peroxidase, Rabbit IgG)	Vector Laboratories	#PK-4001	Followed protocol within the kit

Table 2.4 antibodies used for Flow cytometry analysis

Surface marker	Conjugate	Company	Dilution
CD45	APC	eBioscience	1:200
CD11b	PE	eBioscience	1:200
B220	PerCP-Cy5.5	eBioscience	1:200
CD3	FITC	eBioscience	1:200

Surface marker	Conjugate	Company	Dilution
CD45	APC-Cy7	eBioscience	1:200
CD11b	FITC	eBioscience	1:200
F4/80	APC	eBioscience	1:200
Ly6C	PerCP-Cy5.5	eBioscience	1:200
Ly6G	Pe-Cy7	Invitrogen	1:200
Siglec F	PE	eBioscience	1:800

Surface marker	Conjugate	Company	Dilution
CD45	APC	eBioscience	1:200
CD11b	FITC	eBioscience	1:200

F4/80	PE	eBioscience	1:200
MHCII	AF700	eBioscience	1:200
Ly6G	Pe-Cy7	Invitrogen	1:200

2.1.5. Histology and microscopy materials

Eukitt quick-hardening mounting medium	Sigma-Aldrich
PAP-Pen	Sigma-Aldrich
Microscope slide Superfrost Plus	Thermo Scientific
Coverglasses 24x60 mm	VWR
Citrate Buffer pH 6,0 10x Antigen Retriver	Sigma-Aldrich
30% H_2O_2	Merck
Biotin / Avidin blocking Kit	Vektorlabs
ImmPACT DAB	Vektorlabs

2.1.6. Molecular biology materials

DNA Hyperladder	Bioline
Agarose	Sigma-Aldrich

Ethidium bromide	Merck
dNTPs	Bioline
Tag DNA Polymerase (MO267X)	New England Biolaps
OneTaq Quick-Load 2X MasterMix with Standard Buffer (MO486L)	New England Biolaps
High Capacity cDNA Reverse Transcription Kit	Applied Biosystems
Platinum SYPR Green qPCR SuperMix-UDG	Invitrogen
RNAse OUT	Invitrogen
Qiagen RNeasy kit	Qiagen
Trizol	Invitrogen
BCA protein assay	Thermo Scientific Pierce
Cytokine & Chemokine 36-Plex Mouse ProcartaPlex™ Panel 1A	Invitrogen
Bio-Plex Pro Mouse Cytokine 8-plex Assay	BIO-RAD
Bio-Plex Pro Mouse Cytokine 23-plex Assay	BIO-RAD

2.1.7. Cell culture materials

12-Well plates	Sarstedt

6-Well plates	Sarstedt
10 cm cell culture dish	Sartstedt
Cell culture filter 0,45 µm	Sartorius stedim biotech
Petri dishes 10 cm	Sarstedt
Reaction tubes 0,5 ml, 1,5 ml, 2 ml	Eppendorf
Reaction tubes 15 ml, 50 ml	Sarstedt
DMEM	Sigma-Aldrich
FBS	Sigma-Aldrich
HEPES	Gibco
Glutamine	Sigma-Aldrich
Sodium Pyrovat	Sigma-Aldrich
Peniciline-Streptomycin	Sigma-Aldrich
Dexamethasone	Sigma-Aldrich
Recombinant Interleukin-1β	Immunotools
Trypan Blue solution	Fuka analytica

2.1.8. Laboratory Equipment

Camera DFC 295 / 365	Leica
Centrifuge 5424	Eppendorf
Centrifuge 5810R	Eppendorf
Table centrifuge 3722L	Fisher Scientific
Gel Chamber	Peqlab Biotechnology
Microtome RM2255	Leica
OV1 Mini Hybridisation Oven	Biometra
PCR flexid Mastercycler	Eppendorf
Precellys 24 homogenizer	PeqLab Biotechnology
Micro CT Scyscan 1176	Bruker
Micro CT Skyscan 1174	Bruker
Spectrophotometer Nanodrop 2000	Eppendorf
Viia7 Real-Time PCR machine	Life Technologies
New Brunswick Galaxy 170S cell culture incubator	Eppendorf
Flow cytometry BD-LSR2	BD Biosciences
Bio-Plex 2000 System	BIO-RAD

Microscope DMI6000B	Leica
Microscope camera DP73	Olympus
ThermoMixer F1.5	Eppendorf
Vortex REAX2000	Heidolph
MR3002 magnetic stir and heater	Heidolph
pHenomenal	VWR
Opsys MR Microplate Reader	Dynex technologies
Waterbath	Julabo
Pippets	Starlab
MSC advantage laminar flow	Thermo Scientific

2.1.9. Software

CTAn	Bruker
CTVol	Bruker
CTVox	Bruker
DataViewer	Bruker
NRecon	Bruker

Prism 7	GraphPad Software
Adobe Illustrator CS6	Adobe
Microsoft Office	Microsoft
Single cell analysis software	FlowJo
Viia7 software version 1.2.2	Applied Biosystems
Bioplex manager 6	BIO-RAD
FACSDiva	BD Biotechnology
CellSens Imaging	Olympus

2.2. Methods

2.2.1. Mouse strains and facilities

Mice were bred in the animal facility of Ulm University (TFZ) and animal experiments were approved by the review board of the Land Baden-Wuerttemberg, Permit Number 1134 and 1271 and performed in compliance with the guidelines for the welfare of experimental animals issued by the Federal Government of Germany. K/BxN mice of F1 generation were generated as described (Monach et al., 2008) GR^{dim} mice (Nr3c1tm3Gsc) (Reichardt et al., 1998) were maintained in the Balb/c background, GRfl/fl (Nr3c1tm2Gsc) (Tronche et al., 1999) were crossed to the Tg(Col2a-cre)1Star(BL6) (kindly provided by Prof. A. Vortkamp, Essen University), Tg(Camk2a-cre/ERT2)2Gsc (Erdmann et al., 2007), Cdh5(PAC)-CreERT2 (Wang et al., 2010) and (Col(I)a2-CreERT) (C57BL/6) (Singh et al., 2015) mice. CD163fl/fl B6.C-TgN(CMV-Cre)1Cgn/J (unpublished) were kindly provided by Katarzyna Barczyk-Kahlert (WWU Münster) and $GR^{fl/fl}$; Dbh-Cre mice (Parlato et al., 2009) were kindly provided by Dr. Grzegorz Kreiner (Polish academy of Science). All strains were backcrossed at least 3 generations to the Balb/c or C57BL/6 background. Tamoxifen (Sigma-Aldrich) was administered as described, 3 weeks prior to irradiation or 6 weeks prior STIA.

Bone marrow chimeras were generated by lethal irradiation (2 x 4,5 Gy - 2h in-between) and reconstitution with $9x10^6$ bone marrow cells in PBS intra venously. Mice were treated for 3 weeks with Neomycin in the drinking water, 3 weeks later STIA was induced.

2.2.2. Serum transfer-induced arthritis (STIA)

K/BxN serum was collected by heart puncture at the age of 9 weeks (Monach et al., 2008). Full blood was kept at room temperature for 30 min and centrifuged for 15 minutes at 500rcf. Collected serum of mice was pooled and frozen at -80°C. Arthritis was induced by two intra peritoneal (i.p.) injections of 100µl (for Balb/c background) and 200µl (for C57BL/6 background) pooled sera from K/BxN mice at

day 0 and 2. Disease severity was measured by assessment of the clinical score (Rose et al., 2013) and thickness of the left ankle joint by calipers. From day 4 Dex (1mg/kg Sigma-Aldrich) was daily i.p. administered (except for $GR^{Col1a2CreERT}$, for which Dex was applied from day 6 on). Mice were sacrificed on day 14.

2.2.3. Mouse genotyping

For genotyping, tail biopsies were digested at 56°C over night in 200µl NID buffer + 10µl Proteinase K and heat-inactivated afterwards for 10min at 95°C.

Genotyping PCRs were performed for GR^{dim} mice as described elsewhere (Reichardt et al., 1998) with the PCR cycler program in table 2.5. GR^{flox} mice and Cre-straines were genotyped using Primers in table 2.1 with the PCR cycler program table 2.6-2.8. All Cre-lines except of Col2a1-Cre and CamKII-Cre ERT2 were analyzed with a general Cre-PCR (Table 2.5 and 2.6). PCR products were analyzed by agarose gelelectrophoresis, in a 1.5% agarose gel in 1x TAE buffer. For 45 min at 120 Volt in 1x TAE buffer. Sizes of PCR products were determined by 1kb DNA-ladder.

Table 2.5 PCR genotyping program GR^{dim}

5 min	95°C	1 cycle
20 sec	95°C	35 cycles
1 min	58°C	
1 min	72°C	
7 min	72°C	1 cycle

Table 2.6 PCR genotyping program GR^{flox}; general Cre

2 min	94°C	1 cycle
20 sec	94°C	35 cycles
20 sec	55°C	
2.30 min	72°C	
7 min	72°C	1 cycle

Table 2.7 PCR genotyping program Col2a1-Cre

3 min	94°C	1 cycle
30 sec	94°C	35 cycles
30 sec	53°C	
45 sec	72°C	
5 min	72°C	1 cycle

Table 2.8 PCR genotyping program CamKII-Cre ERT2

2 min	95°C	1 cycle
30 sec	95°C	35 cycles
1 min	63°C	

1 min	72°C	
10 min	72°C	1 cycle

2.2.4. RNA isolation, cDNA Synthesis and qRT-PCR

RNA was harvested from both skinned front paws by homogenization with steal beads in the Precellys 24 in 1ml Trizol (Invitrogen). 200µl chlorophorm (Merck) was added and incubated for 3 min at RT and centrifuged at 13.000rpm 4°C. Upper phase was mixed with equal amount of ice-cold ethanol (Sigma) and applied to the Qiagen RNeasy kit columne (Qiagen). Protocol was strictly followed, including DNAse (Qiagen) digestion step. For RNA isolation from cells, cells were washed twice with PBS and collected with a cell scraper in 350µl of RLT buffer (Qiagen Rneasy kit) and 10µl β-mercaptoethanol per ml, were added. Subsequent, protocol was strictly followed, including DNAse digestion step. Quality and amount of RNA was determined with the Nanodrop and 1µg RNA was converted to cDNA (Applied biosystems, high capacity cDNA kit) by addition of 2µl RT-buffer, 0,8µl dNTPs, 2µl of random RT primers and 0,7µl reverse transcriptase and 4,3µl RNAse-free water, with addition of 0,3µl Rnase Inhibitor (Invitrogen Rnase OUT) per reaction. Reaction was performed in a thermocycler with the following program: 10min 25°C, 120min 37°C, 5min 85°C and stored at -20°C. For qRT-PCR cDNA was diluted 1:25 from tissue-derived samples and 1:10 for cell culture-derived samples, and 2,5µl were added to a reaction with 5µl SYBR green (Invitrogen), 0,4µl forward and 0,4µl reverse primers and 1,7µl RNAse-free water. PCR was performed in the Applied Biosystems Vii7 by life technology cycler with the following program: 2min 50°C, 10min 95°C, 40 cycles of 15 sec 95°C and 1min 60°C, 15sec 95°C and 1min 60°C for melt curve analysis. Target gene primer sequences table 2.2.

2.2.5. Histology

Ankle joints were collected at day 14 of STIA, fixed in 4% Formaldehyde and decalcified with 15% EDTA shaking at 37°C for 14 days followed by paraffin

embedding. Paraffin-sections of 7 µm were generated with a Microtom (Leica). Sections were stained with H&E (Hematoxylin Roth and Eosin Applichem), Safranin-O and immunohistochemistry was performed for GR and Cadherin-11 (Table 2.3). Pictures were taken in the Leica DMI6000B microscope with the DP73 Olympus camera, using CellSens program.

2.2.6. Hematoxylin Eosin staining

Sections were de-paraffinazed by 2 x 10 min xylene and a degrading ethanol row (100%, 90%, 70%, 50%), washed in tap water for two minutes and stained with hematoxylin for nuclear staining for 1 min. After 5 min tap water washing, sections were stained for 1.30 min in eosin, followed by a dehydration in an increasing ethanol row (50%, 70%, 90%, 100%) and two times 10 min xylene. Sections were embedded in EuKit (Sigma).

2.2.7. Safranin-O staining

Sections were de-paraffinized by 2 x 10 min xylene and a degrading ethanol row (100%, 90%, 70%), stained for 30min with Safranin-O solution (0,1% in 100ml aqua dest.) and washed in dH2O by dipping the sections 6 times. Sections were washed for 10 sec in 90% ethanol and 100% ethanol and stained for 1.15 min in 0,1% Fast Green in 100% ethanol. Finally sections were washed in a 1:1 xylene/ethanol mixture and after 2 x 10 min xylene washing, embedded in EuKit (Sigma).

2.2.8. Immunohistochemistry

Sections were de-paraffinized by 2 x 10 min xylene and a degrading ethanol row (2x100%, 90%, 70%) and kept for 5 min in PBS. For antigen-retrival, sections were slowly cooked in a waterbath in citrate buffer for 15 min, cooled down to RT for 30 min and washed for 5 min in PBS. For blocking of endogenous peroxidase activity sections were kept in 3% H_2O_2 in dH_2O for 10 min and after 5 min PBS washing blocked in 4% goat serum in 0,1%TritonX100/PBS. Followed by blocking

of endogenous biotin / avidin, sections were kept at 4°C with primary antibodies in blocking solution over night. Sections were washed in PBS for 5 min and incubated in secondary antibody as following strictly protocol of VECTASTAIN ABC HRP Kit (Peroxidase, Rabbit IgG) for 1h. After 5 min washing in PBS ABC reagent following strictly protocol of VECTASTAIN ABC HRP Kit (Peroxidase, Rabbit IgG) was incubated for 30 min at RT. After additional 5 min washing in PBS sections were incubated with DAB substrate to reveal the antigen of interest. Reaction was stopped by incubation in H_2O and counterstaining with Hemalaun was performed for 2 min following 5 min running tap-water washing. Sections were re-hydrated by upgrading ethanol row (70%, 90%, 2x100%) and 2x10 min xylene and embedded in EuKit (Sigma).

2.2.9. Micro Computed Tomography (µCT)

Ankles were fixed in 4% PFA at 4°C, and scanned with the *in vitro* Skyscan 1174 (Bruker, Billerica, USA) at 6,2µm resolution (only wt→GR^{dim} chimeric mice) or with the *in vivo* SkyScan 1176 (Bruker, Billerica, USA) at 9 µm resolution and a rotation step of 1° with a 0.5 mm aluminum filter. Scanned Images were reconstituted with the NRecon software (Bruker) and images were orientated in the same direction using DataViewer software (Bruker) and analyzed with the CT_{AN} software (Bruker). The region-of-interest (ROI) was defined as the full ankle without the tibia for an overview picture. The threshold was set at 85. Volume of interest and binary images were created and analyzed in the Batch-manager of CT_{AN} software. The CT_{Vox} software (Bruker) was used for 3D models.

2.2.10. Flow cytometry

Hind paws of mice were skinned, tendons and muscles removed and digested in DMEM with 1,12 mg/ml Collagenase IV (Worthington) and 480 mg/ml of 0.5U/mg Dispase II (Sigma) for 30 min in 37°C and inactivated with 10%FCS. Digested tissue was mashed through a cell strainer (40 µm), centrifuged 5 min at 1500rpm and pellet was dissolved in FACS Buffer (10%FCS, 1%EDTA in PBS). Cells were blocked with Fc-Block (anti-CD16/32, eBioscience) for 10 min RT and divided into

4 tubes. One sample of each mouse was kept as an un-stained control. The three remaining samples of each mouse were stained with three different antibody-mixtures (table 1). Each antibody was diluted 1:200 except of Siglec F (1:800) in FACS Buffer and samples were stained for 30min 4°C in the dark (only FACS-Buffer for unstained controls). For compensation single staining of each antibody was performed and automatic compensation of the FACSDiva software. Cells were washed to remove unbound antibodies and analyzed with the BD-LSR2 flow cytometer. Final evaluation was performed with the FlowJo™ Software.

2.2.11. Multiplex cytokine profiling

Multiplex analysis of cytokines was performed from blood serum gained by heart puncture as described above (2.2.2) or from supernatant of FLS cell culture. Protocol was strictly followed and plates analyzed in the Bio-Plex 2000 System by BIO-RAD.

2.2.12. iTRAQ proteomics protocol

Ankles of mice were collected and skin, tendons, muscles, fingertips and tibia were removed and immediately snap frozen in liquid nitrogen. Frozen tissue was homogenized with the Precellys 24 in T-PER buffer (Pierce) supplemented with Roche Complete protease inhibitor cocktail and 10 mM EDTA. After centrifugation (15 min, 13000 rpm, 4°C) supernatants were transferred to a new tube, and protein concentrations were determined by BCS protein assay. Subsequently, 60 µg of total protein of each sample were precipitated using 6 volumes of ice-cold acetone and re-suspended in 20µl iTRAQ Dissolution Buffer according to the manufacturer's instructions (AB SCIEX, Inc.). Samples were further processed at the functional genomics center Zürich (FGCZ) by collaborator Prof. Dr, Ulrich auf dem Keller, Dr. Tobias Kockmann and Hans Kaltenbach of the ETH Zürich, who also performed bioinformatics analysis.

2.2.13. BCA protein assay

Protein concentrations were determined using BCA protein assay Kit (Thermo Scientific Pierce). Diluted protein samples (1:5) were incubated with BCA working solution for 30 min at 37°C. Optical density was measured at 570 nm using Opsys MR Microplate Reader (Dynex Technologies). Concentrations were automatically determined by comparison to an albumin standard curve.

2.2.14. FLS isolation

Ankles of mice were collected and skin, tendons, muscles, fingertips and tibia were removed under sterile laminar flow. Tissue was transferred into collagenase digestion solution (4mg/ml collagenase IV (Worthington) in DMEM (Sigma) substituted with 10% FCS (Gibco) and 1% Penicillin and Streptomycin (Sigma)). Ankles were digested for 1.5h at 37°C shaking. 10 ml FLS-Medium (DMEM, 10%FCS, 1% Penicillin/Streptomycin and 0,025 M HEPES buffer (Sigma)) was added and cells and tissue transferred into 10 cm cell culture dish. Tissue pieces were removed 4 days later and medium renewed. RNA of cells was isolated when confluence was reached, with RNAeasy Mini kit (Qiagen). For RNA-Sequencing and cytokine analysis FLS were treated for 72h with 5 ng interleukin-1β (Immunotools) and/or 1 µM dexamethasone (Sigma).

2.2.15. Isolation of bone marrow-derived macrophages

Mice tibia and femur were isolated and kept on ice in PBS until all mice were dissected. Bones were transferred into sterile hood and kept in 80% EtOH for 30 sec and transferred into BMDM medium (DMEM, 10% heat-inactivated serum, Penicillin/streptomycin, sodium-pyruvate and L-Glutamate). Ends of the bones were cut with sterile scissors and bone marrow flushed out with BMDM medium through a syringe. Cells were dispersed into the medium by pipetting through a cell strainer (40µm) and seeded into four 10cm dishes per mouse (non coated). After 4 days cells were washed once with PBS and medium renewed. On day 7 cells were washed once with PBS, detached with 5xTrypsin (Sigma) and collected

with BMDM medium. Cells were centrifuged at RT, 1500rpm for 5 min and pellet re-suspended. 10 µl of cell suspension was stained with Trypan Blue solution (Sigma) for dead/alive differentiation and counted in “Neubauer”-counting chamber and seeded as indicated.

2.2.16. Efferocytosis assay

200.000 macrophages/well were seeded in a 12-well dish and 50.000 FLS/well from wt or GR^{dim} mice were added. To obtain apoptotic thymocytes, thymus of two wild type mice were isolated, mashed trough a cell strainer (100µm) for single cell suspension and cells were counted. $5x10^6$cells/ml were cultured in RPMI medium substituted with 10% FCS, 1% Penicillin and Streptomycin (Sigma), 2mM L-Glutamate and 20mM HEPES buffer (Sigma). Thymocytes were exposed to 1 µM dexamethasone (Sigma) over-night and apoptosis efficiency validated by Annexin V/PI Staining (eBioscience) followed by flow cytometry. Apoptotic thymocytes were washed through a FCS cushion to eliminate dexamethasone and washed several times with PBS. CFSE (Invitrogen) was added in a 1 to 2500 dilution and cells incubated for 20 min at 37°C. 800.000 apoptotic thymocytes per well were added to co-cultures and kept for 2.5 h. Cells were washed twice with cold PBS, trypsinized and scraped and stained for F4/80 (staining protocol see 2.2.5) and analyzed by flow cytometry (2.2.5).

2.2.17. RNA-Sequencing

For RNA Seq analysis, we cultured FLS isolated from 3 wt and 3 GR^{dim} mice and treated them for 72h with interleukin-1β (5ng/ml) alone or in combination with dexamethasone (1µM). Total RNA was isolated and used for RNA-Sequencing analysis. cDNA library construction and sequencing were performed by Beijing Genomics Institute using BGISEQ-500 platform. Bioinformatics Workflow including data filtering, mapping transcript prediction, differential gene expression analysis and GO and Pathway analysis were performed by procedures established at BGI. Details can be provided upon request. Over all we got an average of 45,19 Mb clean reads, with an average genome mapping rate of 93,44%. The total gene

number identified was 19773 genes and we found an average of 26893 total transcripts per sample.

2.2.18. Statistical analysis

Results are presented as mean ± SEM and statistical analysis was performed with two-way ANOVA, followed by Tukey's post hoc multiple comparison test for qRT-PCR, flow cytometry, area under the curve and supernatant cytokine measurements, with a two-tailed Student's *t*-test (cytokine analysis and efferocytosis measurements).

3. RESULTS

3.1. GR dimerization, but not in immune cells, is a general necessity for GC-mediated suppression of arthritis

3.1.1. Mice with a complete impaired GR dimerization are refractory to DEX treatment in STIA

Previous work in the laboratory demonstrated the role of GR dimerization for anti-inflammatory effects in AIA and G6IP-induced arthritis (Baschant et al., 2011). To determine the role of GR dimerization as a universal model for anti-inflammatory actions of the GR in arthritis, we induced STIA in wt and GR^{dim} mice and treated them with either 1mg/kg dexamethasone (DEX) per day for 10 consecutive days, or with PBS as a control.

To resemble the clinical situation, in which patients first develop the disease and subsequently receive GC treatment, we only started DEX-treatment after the onset of disease (on day 4). By measuring the ankle thickness by calipers (Figure 3.1A) and by assessing the clinical score (Figure 3.1B), we could show that GR^{dim} mice are refractory to DEX treatment (Figure 3.1), thereby verifying a first analysis performed by a former institute member, Dr. Ulrike Baschant (FLI Jena, Technische Universität Dresden). The area-under-the-curve (AUC) was also determined for both, the ankle thickness (Figure 3.1C) and the clinical score (Figure 3.1D) and was significant reduced after DEX treatment in wt (PBS 10,41±0,92 versus DEX 4,78±1,77) but not GR^{dim} mice (PBS 10,21±1,04 versus DEX 10,19±1,28) for the ankle thickness (Figure 3.1C). The AUC of the clinical score showed the same tendency for a reduced AUC after DEX treatment only in wt (PBS 68,75±12,29 versus DEX 37,35±4,42) but not GR^{dim} mice (PBS 78,34±8,24 versus DEX 65,13±5,63) compared to PBS treated littermates (Figure 3.1D).

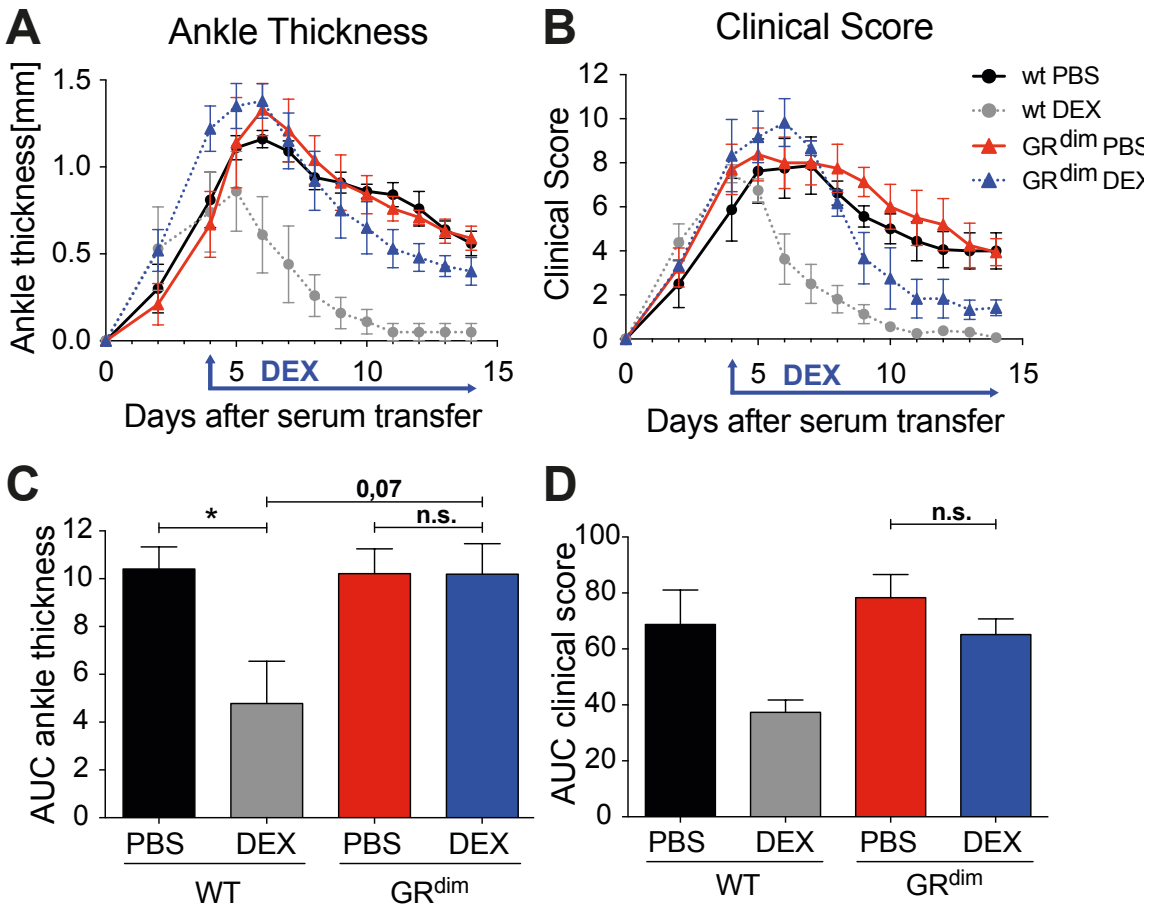

Figure 3.1 GR dimerization is crucial for proper anti-inflammatory actions in STIA

(A) Ankle thickness and (B) clinical score of wt mice and mice with an impaired GR dimerization (GR^{dim}) treated with PBS (black and red) or dexamethasone (DEX) (grey and blue). The area under the curve (AUC) was calculated for the ankle thickness (C) and the clinical score (D). n=3-5 mice. Asterisks indicate significant changes (*p≤0,05, n.s.=not significant) by two-way ANOVA with Tukey's multiple comparison correction.

Histological analysis on sagittal sections of the left hind paw (3D scheme Figure 3.2A) revealed a strong infiltration of cells into the joints of PBS treated wt and GR^{dim} mice (Figure 3.2B, asterisks indicate area of cell infiltration). In wt mice, DEX treatment results in a clear reduction of infiltrating cells in the joint (Figure 3.2B). Contrary to that DEX-treated GR^{dim} mice exhibit a sustained infiltration of cells into the joint cavity (Figure 3.2B).

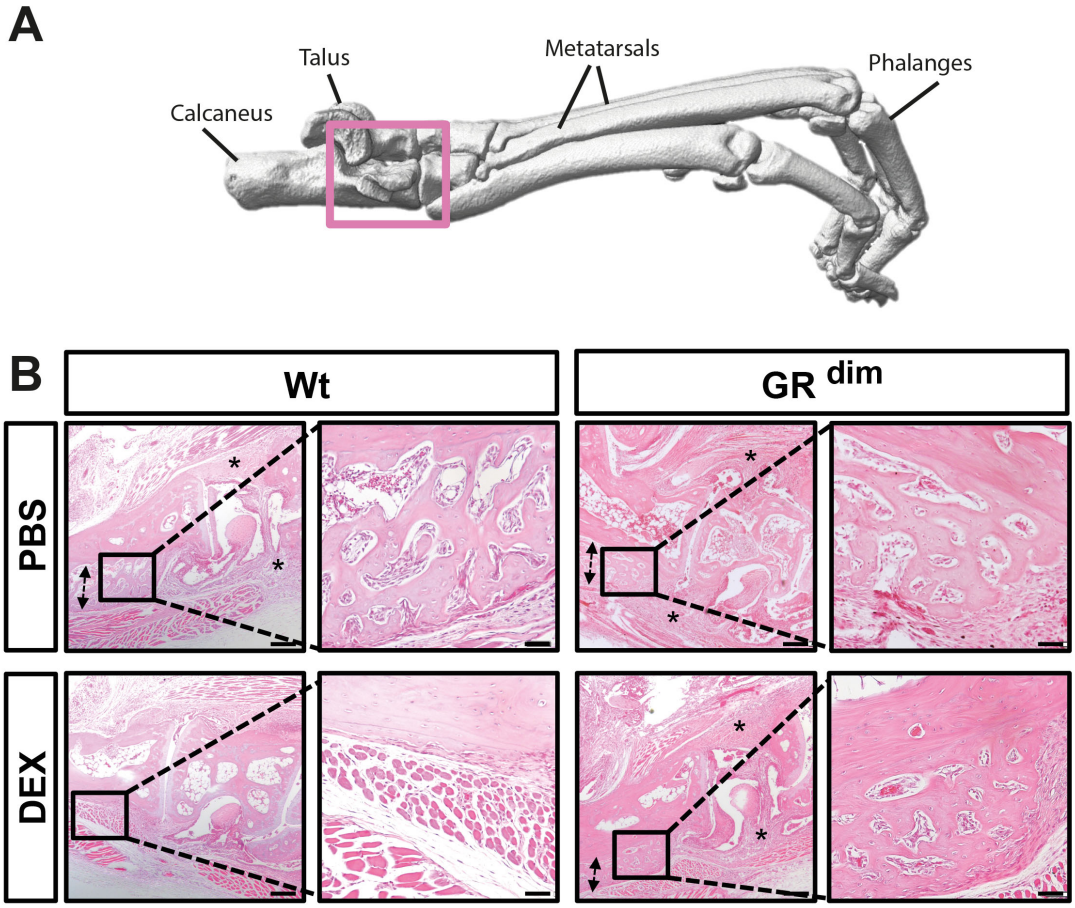

Figure 3.2 GR dimerization is crucial for DEX-mediated clearance of arthritis and suppression of osteophyte development

(A) 3D model of a mouse ankle joint (by µCT). Pink square indicates the area of (B) Hematoxylin and eosin (H&E) staining on ankle sections of wt and GR^{dim} mice treated with PBS or dexamethasone (DEX). Original magnification: 5x (bar = 200µm). Cutout original magnification: 20x (bar = 50µm). Asterisks show area of cell accumulation in the joint cavity. Double-headed arrows indicate the thickness of osteophytes. (B was published in Koenen et al., 2018 under a CC BY-NC 4.0 license, https://creativecommons.org/licenses/by-nc/4.0/deed.de).

In addition to the massive cell infiltration, we could also detect strong osteophyte development at the calcaneus (Figure 3.2A for orientation) in PBS treated wt and GR^{dim} mice. Osteophytes are periosteal bone spurs, which develop through abnormal bone formation induced e.g. by inflammatory joint diseases like arthritis (Finzel et al., 2013). DEX treatment clearly reduced the osteophyte size in wt mice; however, in GR^{dim} mice we could not observe any change in the size of osteophytes (Figure 3.2B). To analyze whether these bone spurs develop also at other sites of the paw we generated micro computed tomography (µCT) 3D

models of the complete hind paw (Figure 3.3). This 3D analysis revealed that most osteophytes developed on the calcaneus and only rarely at the inner metatarsal (Figure 3.3). No osteophyte development was detected at the phalanges (Figure 3.3).

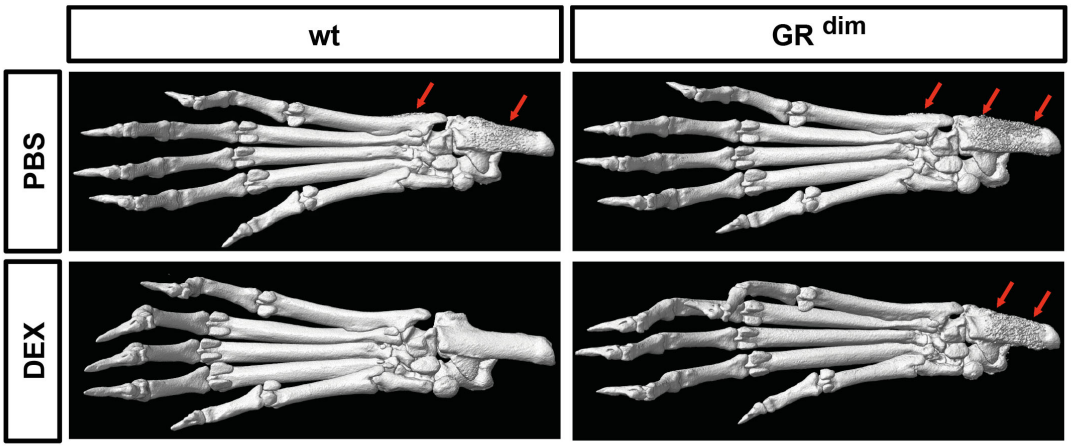

Figure 3.3 Osteophyte development is reduced in wt but not GR^{dim} mice after GC treatment
Inferior view of µCT 3D reconstructed complete ankles of wt and GR^{dim} mice, treated with dexamethasone (DEX) or PBS. Red arrows indicate site of osteophyte formation on the calcaneus and the inner metatarsal.

Due to this observation we defined the area of the osteophyte as region-of-interest in the CT_{AN} program and calculated the percentage of osteophyte area of the total calcaneus area (Figure 3.4A and B). These analyses confirmed the reduction of osteophytes in DEX-treated wt (PBS 0,095%±0,018 versus DEX 0,008%±0,004) but not in GR^{dim} mice (PBS 0,077%±0,021 versus DEX 0,096%±0,026) (Figure 3.3B, 3.4A-B).

Thus, GR dimerization is crucial for the reduction of ankle swelling, the proper clearance of infiltrating immune cells from joints and the inhibition of osteophytes by DEX treatment in STIA. In accordance to our previous work, we can conclude, that GR dimerization is a general necessity for DEX-mediated suppression of several mouse models of arthritis (AIA, G6PI and STIA).

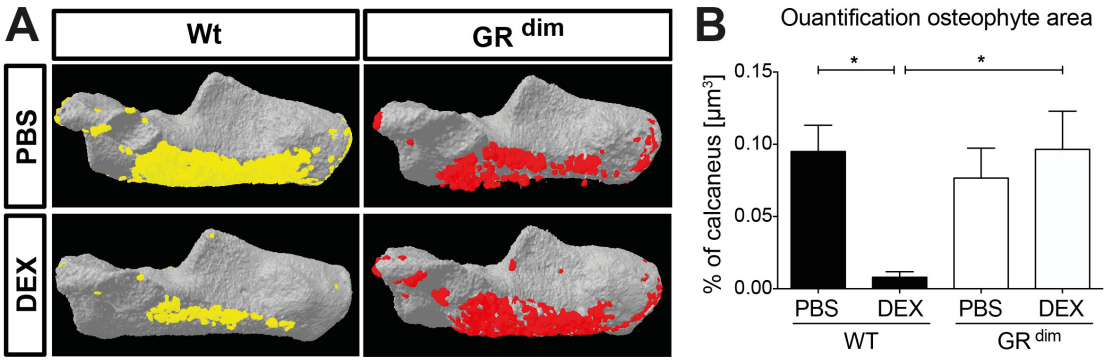

Figure 3.4 Quantification of osteophyte area in calcaneus of wt and GR^{dim} ankles in STIA after GC treatment

(A) Representative 3D model of the calcaneus with artificially colored osteophyte are in wt (yellow) and GR^{dim} (red) mice treated with dexamethasone (DEX) or PBS. (B) Quantification of the percentage of the area of osteophyte of the total calcaneus in µm^3. n=3-5 mice. Asterisks indicate significant changes (p≤0,05) by two-way ANOVA with Tukey's multiple comparison correction.

3.1.2. Non-immune cells mediate the GR dimer-dependent anti-inflammatory effects of DEX in STIA

To determine the role of GR dimerization in immune (mostly radio-sensitive) versus non-immune (radio-resistant) cells in mediating the anti-inflammatory actions of GCs, we generated chimeric mice with a GC competent immune system but an impaired GR dimerization in all peripheral, radio-resistant tissue. For this purpose, we irradiated wt and GR^{dim} mice to destroy all radiosensitive immune cells and reconstituted them with wt bone marrow cells (wt→wt and wt→GR^{dim}). PBS treated wt→wt and wt→GR^{dim} mice showed no differences in the development of STIA, and DEX treatment strongly reduced the joint swelling in wt→wt mice, however, unexpectedly DEX treated wt→GR^{dim} mice showed no reduction in ankle swelling (Figure 3.5A) and clinical score (Figure 3.5B). This result is strongly supported by the AUC of the ankle thickness (Figure 3.5C) and the clinical score (Figure 3.5D) that are significantly reduced in DEX treated wt→wt mice (wt→wt DEX AUC thickness 4,95±0,45 and AUC score 52,25±3,00) compared to DEX-treated wt→GR^{dim} mice (wt→GR^{dim} DEX AUC thickness 9,22±1,63 and AUC score 75,80±15,99) and PBS controls (wt→wt PBS AUC thickness 11,85±0,6 and AUC score 95,50±1,48 versus wt→GR^{dim} PBS AUC thickness 10,78±0,55 and AUC score 91,60±5,12).

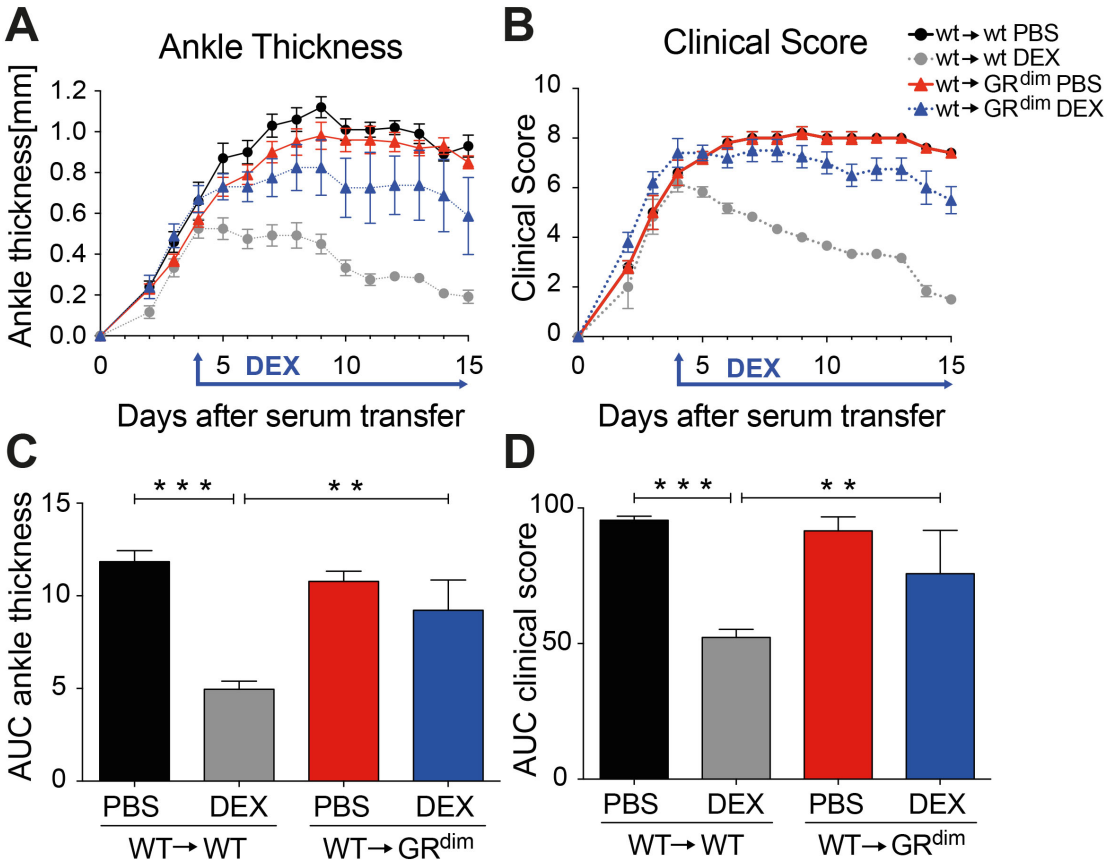

Figure 3.5 GR dimerization in radio resistant cells is crucial for DEX-mediated suppression of STIA.

(A) Ankle thickness and (B) clinical score of irradiated wt recipient mice reconstituted with wt bone marrow cells (wt→wt) and irradiated GR^{dim} recipient mice reconstituted with wt bone marrow cells (wt→GR^{dim}) treated with PBS (black and red) or dexamethasone (DEX) (grey and blue) . The area under the curve (AUC) was calculated for the ankle thickness (C) and the clinical score (D). n=4-6 mice. Asterisks indicate significant changes (*p≤0,05, **p≤0,01 and n.s.=not significant) by two-way ANOVA with Tukey's multiple comparison correction. (Dr. U. Baschant, FLI Jena performed the transplantation and assessment of ankle swelling). (A, B and D were published in Koenen et al., 2018 under a CC BY-NC 4.0 license, https://creativecommons.org/licenses/by-nc/4.0/deed.de).

This finding is striking, since radiosensitive immune cells of wt→GR^{dim} mice are still expressing the complete functional GR, capable of reacting to DEX treatment, directly. To further exclude potentially involved radio resistant immune cells we and collaborators analyzed mice with GR-deficient mast cells (GR^{flox};Mcpt5-Cre, performed by Prof. Dr. A Dudeck (Otto-von-Guericke Universität, Magdeburg)), T-cells (GR^{flox};Lck-Cre) and macrophages (GR^{flox};LysM-Cre) (performed by former member of our Institute Dr. U. Baschant). Our results showed that these cells do not mediate the anti-inflammatory effects of GCs in STIA (data not shown).

Consequently, the direct action of GCs on immune cells is not sufficient for the suppression of STIA. On histological sections we could confirm the ongoing inflammation in DEX-treated wt→GR^{dim} mice by the amount of infiltrating immune cells in the joint (Figure 3.6 indicated by asterisks). In DEX-treated wt→wt mice we see a clear reduction of infiltrating cells in the joint cavity (Figure 3.6). Interestingly, we saw a clear reduction in the size of osteophytes in DEX treated wt→wt and wt→GR^{dim} mice (Figure 3.6), demonstrating the necessity of a potent GR in immune cells for the reduction of osteophytes independent of the ongoing inflammation.

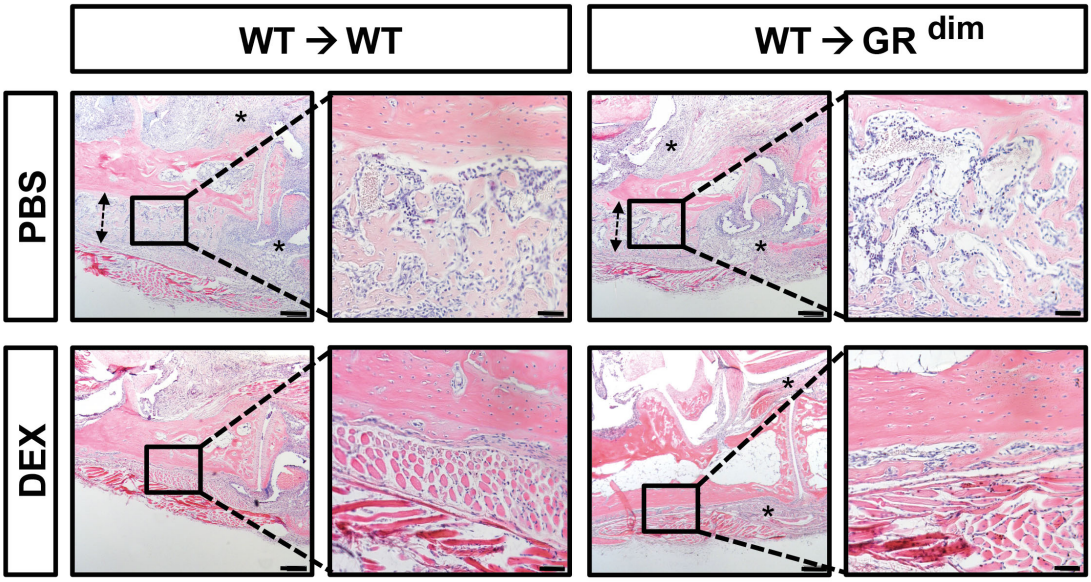

Figure 3.6 GR dimerization in non-immune cells is crucial for DEX-mediated clearance of infiltrating cells but not for reduction of osteophytes

Hematoxylin and Eosin (H&E) staining on ankle sections of irradiated wt mice recipient reconstituted with wt bone marrow cells (wt→wt) and irradiated GR^{dim} recipient mice reconstituted with wt bone marrow cells (wt→GR^{dim}), treated with PBS or dexamethasone (DEX). Original magnification: 5x (bar=200µm). Cutout original magnification: 20x (bar=50µm). Asterisks indicate area of cell accumulation in the joint cavity. Double-headed arrows indicate the thickness of the osteophyte.

To verify the observed osteophyte reduction on histological sections of DEX-treated wt→GR^{dim} mice, we generated µCT 3D models of the calcaneus (Figure 3.7A). Both, the 3D model and the quantification of osteophyte area by µCT revealed a clear reduction of osteophytes not only in DEX-treated wt→wt

(0,01±0,003) but also in DEX-treated wt→GR^{dim} mice (0,017±0,008) (Figure 3.7A-B).

Accordingly, we can conclude that direct actions of GCs on immune cells are insufficient to suppress STIA, however, they are sufficient to reduce osteophytes in the inflamed ankle. Taken together, non-immune cells play a major role in mediating the anti-inflammatory effects of GCs.

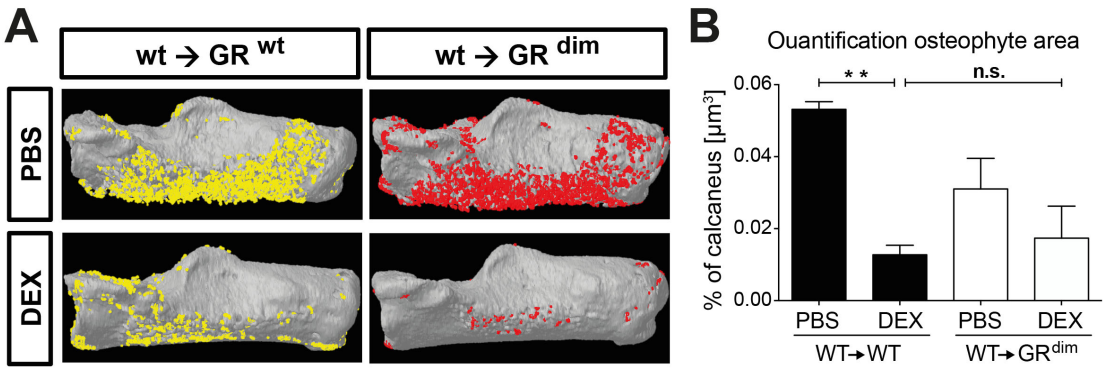

Figure 3.7 Quantification of osteophyte area in calcaneus of wt→wt and wt→GR^{dim} ankles in STIA after DEX treatment

(A) Representative 3D models of the calcaneus with artificially colored osteophyte area of irradiated wt mice reconstituted with wt bone marrow (wt→wt, yellow) and irradiated GR^{dim} mice reconstituted with wt bone marrow (wt→GR^{dim}, red), treated with PBS or dexamethasone (DEX). (B) Quantification of the osteophyte area on the calcaneus in µm3. n=4-6. Asterisks indicate significant changes (*p≤0,05) by two-way ANOVA with Tukey's multiple comparison correction.

3.1.3. GC-mediated cytokine suppression is insufficient to suppress progression of STIA

Since wt→GR^{dim} mice are refractory to GC treatment and show a sustained cell infiltration on histological sections we measured pro-inflammatory cytokine levels in serum of wt→wt and wt→GR^{dim} mice treated with PBS or DEX. Cytokines are major pro-inflammatory mediators, directing cell infiltration and migration and thought to be rapidly suppressed by DEX in wt mice. Due to this fast interaction, we analyzed cytokine levels after 24h and 72h of DEX treatment (day 5 and day 7 of STIA course). After 24h treatment we did not see any differences in the swelling of the ankles nor the clinical score of wt→wt or wt→GR^{dim} mice treated with either

PBS or DEX (Figure 3.8A). Correspondingly we did not observe any significant changes in cytokine levels of wt→wt or wt→GR^{dim} mice after 24h of DEX treatment (Figure 3.8B-D). Interestingly, we saw already a tendency for reduced levels of TNFα and IFNγ in the DEX-treated wt→GR^{dim} mice (Figure 3.8C, D), suggesting a potent suppression independent of GR dimerization in non-immune cells.

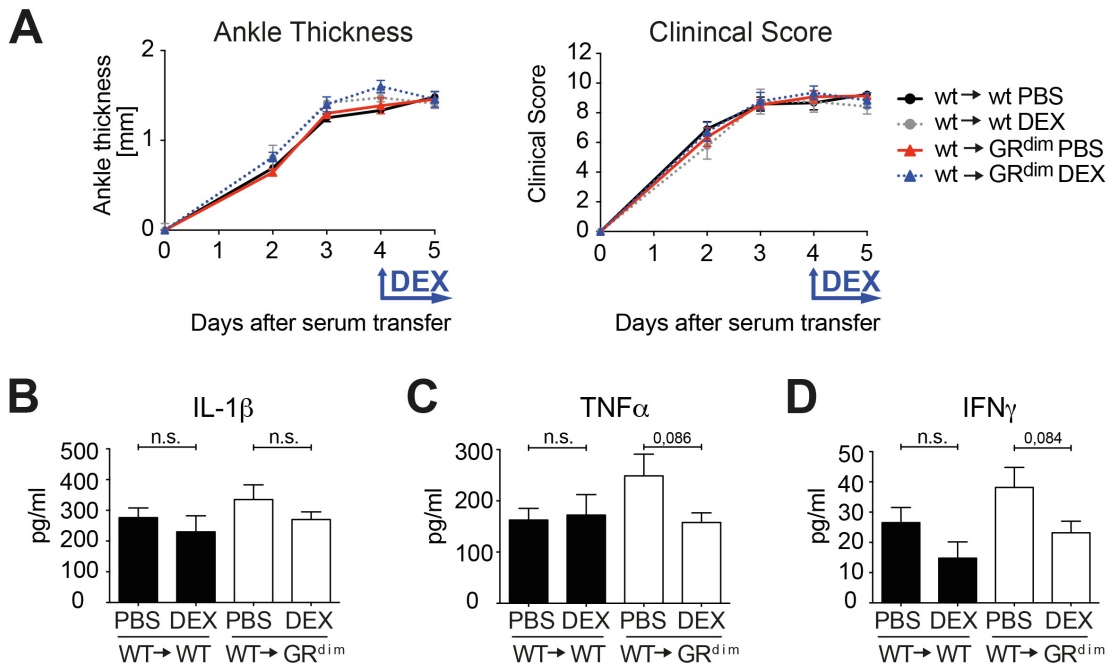

Figure 3.8 Serum cytokines are not changed after 24h of DEX treatment

(A) Ankle thickness and clinical score of irradiated wt recipient mice reconstituted with wt bone marrow cells (wt→wt) and irradiated GR^{dim} recipient mice reconstituted with wt bone marrow cells (wt→GR^{dim}), treated for 24h with PBS (black and red) or dexamethasone (DEX) (grey and blue). Serum cytokine multiplex analysis of pro-inflammatory (B) Il-1β, (C) TNFα and (D) IFNγ of wt→wt and wt→GR^{dim} mice treated for 24h with PBS or DEX. n=4-5 mice. Asterisks indicate significant changes (*p≤0,05) by student's t-test.

After 72h of DEX treatment we did not detect changes in the clinical score of wt→wt and wt→GR^{dim} mice yet, however, ankle thickness was significantly reduced in wt→wt mice (Figure 3.9A). Intriguingly, despite the ongoing swelling in DEX treated wt→GR^{dim} mice there was a clear reduction in pro-inflammatory cytokine levels in the serum of both, wt→wt and wt→GR^{dim} mice after DEX treatment (Figure 3.9B-D).

In intact, non-chimeric GR^{dim} mice we see the same reduction of IL-1β after DEX treatment as in wt mice, pointing towards an important role of the GR monomer in immune cells to regulate this cytokine (Figure 3.10A). TNFα and IFNγ, however, are not reduced after DEX treatment of GR^{dim} mice, indicating a pivotal role of a functional GR dimerization in immune cells for the suppression of some cytokines (Figure 3.10B, C).

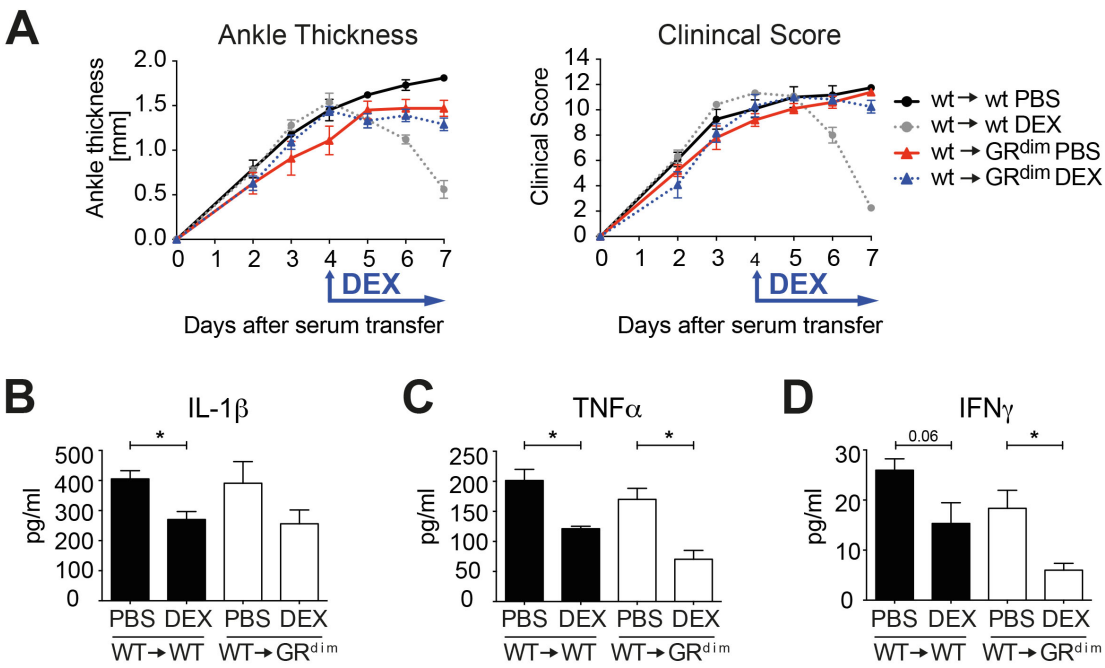

Figure 3.9 Cytokine suppression is independent of GR dimerization in non-immune cells (A) Ankle thickness and clinical score of irradiated wt recipient mice reconstituted with wt bone marrow cells (wt→wt) and irradiated GR^{dim} recipient mice reconstituted with wt bone marrow cells (wt→GR^{dim}), treated for 72h with PBS (black and red) or dexamethasone (DEX) (grey and blue). Serum cytokine multiplex analysis of pro-inflammatory (B) Il-1β, (C) TNFα and (D) IFNγ of wt→wt and wt→GR^{dim} mice treated for 72h with PBS or DEX. n=5-6 mice. Asterisks indicate significant changes (*p≤0,05) by student's t-test. (Koenen et al., 2018 published under a CC BY-NC 4.0 license, https://creativecommons.org/licenses/by-nc/4.0/deed.de).

Thus, impaired GR dimerization in non-immune cells has no effect on direct suppression of cytokine production; however, this is insufficient to prohibit the progression of STIA.

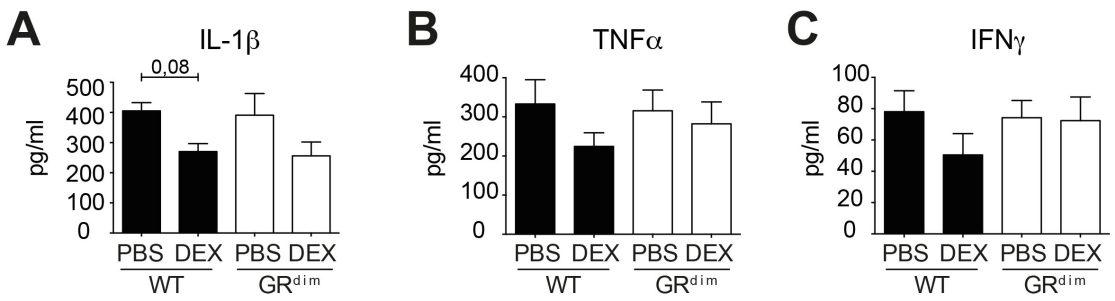

Figure 3.10 Cytokine suppression is independent of GR dimerization in non-immune cells Serum cytokine multiplex analysis of pro-inflammatory (A) Il-1β, (B) TNFα and (C) IFNγ of wt and GR^{dim} mice treated for 72h with PBS or dexamethasone (DEX). n=5. Asterisks indicate significant changes (*p≤0,05) by student's t-test.

3.1.4. Induction of anti-inflammatory macrophages by GCs depend on GR dimerization in non-immune cells

Since impairment of cytokine suppression was not the cause for the sustained cell infiltration and ongoing swelling of the DEX-treated ankles in wt→ GR^{dim} mice, we further analyzed the cell composition in wt→wt and wt→GR^{dim} ankles treated with PBS or DEX. Therefore, we chose the 72h time point where we already detected significant effects on cytokine suppression but no changes in the clinical score or only slight changes in ankle swelling respectively. Flow cytometry analysis of digested ankles revealed, as expected, a strong and significant reduction of about 70% in both hematopoietic ($CD45^+$) (Figure 3.11A) and myeloid ($CD11b^+$) cells (Figure 3.11B) after DEX treatment of wt→wt mice compared to PBS controls. PBS treated wt→GR^{dim} digests showed already about 40% fewer hematopoietic and myeloid cell infiltrate than PBS treated wt→wt cell extracts, however, there was no change between PBS-treated wt→GR^{dim} and DEX-treated wt→GR^{dim} cell extracts (Figure 3.11A-B). Despite this basal difference between PBS treated wt→wt and wt→GR^{dim} infiltrates, DEX treated wt→wt mice still displayed 50% lower numbers of hematopoietic and myeloid cells than DEX treated wt→GR^{dim} mice (Figure 3.11 A-B).

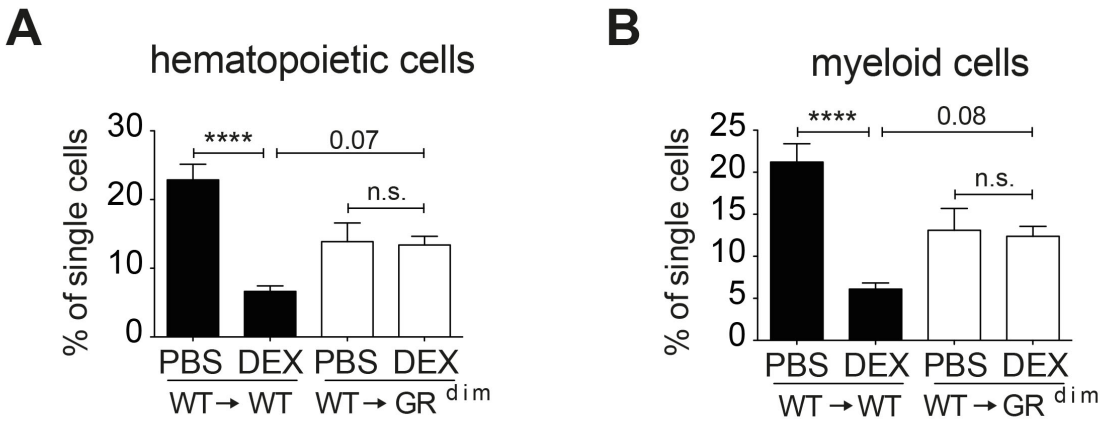

Figure 3.11: Hematopoietic and myeloid cells are repressed by DEX in a GR dimer-dependent manner

(A) Percentage of hematopoietic cells ($CD45^+$) of single cells in ankle digests of irradiated wt mice reconstituted with wt bone marrow (wt→wt) and irradiated GR^{dim} mice reconstituted with wt bone marrow (wt→GR^{dim}), treated for 72h with PBS or dexamethasone (DEX). (B) Percentage of myeloid cells ($CD45^+$, $CD11b^+$) of single cells in ankle digests of wt→wt and wt→GR^{dim} mice treated for 72h with PBS or DEX. n=5-6. Two-way ANOVA was performed for statistical analysis with Tukey's multiple comparison correction (*p≤0,05, **p≤0,01, ***p≤0,001, ****p≤0,0001 and n.s.=not significant). (Published in Koenen et al., 2018 under a CC BY-NC 4.0 license, https://creativecommons.org/licenses/by-nc/4.0/deed.de).

Further on we analyzed the percentage of neutrophils, the first inflammatory responders that play a major role in STIA development and progression, but did not observe any significant changes in the percentage of $Ly6G^{pos}$ cells after 72h of DEX treatment in wt→wt or wt→GR^{dim} mice (Figure 3.12A). Although, the STIA model mostly is considered as a T-cell independent arthritis model, we also analyzed the effect of DEX on these cells, since these cells were the direct target of DEX in the AIA and the G6PI arthritis model. Nevertheless, we could not detect any changes in the percentage of T-cells ($CD3^{pos}$) under any condition (Figure 3.12B).

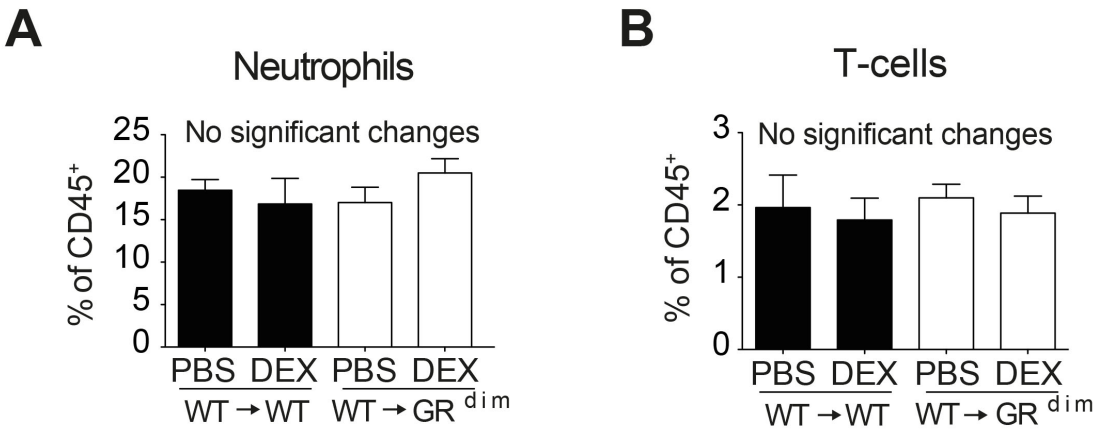

Figure 3.12: DEX treatment does not influence the percentage of neutrophils or T-cells after 72h independent of genotype

(A) Percentage of neutrophils ($CD11b^+$, $Ly6G^+$, FSC/SSC^{high}) of $CD45^+$ cells in ankle digests of irradiated wt mice reconstituted with wt bone marrow (wt→wt) and irradiated GR^{dim} mice reconstituted with wt bone marrow (wt→GR^{dim}), treated for 72h with PBS or dexamethasone (DEX). (B) Percentage of T-cells ($CD11b^-$, $CD3^+$) of single cells in ankle digests of wt→wt and wt→GR^{dim} mice treated for 72h with PBS or DEX. n=5-6. Two-way ANOVA was performed for statistical analysis with Tukey's multiple comparison correction (*p≤0,05). (Published in Koenen et al., 2018 under a CC BY-NC 4.0 license, https://creativecommons.org/licenses/by-nc/4.0/deed.de).

Macrophages are considered the second most important cell type in STIA development and are direct responders to infiltrating neutrophils. To differentiate between infiltrating inflammatory monocytes and macrophages and anti-inflammatory macrophages, we analyzed the respective surface markers in combination. First, we differentiated between activated and non-activated macrophages based on the percentage of $F4/80^{pos}$ cells of $CD11b^{pos}$ cells which either express MHCII or not (Figure 3.13). This first analysis displayed neither changes in the percentage of activated macrophages ($F4/80^{pos}$, $MHCII^{pos}$) between DEX- and PBS-treated wt→wt mice, nor to equally treated wt→GR^{dim} mice (Figure 3.13A). Interestingly, we detected a 1,8-fold increased percentage of non-activated macrophages ($F4/80^{pos}$, $MHCII^{neg}$) after DEX treatment in the wt→wt but not wt→GR^{dim} mice (Figure 3.13B), strongly shifting the ratio of non-activated macrophages to activated macrophages within the ankle joint (Figure 3.13C). Of note non-activated macrophages are considered as anti-inflammatory macrophages.

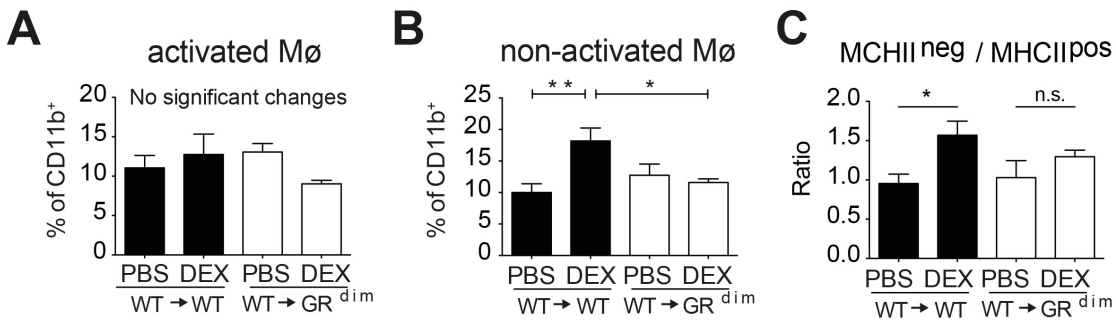

Figure 3.13 Percentage of non-activated macrophages is increased after 72h of DEX treatment in a GR dimer-dependent mechanism

(A) percentage of activated macrophages (Ly6G$^-$, F4/80$^+$, MHCII$^+$) of CD11b$^+$ cells in ankle digests of irradiated wt mice reconstituted with wt bone marrow (wt→wt) and irradiated GR^{dim} mice reconstituted with wt bone marrow (wt→GR^{dim}), treated for 72h with PBS or dexamethasone (DEX). (B) Percentage of non-activated macrophages (Ly6G$^-$, F4/80$^+$, MHCII$^-$) of CD11b$^+$ cells in ankle digests of wt→wt and wt→GR^{dim} mice treated for 72h with PBS or DEX. (C) Ratio of non-activated Mø to activated Mø of wt→wt and wt→GR^{dim} mice treated 72h with PBS or DEX. n=5-6. Two-way ANOVA was performed for statistical analysis with Tukey's multiple comparison correction (*p≤0,05, **p≤0,01 and n.s.=not significant). Mø=macrophages. (Published in Koenen et al., 2018 under a CC BY-NC 4.0 license, https://creativecommons.org/licenses/by-nc/4.0/deed.de).

To substantiate this finding, we analyzed the percentage of infiltrating monocytes (F4/80^{neg}, Ly6C^{pos}) and classical macrophages (F4/80^{pos}, Ly6C^{pos}) considered as pro-inflammatory cells and anti-inflammatory non-classical macrophages (F4/80^{pos}, Ly6C^{neg}) (Figure 3.14). We observed a similar reduction of infiltrating monocytes (F4/80^{neg}, Ly6C^{pos}) in DEX-treated wt→wt (1,27-fold) and wt→GR^{dim} mice (1,35-fold) (Figure 3.14A) but no changes for classical macrophages (F4/80^{pos}, Ly6C^{pos}) (Figure 3.14B). Hence, these data provided no explanation for the observed resistance of DEX-treated wt→GR^{dim} mice. Strikingly, however, we observed a significant 1,7-fold increase of non-classical macrophages (F4/80^{pos}, Ly6C^{neg}) in DEX-treated wt→wt mice but not in DEX-treated wt→GR^{dim} mice, which is in line with the increase of non-activated macrophages (F4/80^{pos}, MHCII^{neg}, Figure 3.13B).

In more detail, in PBS-treated wt→wt mice as well as PBS- or DEX-treated wt→GR^{dim} mice, we detected more infiltrating cells then non-classical macrophages (with a ratio of 0,56 in PBS treated wt→wt and 0,5 and 0,57 for DEX- and PBS treated wt→GR^{dim} mice). However, this ratio completely shifts to

higher levels of non-classical macrophages (with a ratio of 1,13) in DEX-treated wt→wt mice (Figure 3.14D, E).

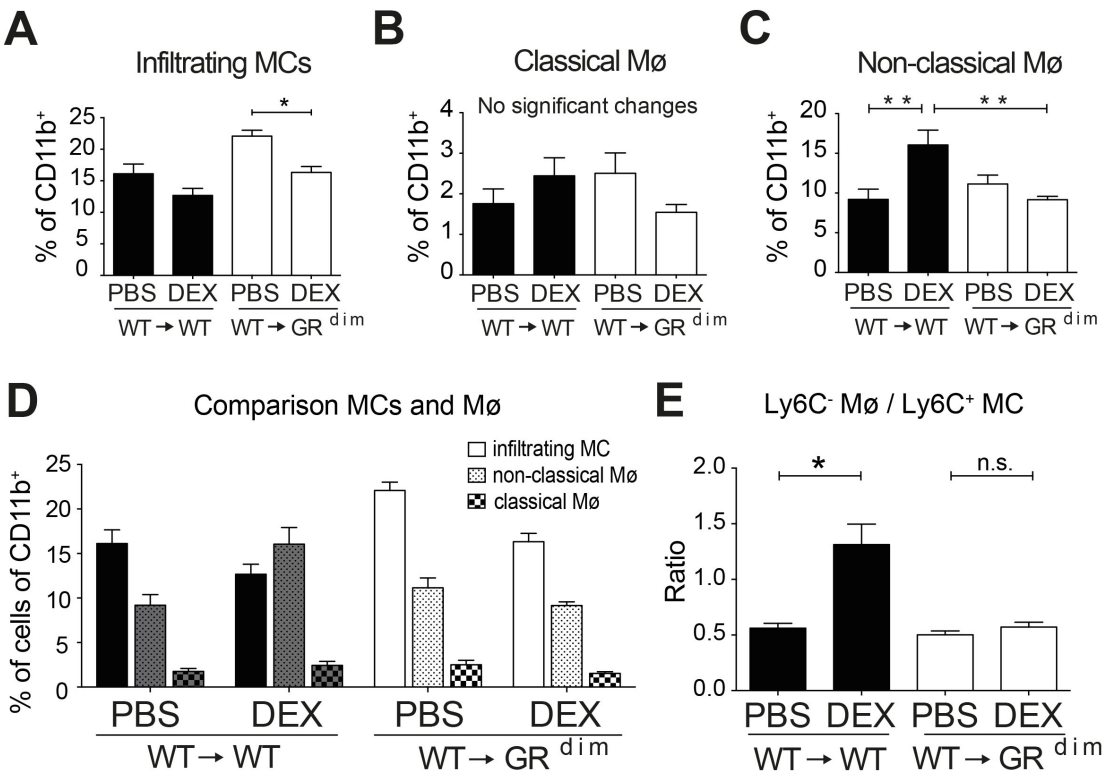

Figure 3.14: GR dimer-dependent increase of non-classical Ly6C^{neg} Mø after 72h of DEX treatment

(A) Percentage of infiltrating monocytes (Ly6G$^-$, F4/80$^-$, Ly6C$^+$) of CD11b$^+$-cells in ankle digests of irradiated wt mice reconstituted with wt bone marrow cells (wt→wt) and irradiated GR^{dim} mice reconstituted with wt bone marrow (wt→GR^{dim}) treated for 72h with PBS or dexamethasone (DEX). (B) Percentage of classical macrophages (Ly6G$^-$, F4/80$^+$, Ly6C$^+$) of CD11b$^+$-cells in ankle digests of wt→wt and wt→GR^{dim} mice treated for 72h with PBS or DEX. (C) Percentage of non-classical macrophages (Ly6G$^-$, F4/80$^+$, Ly6C$^-$) of CD11b$^+$-cells in ankle digests of wt→wt and wt→GR^{dim} mice treated for 72h with PBS or DEX. (D) Direct comparison of percentage of (A, filled), (B, dotted) and (C, squares). Ratio of non-classical Mø to infiltrating monocytes (MC) in ankle digests of wt→wt and wt→GR^{dim} mice treated for 72h with PBS or DEX. n=5-6. Two-way ANOVA was performed for statistical analysis with Tukey's multiple comparison correction (*p≤0,05, **p≤0,01 and n.s.=not significant). Mø=macrophages, (B and C were published in Koenen et al., 2018 under a CC BY-NC 4.0 license, https://creativecommons.org/licenses/by-nc/4.0/deed.de).

3.1.5. Anti-inflammatory macrophage marker genes, associated with phagocytosis activity are increased in a GR dimer-dependent manner

To further validate the characteristics of this non-classical, non-activated macrophage population, we analyzed macrophage specific marker genes, known to be associated with anti-inflammatory macrophages, in the ankles of wt→wt and wt→GR^{dim} mice treated with DEX or PBS. These marker genes include genes involved in phago- and efferocytosis associated with anti-inflammatory properties.

At an early time point of treatment (24h treatment, day 5 of STIA course) we could not detect DEX-induced changes of any of the analyzed maker genes (*CD163*, *CD36*, *AnxA1* and the TAM receptors *MerTK* and *Axl*) (Figure 3.15). Only the TAM receptor Tyro3 showed a trend toward an up regulation in DEX-treated wt→wt mice compared to DEX-treated wt→GR^{dim} mice (Figure 3.15F). Surprisingly, we observed an increased expression of *CD163* and *MerTK* in PBS treated wt→GR^{dim} mice compared to PBS-treated wt→wt mice (1,5-fold in both *CD163* and *MerTK*) (Figure 3.15A, D), but no obvious difference was detected for CD163 between DEX treated wt→wt and wt→GR^{dim} mice (Figure 3.15A). For *MerTK*, we observed significant higher level in DEX-treated wt→GR^{dim} mice compared to DEX-treated wt→wt mice, however, no differences to PBS-treated wt→GR^{dim} mice (Figure 3.15D).

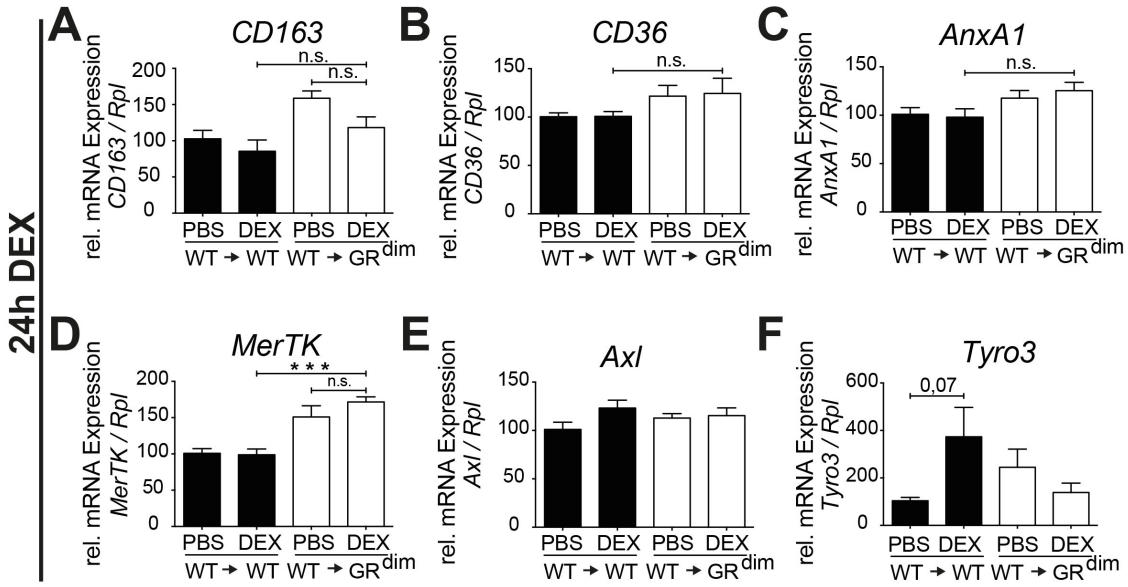

Figure 3.15 No changes in phago- and efferocytosis associated genes after 24h of DEX treatment

QRT-PCR analysis of (A) CD163, (B) CD36, (C) AnnexinA1 (AnxA1) and the TAM receptors (D) MerTK, (E) Axl and (F) Tyro3 in whole ankle mRNA of irradiated wt mice reconstituted with wt bone marrow cells (wt→wt) and irradiated GR^{dim} mice reconstituted with wt bone marrow (wt→GR^{dim}) treated for 24h with PBS or dexamethasone (DEX). n=4-5. Two-way ANOVA was performed for statistical analysis with Tukey's multiple comparison correction (*p≤0,05, **p≤0,01, ***p≤0,001 and n.s.=not significant).

After 72h of DEX treatment, the time point similarly used in the flow cytometry analysis showing an increased percenta of non-classical, non-activated macrophages in DEX-treated wt→wt mice, we found a strong increase in the expression of all analyzed marker genes in DEX-treated wt→wt mice compared to PBS-treated wt→wt mice. *CD163*, *CD36*, *AnxA1* and the TAM receptor genes *Axl*, *MerTK* and *Tyro3* were up regulated between 1,3- and 2-fold in DEX-treated wt→wt mice compared to PBS-treated wt→wt mice. In contrast, however, in wt→GR^{dim} mice expression of *CD163*, *CD36*, *AnxA1* or the TAM receptors remained unchanged in the presence or absence of DEX (Figure 3.16). For *AnxA1* we saw a significant 1,3-fold induction by DEX in wt→wt compared to PBS-treated wt→wt mice, a value insignificant compared to DEX-treated wt→GR^{dim} mice (Figure 3.16C). For *Tyro3* we only detected a trend in wt→wt mice between PBS- and DEX-treated mice (p=0,059) that was not significant compared to DEX-treated wt→GR^{dim} mice (Figure 3.16F).

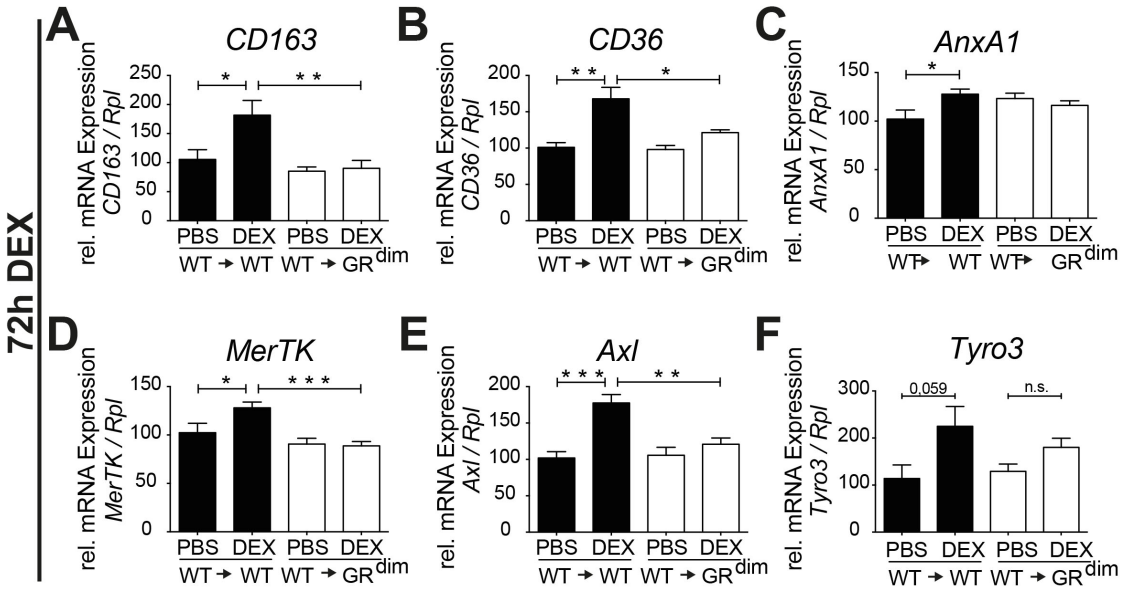

Figure 3.16: GR dimer-dependent up regulation of phago- and efferocytosis associated genes after 72h of DEX treatment

QRT-PCR analysis of (A) CD163, (B) CD36, (C) AnnexinA1 (AnxA1) and the TAM receptors (D) MerTK, (E) Axl and (F) Tyro3 in whole ankle mRNA of irradiated wt mice reconstituted with wt bone marrow cells (wt→wt) and irradiated GR^{dim} mice reconstituted with wt bone marrow (wt→GR^{dim}) treated for 72h with PBS or dexamethasone (DEX). n=5-6. Two-way ANOVA was performed for statistical analysis with Tukey's multiple comparison correction (*p≤0,05, **p≤0,01, ***p≤0,001 and n.s.=not significant). (Published in Koenen et al., 2018 under a CC BY-NC 4.0 license, https://creativecommons.org/licenses/by-nc/4.0/deed.de).

This observed induction is mostly stable throughout the time course of arthritis (14 days of STIA, 10 days DEX/PBS treatment) with an increased expression of *CD163*, *CD36*, *AnxA1* and *Axl* (between 1,6- to 2,8-fold), but not *MerTK* and *Tyro3* after 10 days of DEX treatment in wt→wt mice compared to wt→wt PBS-treated and wt→GR^{dim} DEX- or PBS-treated mice (Figure 3.17A-F).

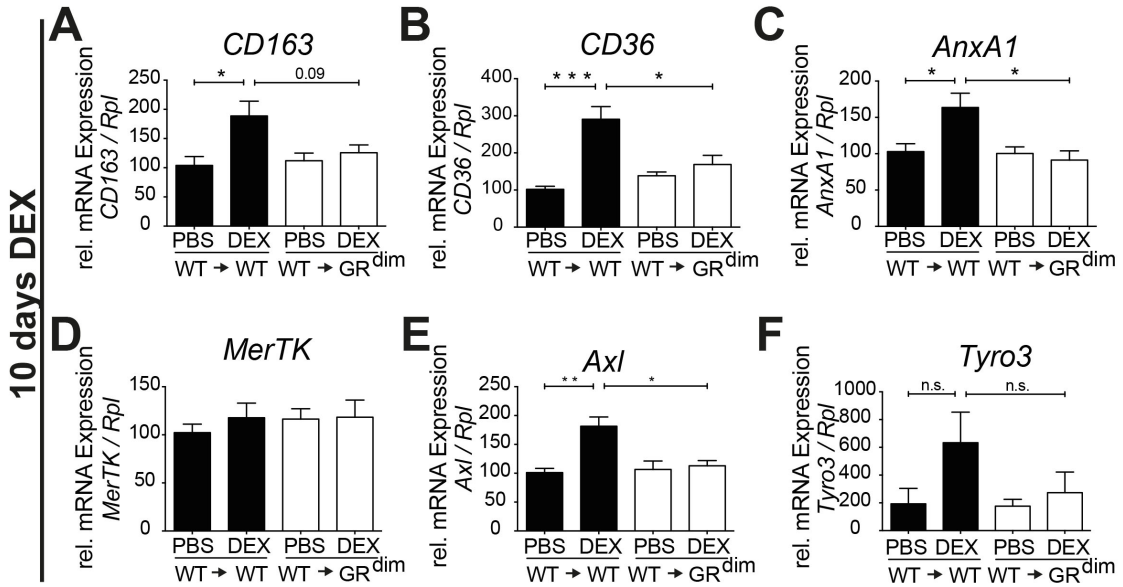

Figure 3.17: GR dimer-dependent induction of phago- and efferocytosis associated genes is stable for 10 days of DEX treatment

QRT-PCR analysis of (A) CD163, (B) CD36, (C) AnnexinA1 (AnxA1) and the TAM receptors (D) MerTK, (E) Axl and (F) Tyro3 in whole ankle mRNA of irradiated wt mice reconstituted with wt bone marrow (wt→wt) and irradiated GR^{dim} mice reconstituted with wt bone marrow (wt→GR^{dim}) treated for 10 days with PBS or dexamethasone (DEX). n=4-6. Two-way ANOVA was performed for statistical analysis with Tukey's multiple comparison correction (*p≤0,05, **p≤0,01, ***p≤0,001 and n.s.=not significant).

Of note, qRT-PCR analysis of not irradiated, complete GR^{dim} mice treated with DEX or PBS showed an equal lack of up regulation of *CD163*, *CD36*, AnxA1, *Axl* and *Tyro3* compared to DEX-treated wt mice (Figure 3.18).

Thus, in STIA, DEX induces anti-inflammatory macrophage marker genes associated with increased phagocytosis capacity, which essentially depends on GR dimerization in stromal cells. The observed changes in macrophage subsets (revealed by flow cytometry and qRT-PCR), however, must be mediated by cross talk of macrophages to stromal cells, since GR in stromal cells, as shown herein, is decisive for STIA suppression.

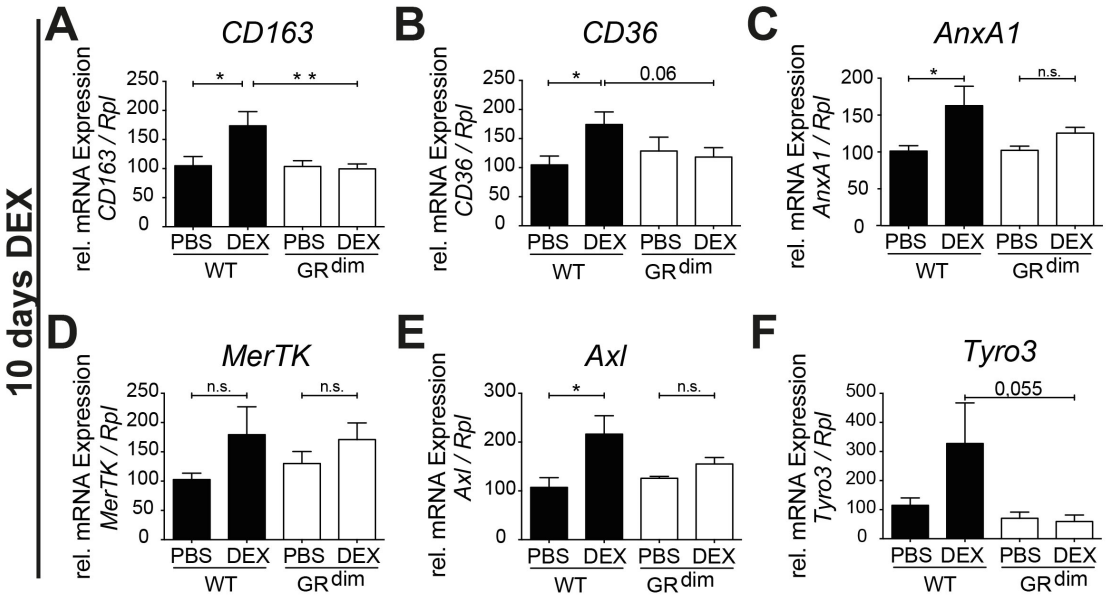

Figure 3.18: DEX-mediated up regulation of phago- and efferocytosis associated genes is independent of GR dimerization in immune cells

QRT-PCR analysis of (A) CD163, (B) CD36, (C) AnnexinA1 (AnxA1) and the TAM receptors (D) MerTK, (E) Axl and (F) Tyro3 in whole ankle mRNA of wt and GR^{dim} mice treated for 10 days with PBS or dexamethasone (DEX). n=5-7. Two-way ANOVA was performed for statistical analysis with Tukey's multiple comparison correction (*p≤0,05, **p≤0,01, ***p≤0,001 and n.s.=not significant), (A, B and E were published in Koenen et al., 2018 under a CC BY-NC 4.0 license, https://creativecommons.org/licenses/by-nc/4.0/deed.de).

3.1.6. Proteomics analysis revealed several potential dimerization-depended, DEX-regulated target proteins

Here, we could show that DEX treatment of STIA results in an increased fraction of specific anti-inflammatory macrophages. However, our transplantation model clearly shows that DEX mediates the suppression of STIA by direct effects on non-immune cells, pointing towards a cross talk of stromal cells and macrophages. To delineate possible factors within this cross talk, we examined (in cooperation with the functional genomic center Zürich (FGCZ) and PD. Dr. U. Auf dem Keller and Dr. T. Kockmann, ETH Zürich) the proteome of ankles of wt→wt and wt→GR^{dim} mice treated with PBS or DEX. We analyzed ankles at early (after 24h of treatment) and late stages of STIA course (after 10days of treatment) and found several proteins up (Figure 3.19A) or down regulated (Figure 3.19B) in DEX treated wt→wt but not in wt→GR^{dim} mice. Only considering significant changes due to genotype- and treatment-interaction, we found 190 proteins significantly

different between wt→wt and wt→GR^{dim} mice treated with PBS or DEX for 24h and 10 days.

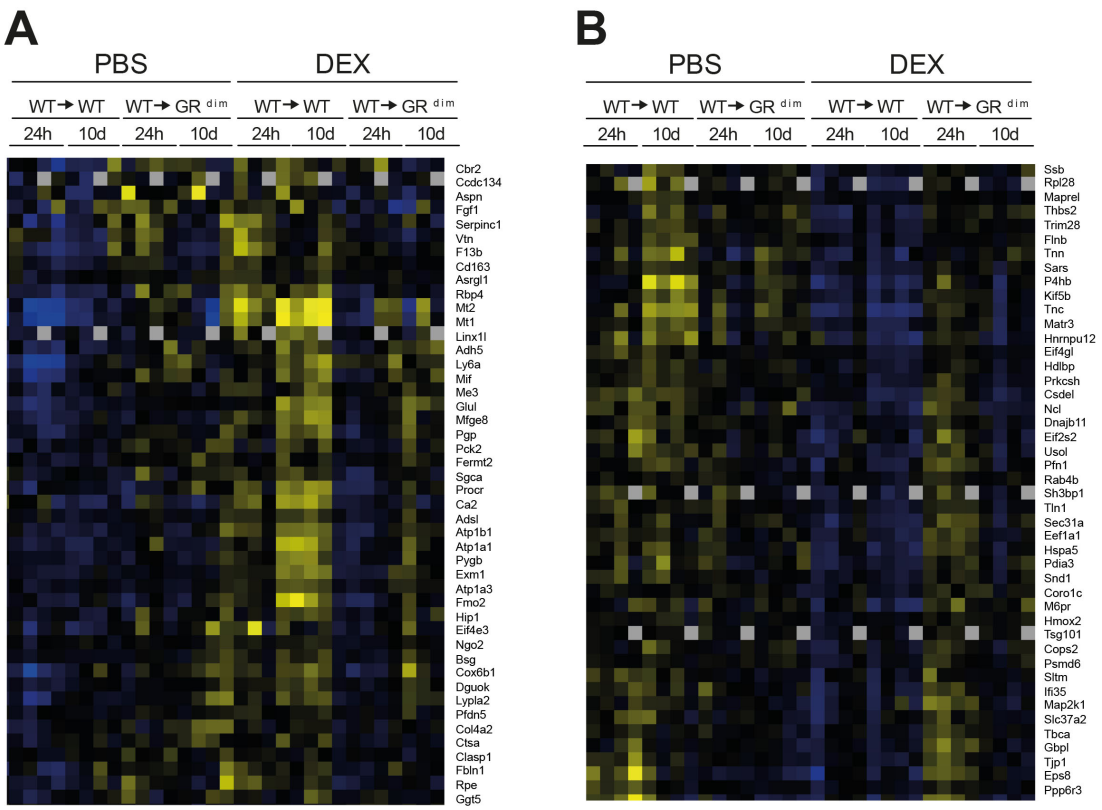

Figure 3.19 GR dimer-dependent regulation of proteins after DEX treatment in ankle digests of wt→wt and wt→GR^{dim} mice

iTRAQ proteomics analysis of ankle digests of irradiated wt mice reconstituted with wt bone marrow (wt→wt) and irradiated GR^{dim} mice reconstituted with wt bone marrow (wt→GR^{dim}) treated for 24h or 10 days (10d) with PBS or dexamethasone (DEX). (A) 45 significantly up regulated and (B) down regulated proteins by DEX in wt→wt mice but not in wt→GR^{dim} mice. n=4. (Performed by the Functional Genomics Center Zürich and ETH Zürich).

In addition, we found 264 proteins significantly altered by DEX treatment regardless of the genotype, thus, being regulated independently of GR dimerization in immune cells. The most prominent up regulated genes in DEX-treated wt→wt mice are Metallothionein-1 and -2, both classical GC-target genes that were absent from DEX-treated wt→GR^{dim} mice (Figure 3.19).

3.1.7. Metallothionein-1 and -2-deficiency does not affect the outcome of DEX treatment in STIA

Metallothionein-1 and -2 are promising candidates for GC-mediated suppression of STIA since RA patients treated with cortisone equally showed a strong induction of MT-1/-2 and subsequent clinical improvement (Miesel and Zuber, 1993). In addition, Mt-1/-2 treatment (100µg/day) of CIA mice resulted in the suppression of arthritis (YOUN et al., 2002). To support the result of our proteomics screen, we measured the expression of *Mt-1* and *Mt-2* on mRNA levels of ankle extracts of wt→wt and wt→GR^{dim} mice after 24h and 72h as well as after 10 days of PBS or DEX treatment, respectively (Figure 3.20A-C).

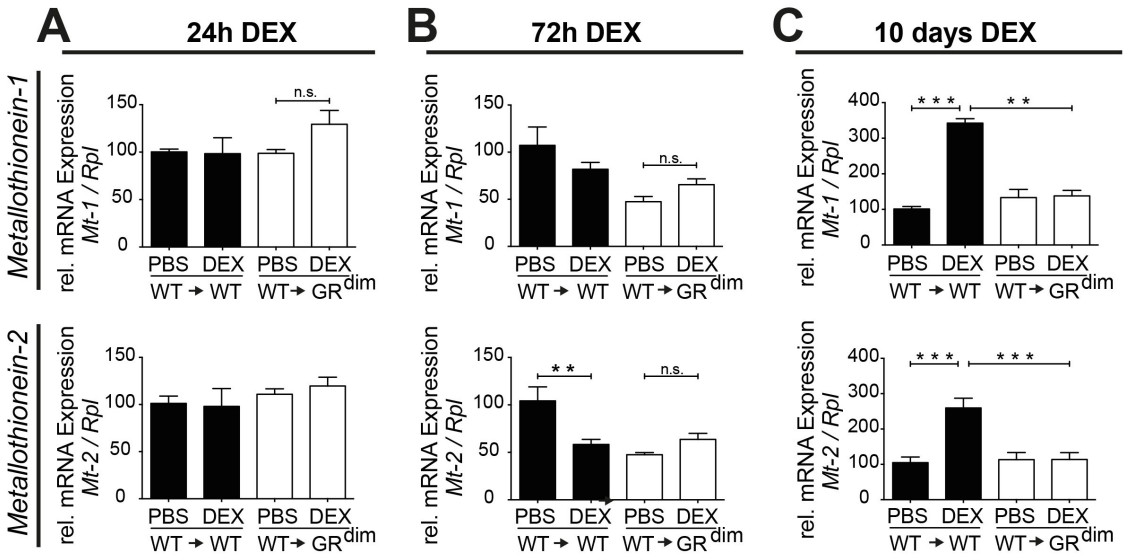

Figure 3.20 GR dimer-dependent induction of Metallothionein-1 and .2 after 10 days of DEX treatment

Metallothionein-1 and -2 qRT-PCR analysis of whole ankle mRNA of irradiated wt mice reconstituted with wt bone marrow (wt→wt) and irradiated GR^{dim} mice reconstituted with wt bone marrow (wt→GR^{dim}) treated for (A) 24h (n=4-5), (B) 72h (n=5-6) or (C) 10 days (n=4-6) with PBS or dexamethasone (DEX). Two-way ANOVA was performed for statistical analysis with Tukey's multiple comparison correction (*p≤0,05, **p≤0,01, ***p≤0,001 and n.s.=not significant).

In contrast to the proteomic screening results, we did not observe changes in *Mt-1* or *Mt-2* expression after 24h DEX treatment in wt→wt or wt→GR^{dim} mice (Figure 3.21A). In addition to the missing *Mt-1* and *-2* induction after 24h, we even

observed a significant reduction (1,8-fold) of Mt-2 after 72h DEX-treatment of wt→wt mice (Figure 3.21B, lower panel). Only after 10 days of DEX treatment we could validate the proteomics results with a 3,6- respectively 2,5-fold increased expression of *Mt-1* and *-2* in wt→wt but not in wt→GR^{dim} mice compared to PBS-treated mice (Figure 3.21C). The mRNA levels, thus did not support the results gained by the proteomics approach, however, translational modifications or mRNA stability might cause the observed changes. Accordingly, we analyzed the influence of Metallothionein-1/-2 double knockout mice (performed by Dr. Ulrike Baschant, FLI Jena, Technische Universität Dresden), since in mice, other then in human, *Mt-1* and *Mt-2* are simultaneously expressed and substitute for each other in single knockout mice. Finally, and in accordance to the lack of induction of mRNA levels at early time points (24h and 72h), but in contrast to the proteomics analysis, double *Mt-1* and *-2* knockout mice were not resistant to DEX treatment in STIA (results not shown).

3.1.8. CD163-deficiency does not affect DEX-mediated suppression of STIA

CD163, another DEX-induced protein induced in wt→wt but not wt→GR^{dim} mice identified in our iTRAQ proteomics screen (Figure 3.20), is solely expressed on monocytes and macrophages (Heuvel et al., 1999) and was shown to be strong and rapidly induced by DEX also in human *in vivo* and *in vitro* studies (Zwadlo-Klarwasser et al., 1990; Wenzel et al., 1996). Importantly, CD163 was the only anti-inflammatory gene up regulated by liposomal delivery of prednisolone in immune complex-induced arthritis that together with the down regulation of pro-inflammatory genes led to the suppression of arthritis (Hofkens et al., 2013). Since we showed that direct suppression of pro-inflammatory cytokines is not sufficient to suppress STIA and in addition detected an up regulation of several anti-inflammatory macrophage genes by mRNA analysis, we analyzed the role of CD163 in STIA suppression and showed that GCs directly act on non-immune cells to suppress STIA. Thus, CD163 seemingly is not a direct target of GCs in STIA but might be the critical factor to induce the DEX-mediated suppression.

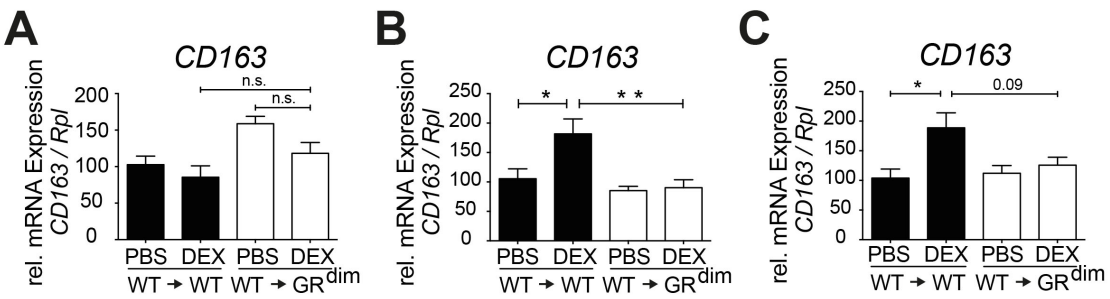

Figure 3.21 GR dimer-dependent induction of CD163 after 72h and 10 days of DEX treatment CD163 qRT-PCR analysis of whole ankle mRNA of irradiated wt mice reconstituted with wt bone marrow (wt→wt) and irradiated GR^{dim} mice reconstituted with wt bone marrow (wt→GR^{dim}) treated for (A) 24h (n=4-5), (B) 72h (n=5-6) or (C) 10 days (n=4-6) with PBS or dexamethasone (DEX). Two-way ANOVA was performed for statistical analysis with Tukey's multiple comparison correction (*p≤0,05, **p≤0,01, ***p≤0,001 and n.s.=not significant).

On *mRNA* level, *CD163*, like *Mt-1* and *-2*, was not changed after 24h of DEX treatment in wt→wt or wt→GR^{dim} mice (Figure 3.15A and 3.21A). In contrast to *Mt-1* and *-2*, it was however strongly induced after 72h (1,7-fold) in DEX-treated wt→wt but not DEX-treated wt→GR^{dim} mice (Figure 3.16A and Figure 3.21B) and this induction was stable even after 10 days treatment (1,8-fold) (Figure 3.18A and 3.21C). To determine if the induction of CD163 alone would be crucial for the DEX-mediated suppression of STIA, we analyzed CD163-deficient mice (a kind gift from Katarzyna Barczyk-Kahlert, WWU Münster) in STIA.

Both, $CD163^{flox}$ and CD163-deficient ($CD163^{del}$) mice developed a strong inflammatory arthritis, measured by the ankle thickness (Figure 3.22A) and the clinical score (Figure 3.22B). In addition, both genotypes equally repress the swelling of the ankles by DEX treatment as shown by the ankle thickness, clinical score and the AUC of both (AUC-thickness $CD163^{flox}$ 10,1 ± 0,7 and $CD163^{del}$ 8,8 ± 1,2 and AUC-score $CD163^{flox}$ 84,8 ± 4,4 and $CD163^{del}$ 59,5 ± 9,2, respectively (Figure 3.22C, D). Thus, CD163 alone is not sufficient to mediate DEX-induced suppression of STIA and is rather part of a pattern of genes indirectly induced by GC-treatment *via* non-immune cells.

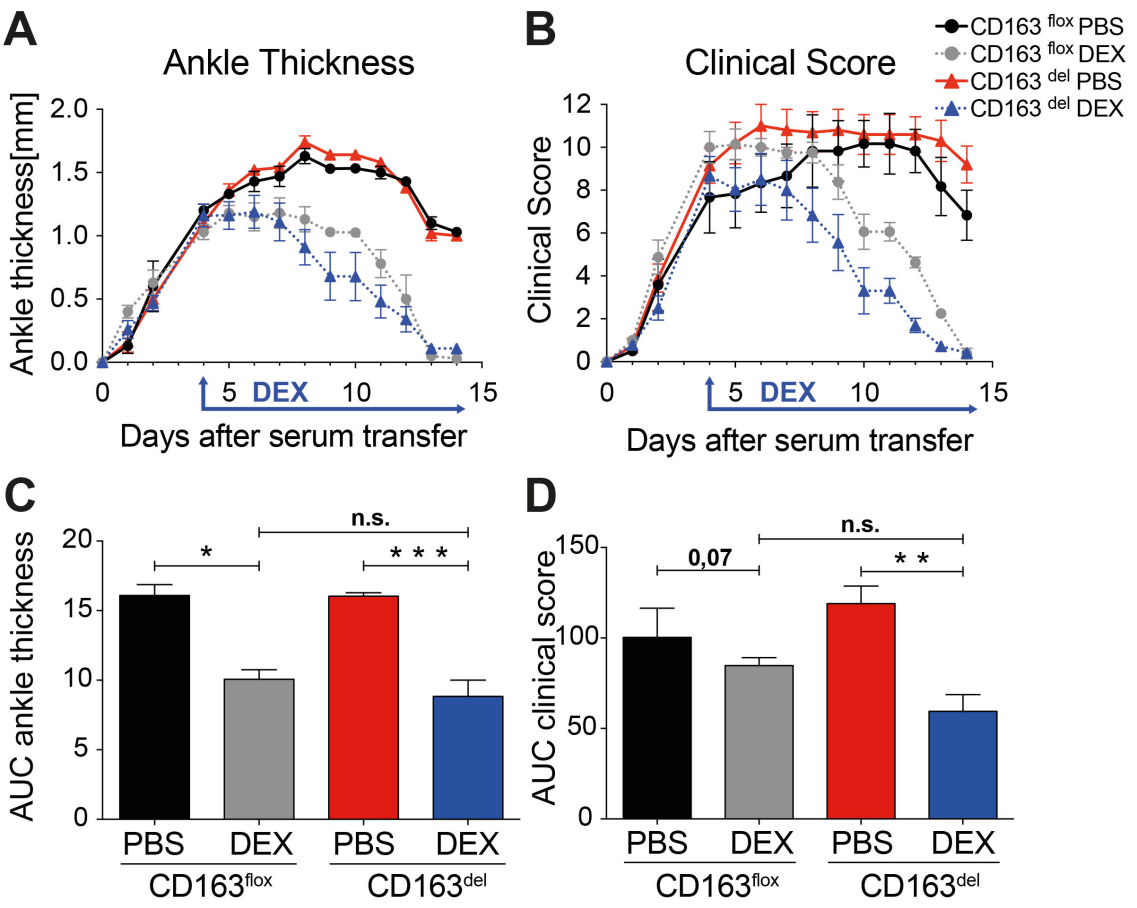

Figure 3.22 Deletion of *CD163* does not abrogate the DEX-mediated suppression of STIA (A) Ankle thickness and (B) clinical score of wt ($CD163^{flox}$) and CD163-deficient mice ($CD163^{del}$) treated with PBS (black and red) or dexamethasone (DEX) (grey and blue). The area under the curve (AUC) was calculated for the ankle thickness (C) and the clinical score (D). n=3-8. Asterisks indicate significant changes (*p≤0,05, **p≤0,01 and n.s.= not significant) by two-way ANOVA with Tukey's multiple comparison correction.

Taken together, this approach did not provide primary mediators of GR actions in non-immune cells. We therefore aimed to identify the specific non-immune target cell type, which directly mediates the DEX-induced suppression of STIA.

3.2. Cell type-specific deletion of the GR in fibroblast-like synoviocytes results in delayed anti-inflammatory actions of GC treatment in STIA

Experiments from bone marrow-chimeric mice and analysis of conditional knock-out mice for radio resistant immune cells (GR^{flox};Mcpt5-Cre, GR^{flox};Lck-Cre and GR^{flox};LysM-Cre, data not shown), revealed the necessity of GC actions on non-immune cells to suppress STIA. In addition, cell type specific delivery of GCs was shown to be an interesting alternative to induce anti-inflammatory effects in AIA (Hofkens et al., 2013; Vanniasinghe et al., 2014) and might reduce potential side effects. To determine the non-immune cell essentially required in GC-mediated suppression in STIA, we analyzed several inducible and non-inducible cre-recombinase-based mouse models for conditional GR-deficiency in endothelial cells, chondrocytes, neurons and fibroblast-like synoviocytes in their GC responsiveness in STIA.

3.2.1. GR in endothelial cells does not mediate the anti-inflammatory effects of DEX treatment in STIA

Endothelial cells share classical features of immune cells like cytokine and chemokine production but do not belong to the group of immune cells. Endothelial cells are resistant to irradiation and GC treatment results in the tightening of the endothelial cell barrier and subsequent reduced infiltration of immune cells from the blood stream into the site of inflammation. We used a tamoxifen-inducible conditional knockout mouse model, Cdh5-Cre-ERT2 ($GR^{Cdh5\text{-}ERT}$), shown to generate a sophisticated deletion of the target gene after tamoxifen treatment (Wang et al., 2010, 2013), and crossed it with GRflox mice (Tronche et al., 1999), to generate mice with an inducible GR-deficiency in endothelial cells. We induced STIA in GR^{flox} and $GR^{Cdh5\text{-}ERT}$ littermates and started DEX-treatment after the onset of arthritis (on day 4) (Figure 3.23). We could not detect any differences in the ankle thickness (Figure 3.23A) nor the clinical score (Figure 3.23B) between GR^{flox} and $GR^{Cdh5\text{-}ERT}$ mice in development or progression of STIA nor in their ability to respond to DEX treatment with reduced ankle thickness and clinical score

(Figure 3.23A, B). This observation is further supported by a significant reduction of the AUC of the clinical score after DEX treatment, independent of genotype (Figure 3.23D) as well as by a strong tendency for the AUC of the ankle thickness (Figure 3.23C).

Thus, GR-deficiency in endothelial cells is not crucial for the DEX-mediated, anti-inflammatory effects in STIA.

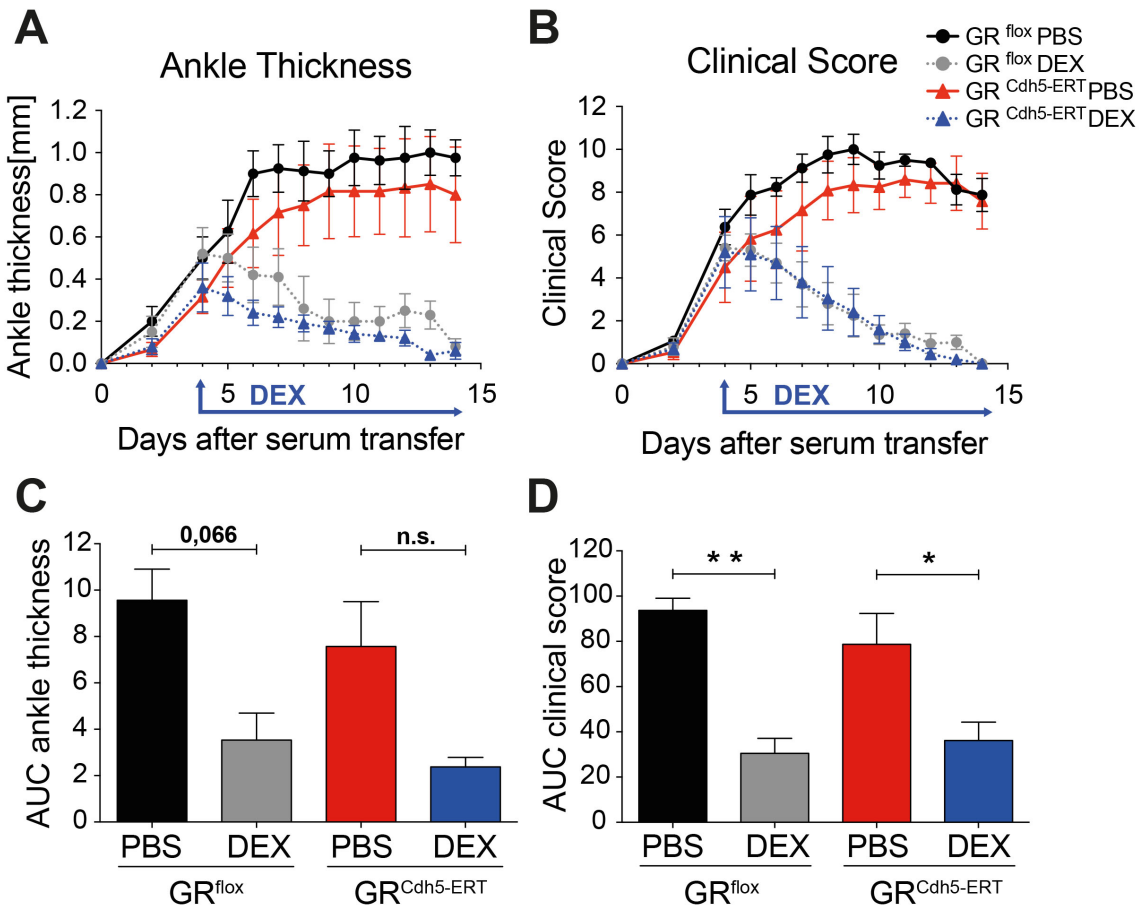

Figure 3.23 GR deletion in endothelial cells does not affect GC-mediated suppression of STIA

(A) Ankle thickness and (B) clinical score of wt mice and mice with a GR-deficiency in endothelial cells ($GR^{Cdh5\text{-}ERT}$) treated with PBS (black and red) or dexamethasone (DEX) (grey and blue). The area under the curve (AUC) was calculated for the ankle thickness (C) and the clinical score (D). n=4-6. Asterisks indicate significant changes (*p≤0,05, **p≤0,01 and n.s=not significant) by two-way ANOVA with Tukey's multiple comparable correction.

3.2.2. GR-deficiency in chondrocytes is not important for exogenous GC-treatment in STIA

Another non-immune cell type that was shown to importantly mediate protective endogenous GC effects in arthritis, are chondrocytes (Tu et al., 2018). Deletion of the GR in chondrocytes resulted in an exacerbation of inflammation and cartilage degradation in STIA and AIA (Tu et al., 2018). Chondrocytes are the major cell type building articular cartilage and ECM. They produce chemokines and high levels of matrix degrading enzymes (MMPs), which can degrade cartilage but are also potentially able to inactivate chemokines by proteolytic processing (Goldring and Otero, 2011; Rose and Kooyman, 2016).

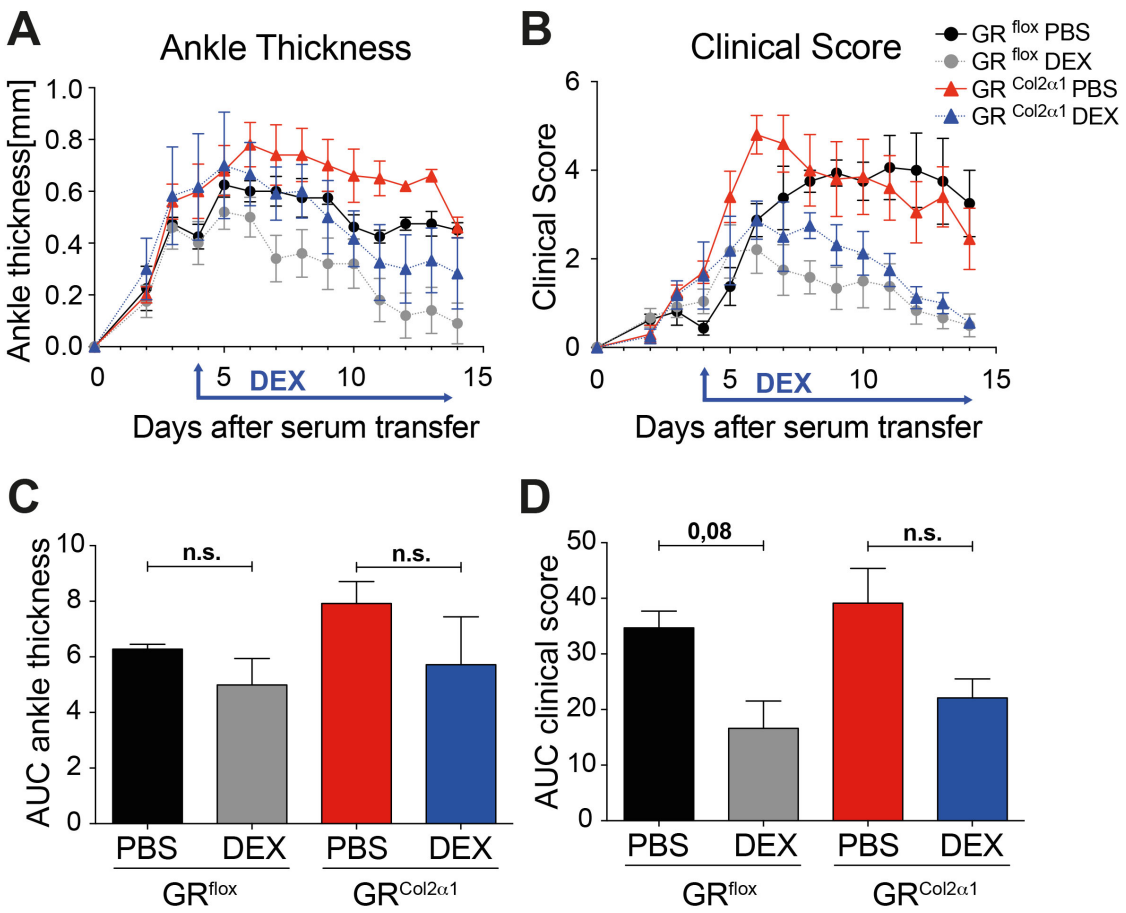

Figure 3.24 GR deletion in chondrocytes does not affect GC-mediated suppression of STIA
(A) Ankle thickness and (B) clinical score of wt mice and mice with a GR-deficiency in chondrocytes (GR^{Col2a1}) treated with PBS (black and red) or dexamethasone (DEX) (grey and blue). The area under the curve (AUC) was calculated for the ankle thickness (C) and the clinical score (D). n=4-6. Asterisks indicate significant changes (*p≤0,05 and n.s=not significant) by two-way ANOVA with Tukey's multiple comparable correction.

In contrast to the study by Tu and colleagues, we did not observe a significant exacerbation of PBS-treated STIA in GRflox;Col2a1-CRE (GR^{Col2a1}) mice, although, we observed an increased AUC by trend of the ankle thickness in PBS-treated GR^{Col1a2} mice compared to PBS-treated GR^{flox} mice (Figure 3.24C).

Nevertheless, exogenous GC treatment resulted in a clear reduction of the clinical score and the AUC of the clinical score in both GR^{flox} and GR^{Col2a1} mice (Figure 3.24B, D). The effective suppression of DEX treatment in both GR^{flox} and GR^{Col2a1} mice was also tendencially observed in the ankle thickness and its AUC (Figure 3.24A, C). In addition, the same effects were repeated in a second experiment (data not shown) and experiments of the group of Prof. Hong Zhou (University of Sydney) confirmed these results independently (unpublished).

3.2.3. GR deletion in neurons of the peripheral or the central nervous system do not influence DEX-mediated suppression of STIA

Peripheral nerves were shown to play an important role in general in arthritis, as their depletion suppresses STIA progression (Stangenberg et al., 2014). Interestingly, the time point of denervation was essential for the outcome. Concurrent denervation and STIA induction resulted in an increased ankle swelling, whereas denervation performed at least 5 days before STIA induction resulted in anti-inflammatory effects. To asses whether GCs may suppress the same inflammatory effects of neurons which are lost by denervation, we analyzed GRflox;Dbh-Cre mice (A kind gift from PhD Grzegorz Kreiner, Polish Academy of Sciences) in STIA (Figure 3.25).

The loss of GR in peripheral nerve cells did not result in obvious differences in the basal level of STIA development or progression (PBS-treated GR^{flox} and GR^{Dbh} mice), nor did it affect the responsiveness towards DEX treatment (Figure 3.25). Especially the ankle thickness and the AUC of the ankle thickness showed a significant potent STIA suppression by DEX treatment, independent of the genotype (Figure 3.25A, C). The clinical score displayed a high variation within the single groups and, thus, the AUC of the latter only displays a trend of suppression by DEX in both genotypes, which, however, is not significant (Figure 3.25B, D).

From this we conclude, that GC-treatment does not resemble the same effects on STIA as a complete denervation and that peripheral neurons do not mediate the anti-inflammatory DEX-effects, observed in our wt mice.

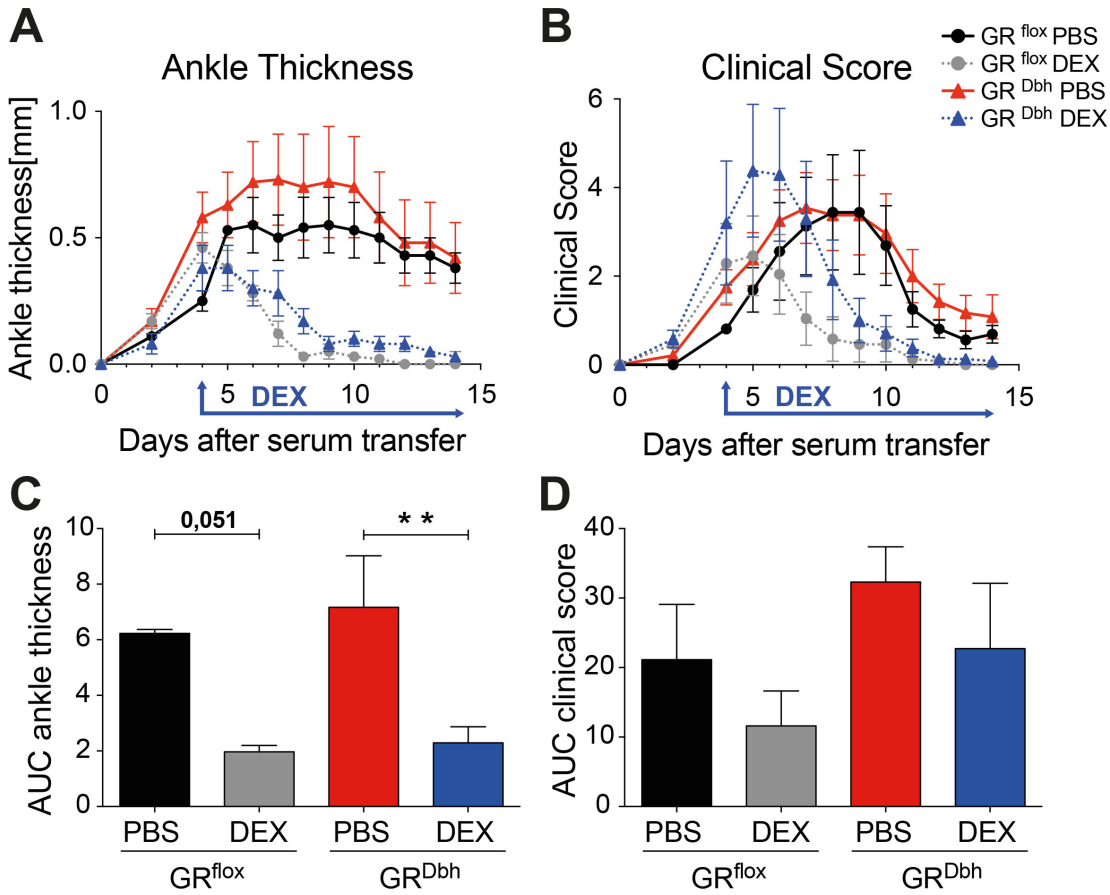

Figure 3.25 GR deletion in peripheral nerve cells does not affect GC-mediated suppression of STIA

(A) Ankle thickness and (B) clinical score of wt mice and mice with a GR-deficiency in peripheral nerve cells (GR^{Dbh}) treated with PBS (black and red) or dexamethasone (DEX) (grey and blue). The area under the curve (AUC) was calculated for the ankle thickness (C) and the clinical score (D). n=5-7. Asterisks indicate significant changes (*p≤0,05, **p≤0,01 and n.s=not significant) by two-way ANOVA with Tukey's multiple comparable correction.

To fully exclude a possible role of neuronal GR in mediating the anti-inflammatory effects of GCs in STIA, we also analyzed mice with a GR deletion in neurons of the central nervous system (CNS). The GR in the central nervous system plays a

pivotal role in HPA-axis feedback regulation and GC secretion, and might as such also affect STIA.

We crossed GR^{flox} mice into the tamoxifen-inducible CamKII-Cre-ERT2 mouse line to generate mice with a neuronal GR-deficient CNS (GRflox;CamKII-Cre-ERT2 mice). Like for the GR deletion in peripheral neurons we did not observe any effects of DEX treatment on STIA in GRflox;CamKII-Cre-ERT2 mice ($GR^{CamKII\text{-}ERT}$). Although not significant, we detected a clear tendency of a proper DEX-mediated suppression of STIA in the ankle thickness and clinical score of both, GR^{flox} and $GR^{CamKII\text{-}ERT}$ mice as represented also in the AUC of the latter (Figure 3.26A-D).

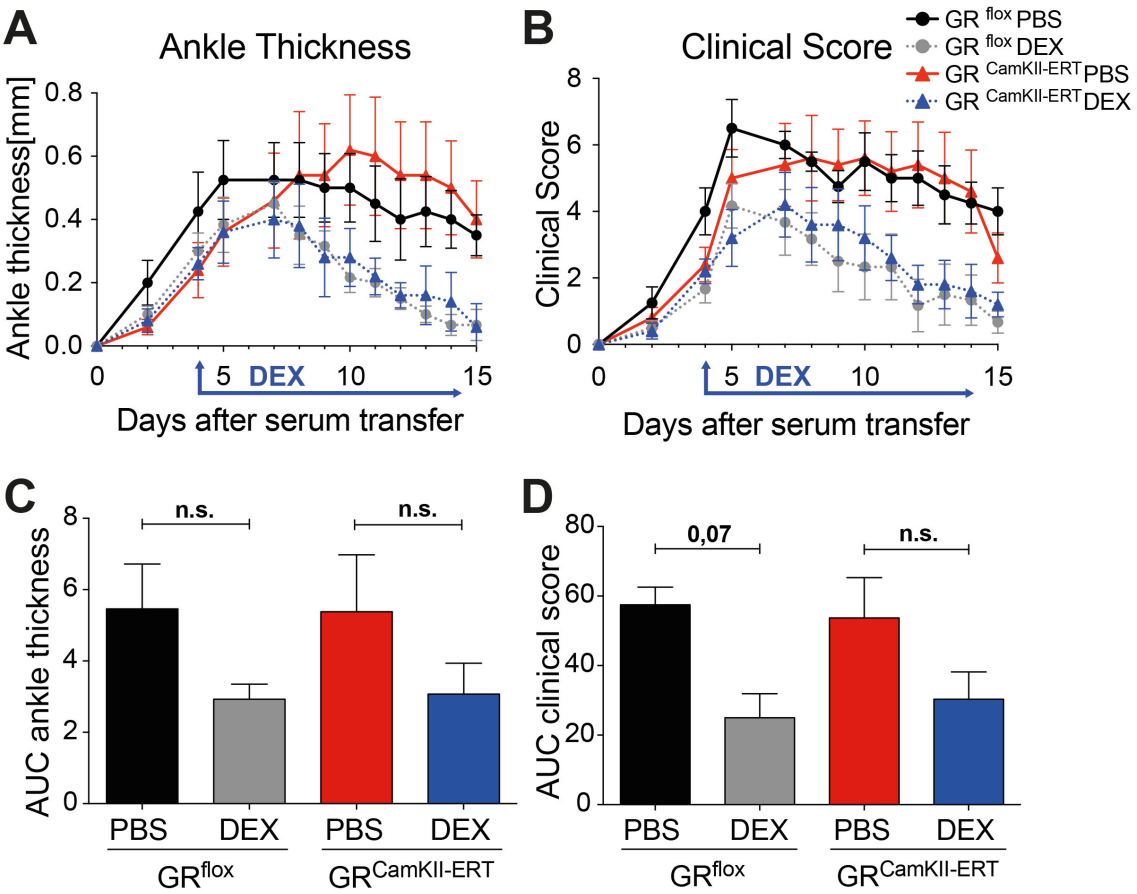

Figure 3.26 GR deletion in neurons of the central nervous system (CNS) does not affect GC-mediated suppression of STIA

(A) Ankle thickness and (B) clinical score of wt mice and mice with a GR-deficiency in nerve cells of the CNS (GR^{CamKII}-ERT) treated with PBS (black and red) or dexamethasone (DEX) (grey and blue). The area under the curve (AUC) was calculated for the ankle thickness (C) and the clinical score (D). n=4-6. Asterisks indicate significant changes (*p≤0,05, **p≤0,01 and n.s=not significant) by two-way ANOVA with Tukey's multiple comparable correction.

In parallel to my work, former lab-member Dr. U. Baschant (FLI Jena, Technische Universität Dresden) performed equal analyses for osteoblast specific GR deletion (GRflox; Osterix-Cre), leading to the conclusion, that osteoblasts do play a role in GC-mediated suppression of STIA (data not shown).

3.2.4. GR-deficiency in FLS attenuates DEX-mediated suppression of STIA

Finally, we addressed to which extend GR expression in fibroblast-like synoviocytes (FLS), mediates the suppression of inflammation in STIA. FLS are lining cells in the joints that are able to produce cytokines and MMPs. Upon activation, as in inflammatory arthritis, FLS start to hyper-proliferate and form a pannus structure that invades into cartilage and bone tissue. To asses the role of GR in FLS for anti-inflammatory effects of GCs we crossed GR^{flox} mice to the inducible Col1α2CreERT mice (Singh et al., 2015) to generate GRflox;Col1a2-CreERT ($GR^{Col1a2\text{-}ERT}$) mice. Since the Col1a2-Cre mouse line was originally described for the deletion in skin fibroblasts we analyzed the recombination efficiency after tamoxifen treatment of these mice in isolated FLS on mRNA level by qRT-PCR and on protein level on histological sections of ankle joints.

After tamoxifen treatment we observed a reduction of GR mRNA expression in FLS of about 50% (Figure 3.27A). Immune histochemistry staining of the GR on serial sections of ankle joints in combination with the FLS marker cadherin-11, revealed a strong deletion of GR protein in cadherin-11 positive cells (3.27B). We conclude that in GRCol1a2-ERT mice, after tamoxifen treatment, GR expression is substantially reduced.

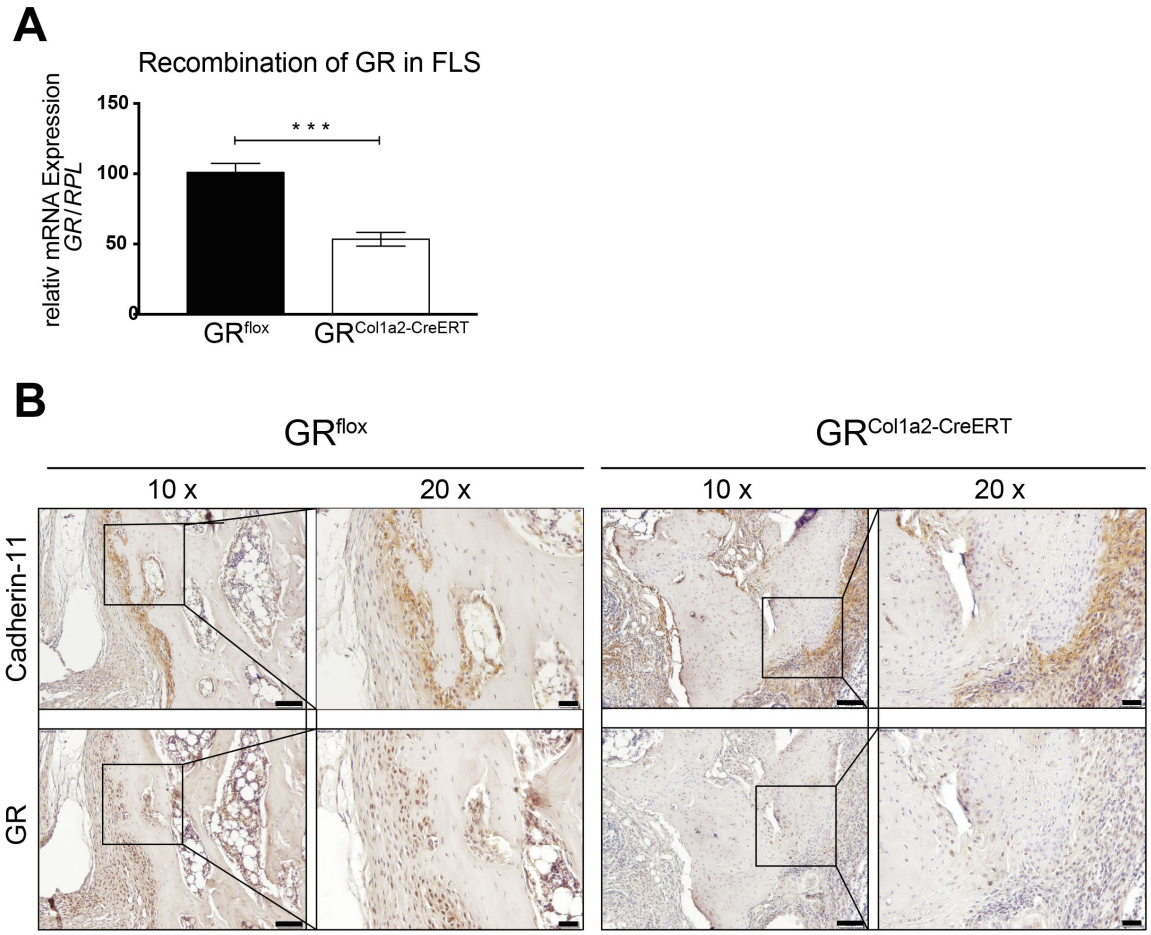

Figure 3.27 GRCo1a2-ERT mice show a reduced GR mRNA expression in isolated mouse FLS and reduced GR protein on ankle sections

(A) qRT-PCR for glucocorticoid receptor (GR) mRNA isolated from articular fibroblast-like synoviocytes (FLS) of GR^{flox} and GRCol1a2ERT mice with STIA. (B) Immunohistochemistry for FLS-specific cadherin-11 and the GR. Original magnification 10x (scale bar=100µm) and 20x (cut outs, scale bar=50µm). ***p≤0,01 and n=3-5. (Published in Koenen et al., 2018 under a CC BY-NC 4.0 license, https://creativecommons.org/licenses/by-nc/4.0/deed.de).

Subsequently, we subjected these mice to STIA after tamoxifen treatment to specifically address the role of GR in FLS. Due to a slower development of STIA independent of the genotypes, we only started DEX treatment on day 6 after STIA induction, when a similar ankle thickness of 0.93 ± 0.12mm and 0.89 ± 0.11mm, respectively and a clinical score of 7 ± 0,85 and 5,38 ±0,75 was reached in mutant and control mice (Figure 3.28A, B). Strikingly, DEX treatment of $GR^{Col1a2\text{-}ERT}$ mice resulted in a delayed reduction of the ankle thickness and clinical score compared to GR^{flox} littermates (Figure 3.28A, B). Furthermore, we saw a clear reduction of the AUC of the ankle thickness in GR^{flox} mice after DEX treatment, which was not

obvious in the $GR^{Col1a2\text{-}ERT}$ mice (Figure 3.28C). This tendency was significant in the AUC of the clinical score (Figure 3.28D).

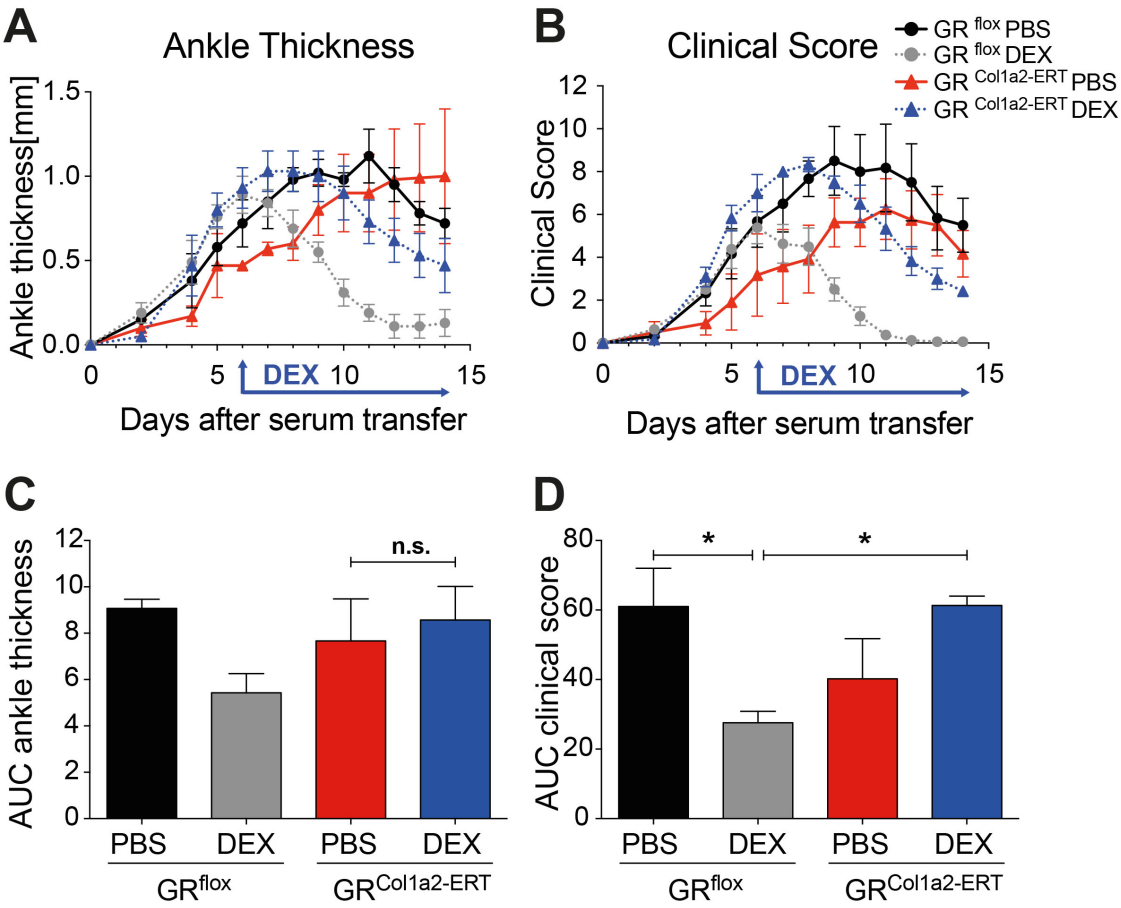

Figure 3.28 GR deletion in FLS strongly reduce the DEX-mediated suppression of STIA (A) Ankle thickness and (B) clinical score of GR^{flox} mice and mice with a GR-deficiency in fibroblast-like synoviocytes (FLS) ($GR^{Col1a2\text{-}ERT}$) treated with PBS (black and red) or dexamethasone (DEX) (grey and blue). The area under the curve (AUC) was calculated for the ankle thickness (C) and the clinical score (D). n=3-6. Asterisks indicate significant changes (*p≤0,05 and n.s.=not significant) by two way ANOVA with Tukey's multiple comparison correction, (A, B and D were published in Koenen et al., 2018 under a CC BY-NC 4.0 license, https://creativecommons.org/licenses/by-nc/4.0/deed.de).

Thus, we can conclude that $GR^{Col1a2\text{-}ERT}$ mice display a delayed reaction to DEX treatment especially within the first 72h, shown by an ongoing swelling of the ankles, however, after this initial delay, $GR^{Col1a2\text{-}ERT}$ mice react to DEX treatment with a reduced ankle swelling and clinical score (Figure 3.28A, B).

Importantly, at the end of the recorded 14 Days of STIA, DEX treated $GR^{Col1a2\text{-}ERT}$ mice did not fully recover compared to their wt littermates, however, compared to their peak of paw swelling at day 8 they showed a strong reduction of the ankle swelling and clinical score (Figure 3.28A, B). Nonetheless, histological analysis revealed ongoing infiltration of immune cells into the joints in DEX treated $GR^{Col1a2\text{-}ERT}$ mice (Figure 3.29), which is resolved in DEX treated GR^{flox} mice (Figure 3.29).

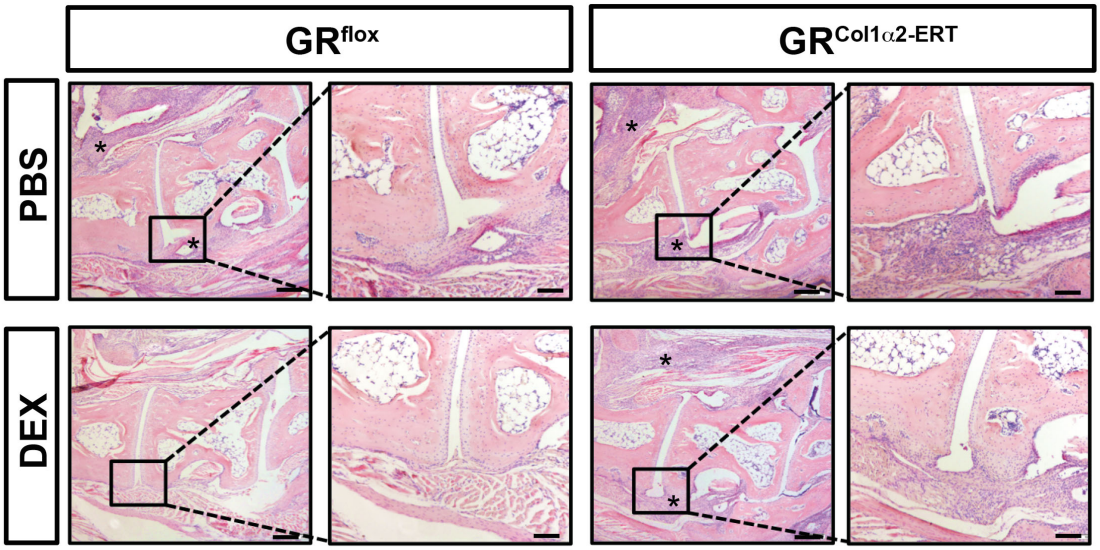

Figure 3.29 GR-deficiency in FLS inhibits DEX-mediated clearance of infiltrating cells into the ankle

Hematoxylin and Eosin (H&E) staining on ankle sections of GR^{flox} and $GR^{Col1a2\text{-}ERT}$ mice treated with PBS or dexamethasone (DEX). Original magnification: 5x (bar=200µm). Original magnification: cutout 10x (bar=100µm). Asterisks show area of cell accumulation in the joint cavity.

Thus, diminished GR expression in FLS reduces the responsiveness towards Dex treatment but does not fully resemble the resistance of mice with a complete GR-deficiency or impaired GR dimerization in all stromal cells. This could be explained by the residual GR expression of 47.5 ± 2.6 percent in the FLS of $GR^{Col1a2\text{-}ERT}$ mice (Figure 3.27). Nevertheless, the partial deletion of GR in FLS already impaired the DEX-induced suppression of STIA strongly, pointing towards an involvement of FLS in stromal cell-mediated DEX-induced resolution of STIA.

3.2.5. Diminished GR expression in FLS does not prevent DEX-mediated cytokine suppression

To analyze whether DEX-mediated suppression of cytokines is still functional in $GR^{Col1a2\text{-}ERT}$ mice, as observed in wt→GR^{dim} mice, we analyzed serum cytokines after 72h of DEX treatment in STIA. Like in wt→wt and wt→GR^{dim} mice we did not observe any significant changes in the ankle swelling between GR^{flox} and GR^{Col1a2} mice after 72h of treatment (Figure 3.31A).

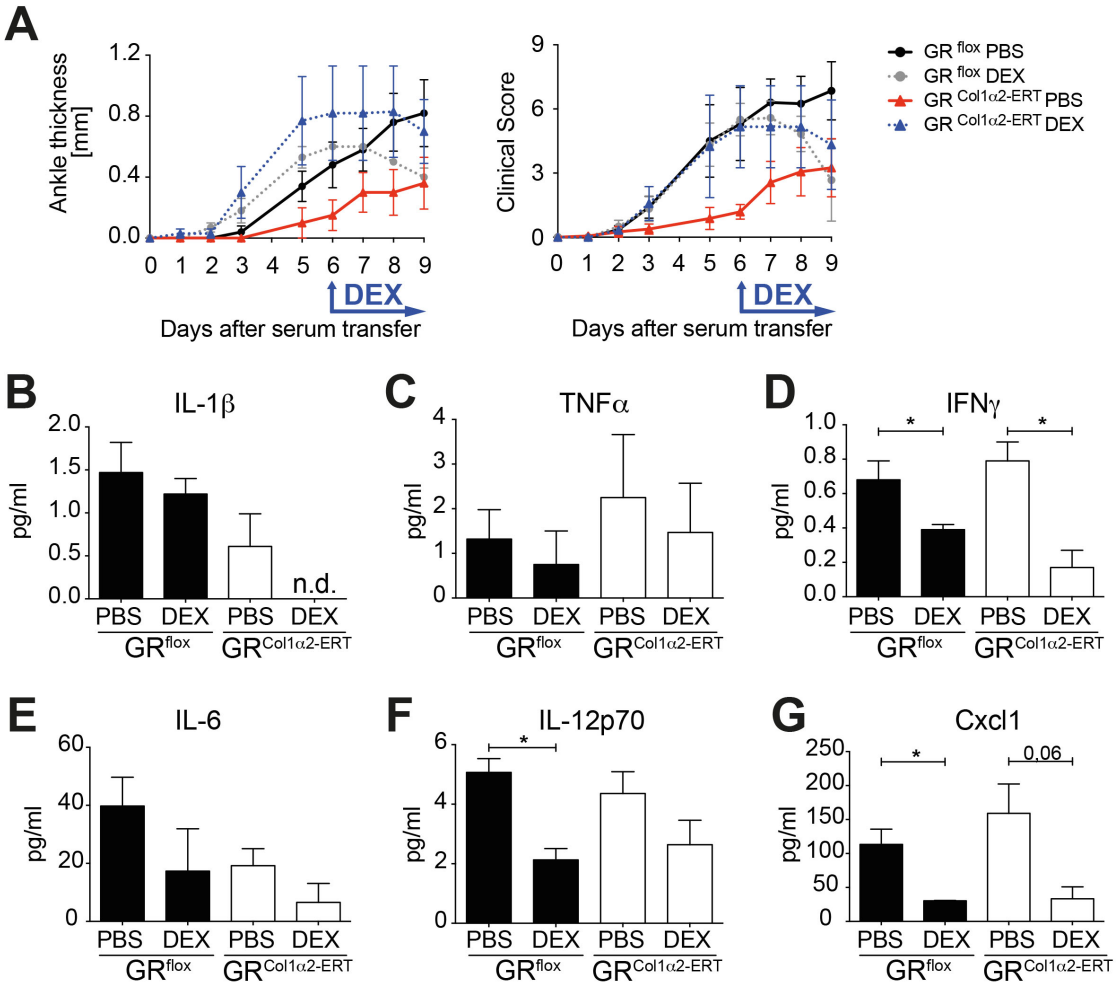

Figure 3.30 GR-deficiency in FLS does not alter cytokine suppression by DEX

(A) Ankle thickness and clinical score of GR^{flox} mice and mice with GR deficient fibroblast-like synoviocytes (FLS) ($GR^{Col1a2\text{-}ERT}$) mice, treated for 72h with PBS (black and red) or dexamethasone (DEX) (grey and blue). Serum cytokine multiplex analysis of pro-inflammatory (B) Il1β (C) TNFα (D) IFNγ (E) Il-6 (F) Il-12p70 and (G) Cxcl1 of GR^{flox} and $GR^{Col1a2\text{-}ERT}$ mice treated for 72h with PBS or

DEX. n=3-5. Asterisks indicate significant changes (*p≤0,05) by student's t-test. n.d.=not detectable, Il=Interleukin, TNF=tumor necrosis factor and IFN=Interferon

Although, serum levels of Il-1β and TNFα were, due to a strong variation, not significantly changed (Figure 3.30B, C), we observed a clear and significant suppression of IFNγ after DEX treatment in both, GR^{flox} and $GR^{Col1a2\text{-}ERT}$ mice (Figure 3.30D). Furthermore, we detected equally suppressed levels of Il-6, Il-12p70 and Cxcl1 in both, GR^{flox} and $GR^{Col1a2\text{-}ERT}$ mice treated with DEX (Figure 3.30E-G). Worth to mention, compared to wt→wt and wt→GR^{dim} mice the detected cytokine levels were reduced (Figure 3.9).

We conclude, that DEX-mediated cytokine suppression is, like in wt→GR^{dim} mice, not impaired by a diminished GR expression in FLS. The reduction of pro-inflammatory cytokines and chemokines is not the decisive factor in STIA suppression.

3.2.6. GR in FLS influences the ratio of non-classical macrophages

To address whether the diminished expression of GR in FLS results in the same changes in cell composition of the ankle joints as observed in the wt→GR^{dim} mice, we analyzed ankle digests by flow cytometer after 72h of DEX-treatment (Figure 3.31-34).

The analysis of hematopoietic ($CD45^{pos}$) (Figure 3.31A) and myeloid cells ($CD11b^{pos}$) (Figure 3.31B) displayed a clear tendency towards a DEX-dependent reduction, which was more prominent in GR^{flox} mice, however also visible in $GR^{Col1a2\text{-}ERT}$ mice (Figure 3.31). The diminished GR expression might result in a diminished suppression of these cells, which is not as strong as in the GR^{flox} littermates (Figure 3.31).

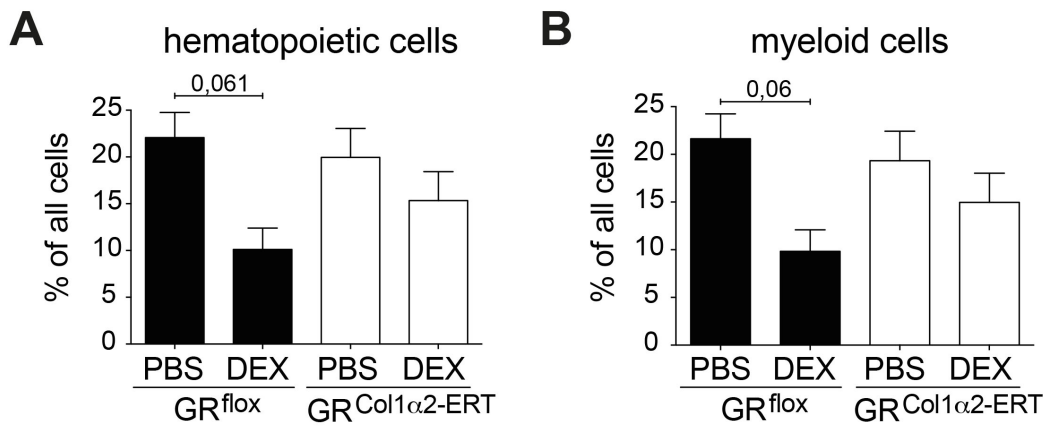

Figure 3.31 DEX reduces the percentage of hematopoietic and myeloid cells is in GR^{flox} but less in $GR^{Col1a2\text{-}ERT}$ mice

Percentage of (A) hematopoietic cells ($CD45^+$) and (B) myeloid cells ($CD45^+$, $CD11b^+$) of all cells in ankle digest of GR^{flox} and $GR^{Col1a2\text{-}ERT}$ mice, treated for 72h with PBS or dexamethasone (DEX). n=3-5. Two-way ANOVA was performed for statistical analysis with Tukey's multiple comparison correction (*p≤0,05 and n.s.=not significant).

We did not observe any significant changes in the percentage of neutrophils ($Ly6G^{pos}$), although, there was a trend towards a reduced percentage of neutrophils in the GR^{flox} mice, which was not the case in $GR^{Col1a2\text{-}ERT}$ mice (Figure 3.32A). No significant changes were observed for T-cells ($CD3^{pos}$) (Figure 3.32B).

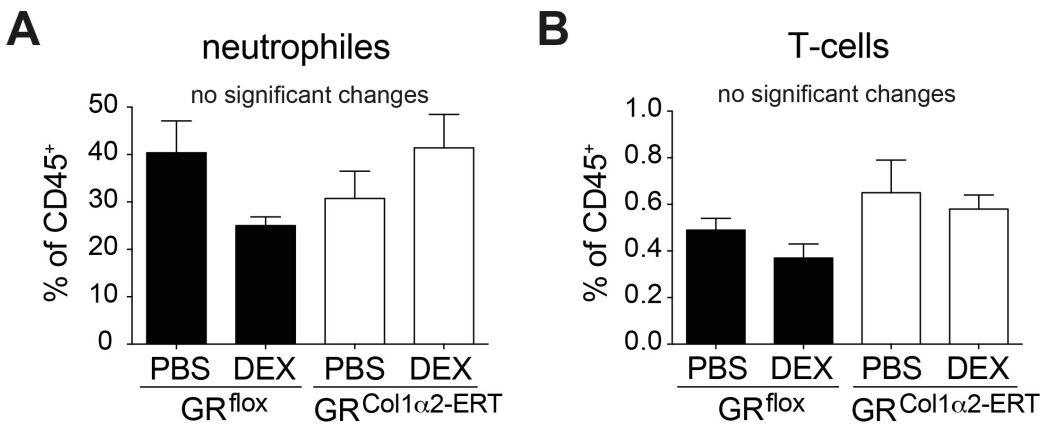

Figure 3.32 Percentage of neutrophils and T-cells is not altered after DEX in $GR^{Col1a2\text{-}ERT}$ mice

Percentage of (A) neutrophils ($CD11b^+$,$Ly6G^+$) and (B) T-cells ($CD11b^-$, $CD3^+$) of $CD45^+$ cells in ankle digest of GR^{flox} and $GR^{Col1a2\text{-}ERT}$ mice, treated for 72h with PBS or dexamethasone (DEX). n=3-5. Two-way ANOVA was performed for statistical analysis with Tukey's multiple comparison correction (*p≤0,05 and n.s.=not significant).

The major difference observed in the cell composition of wt→GR^{dim} mice, was the lack of induction of non-activated and non-classical, anti-inflammatory macrophages. The activation state of macrophages in GR^{flox} and GR$^{Col1a2\text{-}ERT}$ mice (Figure 3.33) as well as analysis of the percentage and ratio of infiltrating monocytes, classical and non-classical macrophages (Figure 3.34) showed an intermediate effect in GR$^{Col1a2\text{-}ERT}$ mice compared to GR^{flox} mice. As in wt→GR^{dim} mice, we did not observe any significant changes in the percentage of activated macrophages (F4/80^{pos}, MHCII^{pos}) (Figure 3.33A); however, we saw a clear tendency for an induction of non-activated macrophages (F4/80^{pos}, MHCII^{neg}) in GR^{flox} mice after DEX treatment (PBS 5,3 ± 1,4 versus DEX 15,5 ± 1,2) (Figure 3.33B). The effect of DEX and a possible lack of induction in GR$^{Col1a2\text{-}ERT}$ mice is, due to a high variation, not clear (10,2 ± 4,5) (Figure 3.33), however, compared to PBS-treated GR$^{Col1a2\text{-}ERT}$ mice, DEX-treated GR$^{Col1a2\text{-}ERT}$ mice had a clear lack of induction of non-activated macrophages (Figure 3.33B). Moreover, the ratio of non-activated macrophages to activated macrophages was once more significantly shifted towards more non-activated macrophages after DEX treatment in the GR^{flox} but not GR$^{Col1a2\text{-}ERT}$ mice (Figure 3.33C).

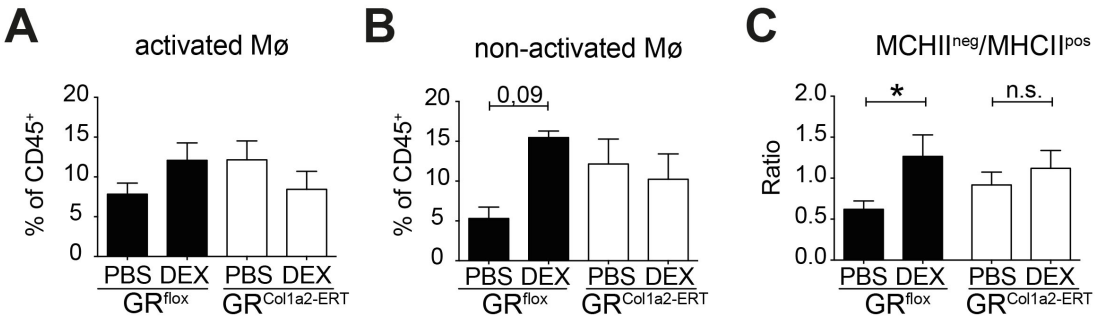

Figure 3.33 Percentage of non-activated macrophages is induced by DEX in GR^{flox} but only partially in GR$^{Col1a2\text{-}ERT}$ mice

Percentage of (A) activated macrophages (CD11b^{+}, Ly6G^{-}, F4/80^{+}, MHCII^{+}) and (B) non-activated macrophages (CD11b^{+}, Ly6G^{-}, F4/80^{+}, MHCII^{-}) of CD45^{+} cells in ankle digest of GR^{flox} and GR$^{Col1a2\text{-}ERT}$ mice, treated for 72h with PBS or dexamethasone (DEX). n=3-5. Two-way ANOVA was performed for statistical analysis with Tukey's multiple comparison correction (*p≤0,05 and n.s.=not significant).

The percentage of infiltrating monocytes (F4/80^{neg}, Ly6C^{pos}), revealed the same reduction through DEX treatment, in GR^{flox} and GR$^{Col1a2\text{-}ERT}$ mice (1,4-fold in GR^{flox} and 2-fold in GR$^{Col1a2\text{-}ERT}$) (Figure 3.34A). For classical activated macrophages we did not observe any significant changes (Figure 3.34B). For non-classical macrophages (F4/80^{pos}, Ly6C^{neg}) we observed a clear, yet not significant induction in DEX-treated GR^{flox} mice compared to PBS treated GR^{flox} mice (PBS 9,97±2,34 versus DEX 22,4±1,99) (Figure 3.34C). Due to a high variation, this induction was not clearly abolished in DEX-treated GR$^{Col1a2\text{-}ERT}$ mice (15,38±5,33), compared to GR^{flox} mice (Figure 3.34C), however once more, compared to PBS-treated GR$^{Col1a2\text{-}ERT}$ mice, DEX-treated GR$^{Col1a2\text{-}ERT}$ mice showed no induction of non-classical macrophages (Figure 3.34C).

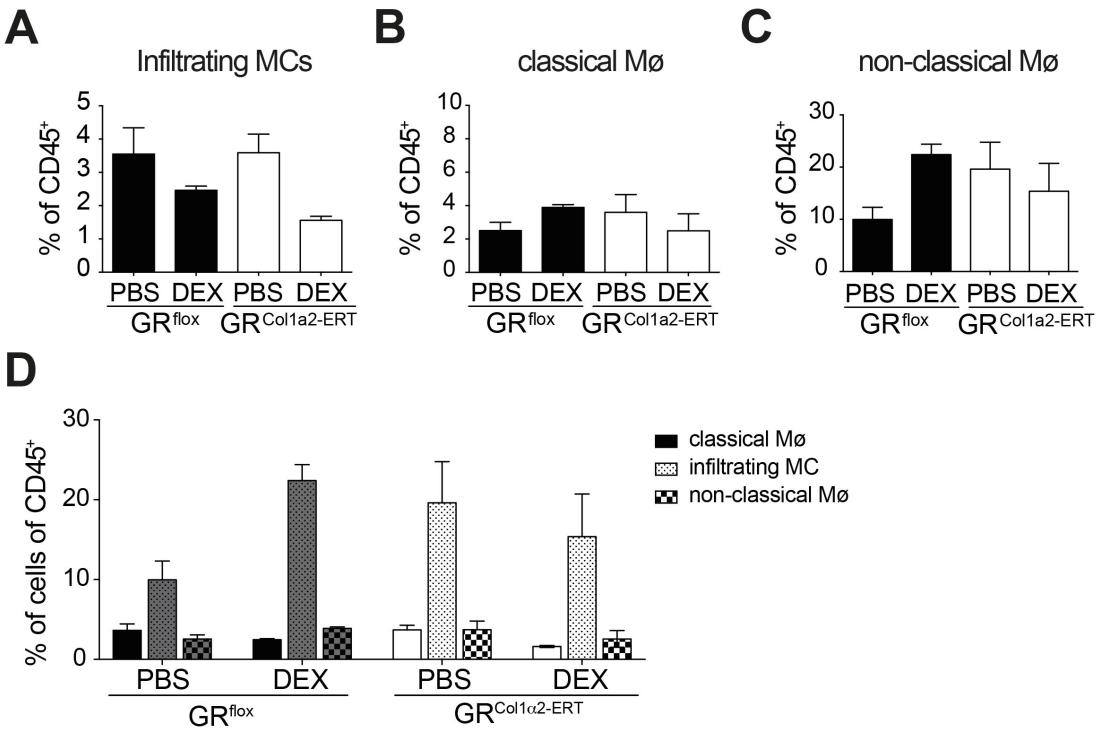

Figure 3.34 GR-deficiency in FLS does not affect DEX-mediated reduction of infiltrating monocytes but lack a clear induction of non-classical macrophages

Percentage of (A) infiltrating monocytes (MC) (CD11b^{+}, Ly6G^{-}, F4/80^{-}, Ly6C^{+}), (B) classical macrophages (CD11b^{+}, Ly6G^{-}, F4/80^{+}, Ly6C^{+}), (C) non-classical macrophages (CD11b^{+}, Ly6G^{-}, F4/80^{+}, Ly6C^{-}) of CD45^{+} cells and (D) direct comparison of the abundance of (A), (B), and (C) in ankle digest of GR^{flox} and GR$^{Col1a2\text{-}ERT}$ mice, treated for 72h with PBS or dexamethasone (DEX). n=3-5. Two-way ANOVA was performed for statistical analysis with Tukey's multiple comparison correction (*p≤0,05 and n.s.=not significant).

The ratio of macrophage sub-populations to each other showed a much lower basal number of infiltrating monocytes in both GR^{flox} and $GR^{Col1a2\text{-}ERT}$ mice compared to the previous experiment in bone marrow chimeric mice (Figure 3.34). Thus, the ratio of infiltrating monocytes to non-classical Mø does not result in a shift towards one or the other (Figure 3.34).

We can conclude, that a diminished GR expression in FLS does reduce the responsiveness to DEX treatment in STIA, but does not show a clear regulation of the anti-inflammatory Mø population.

3.2.7. GR dimer-dependent induction of efferocytosis and associated factors in FLS *in vitro*

To address possible factors affected by an impaired GR dimerization in FLS, we conducted an *in vitro* analysis of isolated primary FLS of wt and GR^{dim} mice. To resemble the inflammation in the ankle joint, we treated the FLS *in vitro* with either Il-1β or DEX alone, or in combination for 72h. Subsequent, qRT-PCR analysis revealed the GR dimer-dependent induction of *Gas6*, the agonist of the TAM-receptors (van den Brand et al., 2013). Interestingly, overexpression of Gas6 was shown to decrease joint inflammation and pathology in collagen-induced arthritis (van den Brand et al., 2013). In our FLS *Gas6* was increased by DEX treatment in wt FLS and to a significant lesser amount in GR^{dim} FLS (Figure 3.35). This induction was even stronger by combinatory treatment of IL-1β and DEX, in wt FLS but not in GR^{dim} FLS (Figure 3.35).

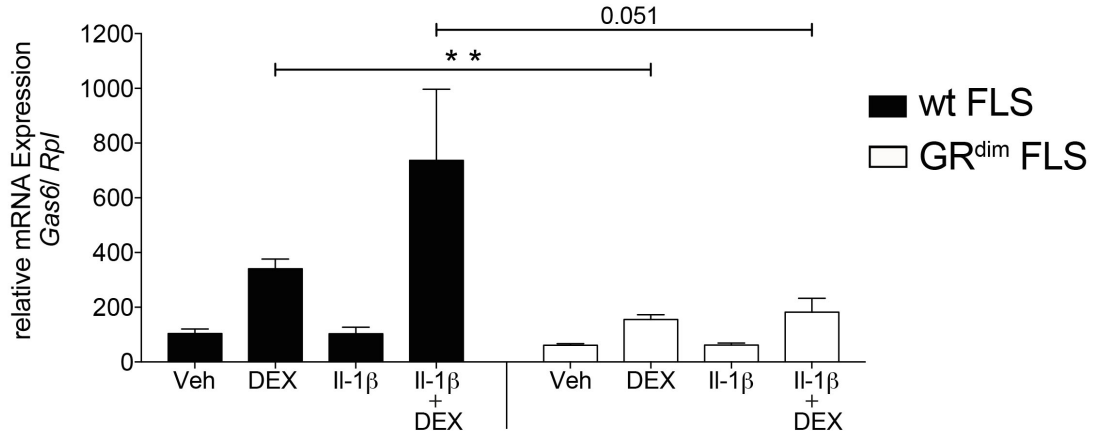

Figure 3.35 DEX-induced increase of *Gas6* expression is stronger in wt FLS then GR^{dim} FLS
qRT-PCR of Gas6 in primary wt (black) and GR^{dim} (white) fibroblast-like synoviocytes (FLS) treated with either vehicle, dexamethasone (DEX) or Interleukin-1β (Il-1β) alone or in combination with DEX for 72h. n=4-5.

To analyze possible functional effects of FLS on macrophages we subsequently, co-cultured wt and GR^{dim} FLS with bone marrow-derived macrophages (BMDMs) and treated these co-cultures for 72h with Il-1β or a combination of Il-1β and DEX. To exclude direct effects of DEX on macrophages we used GR-deficient BMDMs. As a functional read-out we determined the ability of BMDMs to clear an apoptotic cell burden by efficient efferocytosis of apoptotic T-lymphocytes after Il-1β and DEX stimulation. Correspondingly to our *in vivo* results, we found a mild increase of efferocytosis efficiency in GR-deficient BMDMs co-cultured with wt FLS but not with GR^{dim} FLS after IL1β+DEX treatment (Figure 3.36).

This induction supports the hypothesis, that the presence of wt FLS stimulate certain mediators, like *Gas6*, to induce macrophages to change to an anti-inflammatory phenotype, associated with an increased clearance of an apoptotic cell burden in inflammatory arthritis.

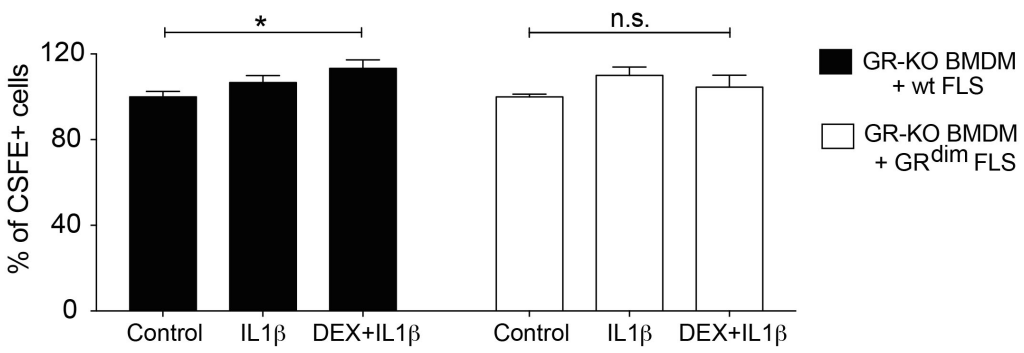

Figure 3.36 DEX slightly induces efferocytosis in BMDMs co-cultured with wt FLS but not with GR^{dim} FLS

Flow cytometry analysis of efferocytosis efficiency of CSFE-labeled apoptotic T-lymphocytes in co-cultures GR-deficient bone marrow-derived macrophages (BMDM) with primary wt (black) or GR^{dim} (white) FLS, treated either with vehicle, Interleukin-1β (Il-1β) or Il-1β and dexamethasone (DEX) for 72h. Asterisks indicate significant changes (p≤0,05, n.s.=not significant) by student's t-test. n=3. (Published in Koenen et al., 2018 under a CC BY-NC 4.0 license, https://creativecommons.org/licenses/by-nc/4.0/deed.de).

3.2.8. RNA sequencing revealed a distinct expression pattern with specifically enriched pathways in GR^{dim} FLS compared to wt FLS treated with IL1β and DEX

To determine potential genes induced or suppressed differentially in wt and GR^{dim} FLS in an unbiased approached, we performed RNA sequencing analysis.

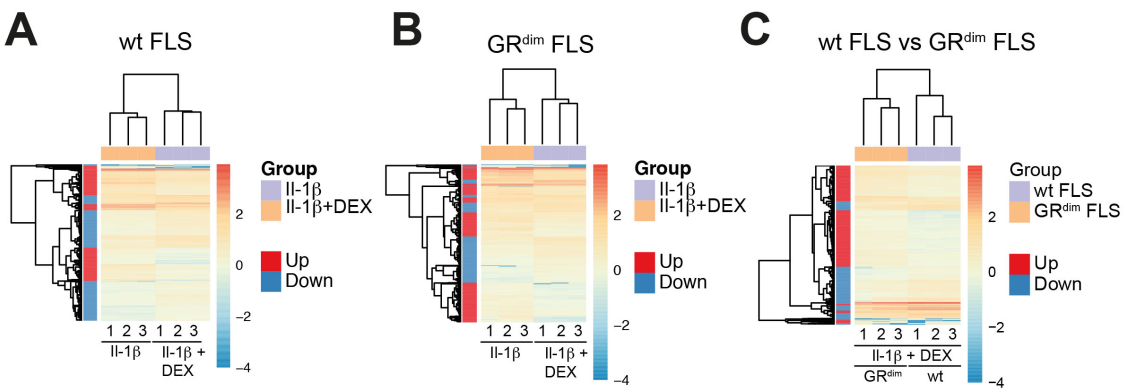

Figure 3.37 RNA Sequencing of wt and GR^{dim} FLS revealed a specific expression pattern after Il-1β and DEX treatment

Hierarchical clustering of differentially expressed genes between (A) wt and (B) GR^{dim} fibroblast-like synoviocytes (FLS) treated with Interleukin-1β (Il-1β) or Il-1β and DEX for 72h. (C) Hierarchical clustering of differentially expressed genes in wt compared to GR^{dim} FLS treated with Il-1β and

DEX for 72h. n=3 (C was published in Koenen et al., 2018 under a CC BY-NC 4.0 license, https://creativecommons.org/licenses/by-nc/4.0/deed.de).

We treated wt and GR^{dim} FLS with Il-1β or Il1-β and DEX for 72h and analyzed differentially expressed genes and pathways, within the treatment groups (Figure 3.37A, B) and between genotypes (Figure 3.37C). Our results revealed several genes associated with pathological effects of FLS, like cell adhesion molecules (CAMs) and cell cycle promoting genes suppressed by DEX in wt FLS stimulated with Il-1β (Figure 3.38A-D), which were not or only slightly suppressed in GR^{dim} FLS (Figure 3.38E-H). A direct comparison of wt and GR^{dim} FLS treated with Il-1β and DEX illustrated that these genes were significantly less regulated in GR^{dim} FLS (Figure 3.38I-L).

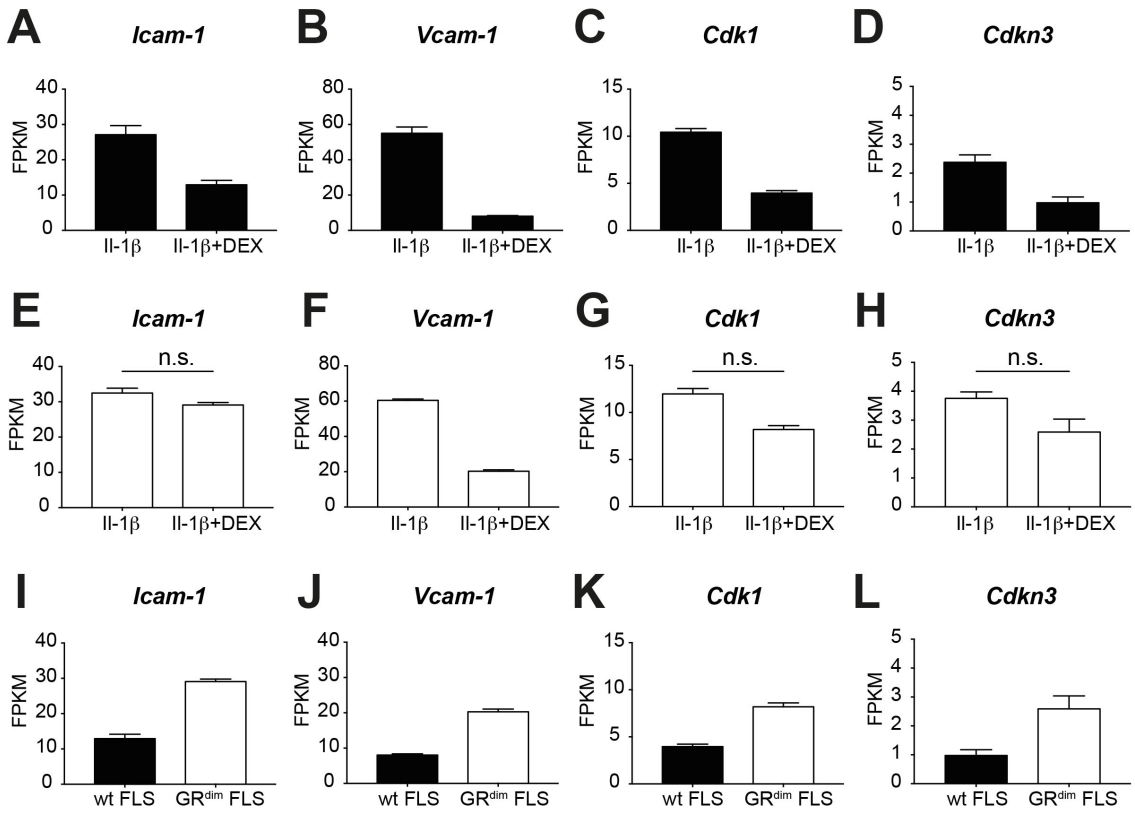

Figure 3.38 GR dimer-dependent regulation of pathogenic FLS marker genes Pathogenic fibroblast-like synoviocytes (FLS) marker genes (A) Icam-1, (B) Vcam-1, (C) Cdk1 and (D) Cdkn3 in wt and GR^{dim} (E-H) FLS treated with Interleukin-1β (Il-1β) or Il-1β and DEX for 72h. Comparison of (I) Icam-1, (J) Vcam-1, (K) Cdk1 and (L) Cdkn3 in Il-1β and DEX treated wt (black) and GR^{dim} (white) FLS. n=3 and n.s.=not significant, if not indicated differently, changes are significant.

Other factors important for cartilage and bone destruction in arthritis like matrix metalloproteinases (Mmps) however were suppressed equally in DEX-treated wt (Figure 3.39A, B) and GR^{dim} FLS (Figure 3.39C, D).

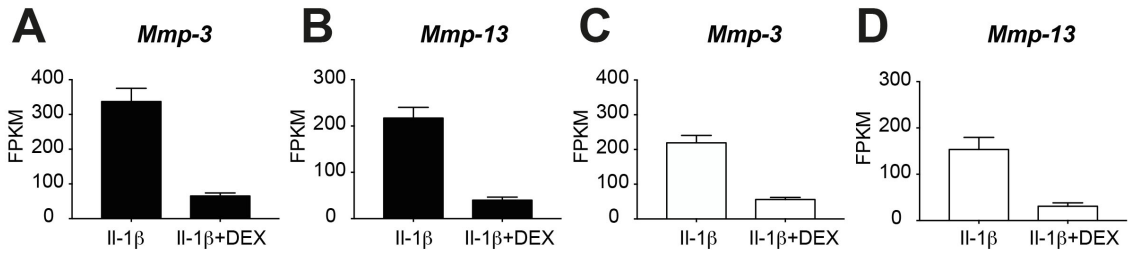

Figure 3.39 Matrix metalloproteinases are regulated in a GR dimer independent manner in FLS

Expression of matrix metalloproteinases (Mmp) (A) Mmp-3 and (B) Mmp-13 in wt fibroblast-like synoviocytes (FLS) (black) and (C) Mmp-3 and (D) Mmp-13 in GR^{dim} FLS (white) treated with interleukin-1β or Il-1β and DEX for 72h.n=3

Furthermore, we identified classical anti-inflammatory GC-target genes (Fkbp5, Gilz, Mt1 and 2), which were significantly less expressed after DEX treatment in GR^{dim} FLS compared to wt FLS (Figure 4.40A-D).

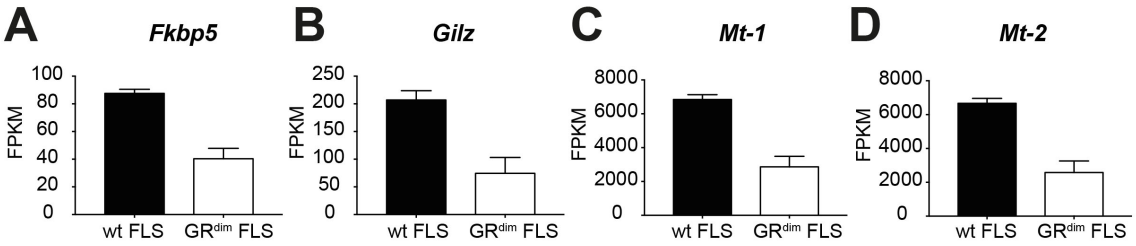

Figure 3.40 GR^{dim} FLS express significantly lower amounts of classical GC-target genes than wt FLS

Expression of (A) Fkbp5, (B) Gilz, (C) Metallothionein (Mt) -1 and (D) Mt-2 in wt (black) and GR^{dim} FLS (white) treated with Interleukin-1β (Il-1β) and dexamethasone (DEX) for 72h. n=3. Fkbp=Fk506 binding protein and Gilz=Glucocorticoid-induced leucine zipper. (Published in Koenen et al., 2018 under a CC BY-NC 4.0 license, https://creativecommons.org/licenses/by-nc/4.0/deed.de).

Interestingly, *Gas6* was also up regulated by DEX treatment in wt FLS but not significantly changed in GR^{dim} FLS, supporting qRT-PCR results (Figure 3.35). As expected, the classical pro-inflammatory cytokines were not expressed differentially between wt and GR^{dim} FLS, however, the chemokine macrophage inflammatory proteins Mip-1α and Mip-1β, associated with macrophage activity, were differentially expressed in DEX-treated GR^{dim} FLS compared to wt FLS (Figure 3.41A, B).

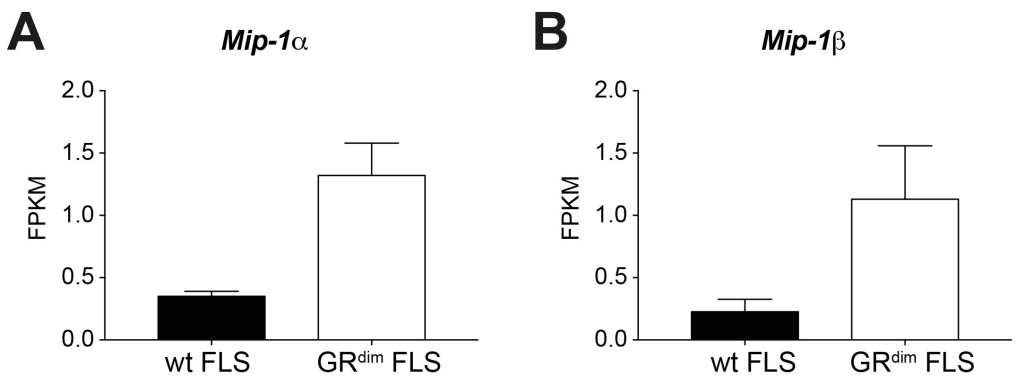

Figure 3.41 GR dimer-dependent suppression of Mip1α and -β in FLS

Expression of (A) macrophage attractant protein (Mip)-1α and (B) Mip-1β inwt (black) and GR^{dim} (white) FLS treated with with Interleukin-1β (Il-1β) and dexamethasone (DEX) for 72h n=3. (Published in Koenen et al., 2018 under a CC BY-NC 4.0 license, https://creativecommons.org/licenses/by-nc/4.0/deed.de).

In addition to the analysis of differentially expressed genes we also performed a pathway enrichment analysis of genes differentially expressed in wt FLS compared to GR^{dim} FLS treated with Interleukin-1β and DEX (Figure 3.42). Interestingly, we found a strong enrichment for pathways associated with cell-cell and cell-matrix contact (cell adhesion molecules, tight junctions, focal adhesion, ECM-receptor interaction, Rap1 signaling pathway) as well as an enrichment for cell cycle associated pathways (cell cycle, p53 signaling pathway and cancer associated pathways) (Figure 3.42), indicating a more pathogenic behavior of GR^{dim} FLS not suppressed by DEX-treatment.

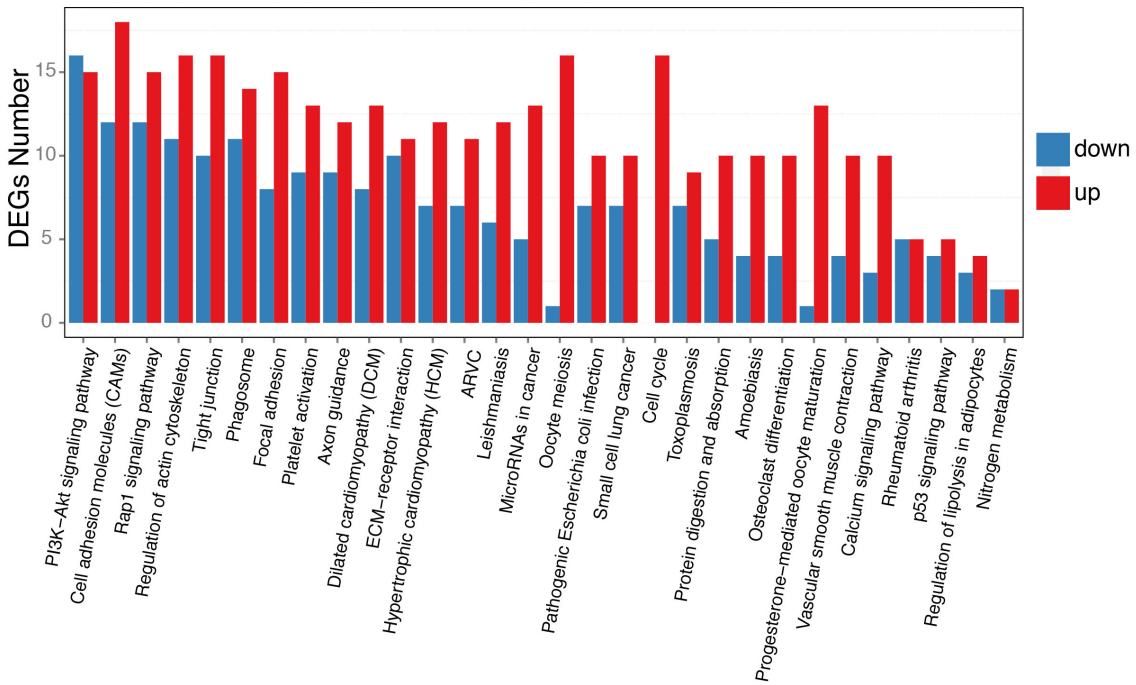

Figure 3.42 Most enriched pathways of differentially enriched genes in wt and GR^{dim} FLS treated with Il-1β and DEX

Most enriched KEGG pathways by differentially expressed genes (DEGs) in Interleukin-1β (Il-1β) and dexamethasone (DEX) treated wt and GR^{dim} FLS. n=3. ARVC=arrythmogenic right ventricular cardiomyopathy ((Published in Koenen et al., 2018 under a CC BY-NC 4.0 license, https://creativecommons.org/licenses/by-nc/4.0/deed.de).

3.2.9. GR dimer-dependent suppression of secreted pro-inflammatory chemokines associated with macrophage biology

Finally, we found that contrary to wt FLS, GR^{dim} FLS not only express higher levels of Mip-1α and Mip-1β mRNA but also secrete significantly higher amounts into their supernatant when stimulated with a combination of Il-1β and DEX (Figure 3.43A). Similar to the serum analysis in wt→GR^{dim} chimeric mice and GR$^{Col1a2\text{-}ERT}$ mice, classical pro-inflammatory cytokines like TNFα and interleukin-6 are equally suppressed in wt and GR^{dim} FLS (Figure 3.43B).

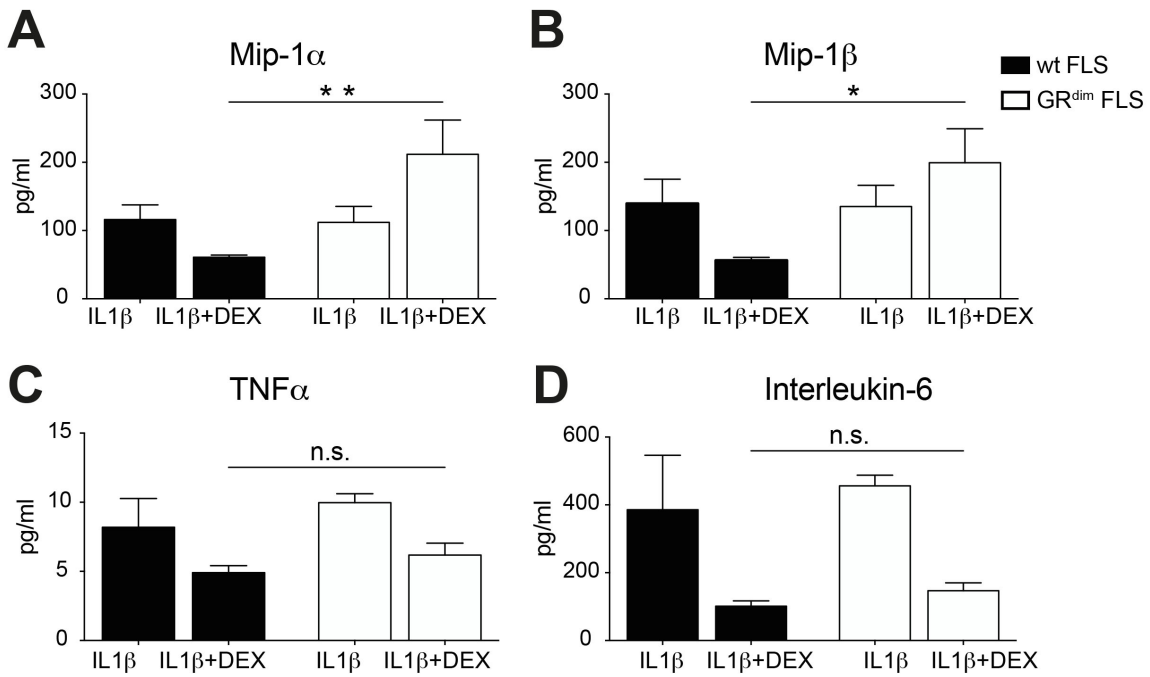

Figure 3.43 GR dimer-dependent suppression of Mip-1α and -β in FLS

Expression of chemokine (A) macrophage attractant protein (Mip)-1α and (B) -β and cytokines (C) TNFα and (D) Interleukin-6 (Il-6) in (black) and GR^{dim} (white) FLS treated with Interleukin-1β (Il-β) and dexamethasone (DEX) for 72h. n=3. TNF=tumor necrosis factor. (A and B were published in Koenen et al., 2018 under a CC BY-NC 4.0 license, https://creativecommons.org/licenses/by-nc/4.0/deed.de).

Taken together we can conclude that GR in non-immune cells, presumably FLS, mediates the suppression of STIA by affecting macrophage populations towards an increased fraction of anti-inflammatory macrophages. Furthermore, GCs regulates the pathological phenotype of FLS in a GR dimer-dependent mechanism by controlling cell-cell and cell-matrix interaction, cell cycle and chemokine secretion.

4. Discussion

Rheumatoid arthritis (RA) is a severe inflammatory autoimmune disease affecting approximately 1% of the world's population (Tsokos et al., 2000) and glucocorticoids (GCs) are still among the most frequently prescribed drugs to suppress inflammation in RA (Bijlsma and Jacobs, 2014; Gaujoux-Viala and Gossec, 2014; Buttgereit and Bijlsma, 2017). Although many *in vitro* (Yang et al., 1998; Hardy et al., 2013; Hofkens et al., 2013) and some *in vivo* studies (Baschant et al., 2011; Patel et al., 2012) have been conducted, the understanding of the critical cell types, especially considering the role of non-immune cells, is still surprisingly vague. A longstanding view considered repression of cytokines by the monomeric GR in immune cells as the pivotal mechanism (Schäcke et al., 2007), however therapies with GR monomer selective ligands were not developed for RA. Furthermore, a predominant part of research is focused on effects on single cell populations and not on the complex interplay of several cell types and their cross talk, which is a prevalent feature of RA. Furthermore, GCs display a variety of desirable anti-inflammatory effects in RA (Baschant et al., 2012) but are under constant clinical audit due to detrimental side effects on bone homeostasis and metabolism (Wassenberg et al., 2005; Hartmann et al., 2016; Wilson et al., 2018). Specific applications by intra-articular administration (Weitoft et al., 2005), joint- and cell type-specific delivery (Hofkens et al., 2011; Vanniasinghe et al., 2014; Quan et al., 2016) and improved drug kinetics were considered to reduce systemic side effects (Jafari et al., 2016; Quan et al., 2016; Lühder and Reichardt, 2017). Thus, it is of utmost interest to determine possible target cells responsible for GC-mediated anti-inflammatory actions and potential pathways that considerably improve GC therapy and reduce the risk for long-term treatment.

In this thesis we show for the first time that stromal cells, specifically FLS, are essential for the suppression of inflammatory arthritis by GCs. We further unraveled that GR dimerization is essentially required for suppression of osteophytes and a proper cross talk of FLS to macrophages, resulting in a shift towards an inflammation-resolving macrophage phenotype.

4.1. A dual role for GR dimerization in immune and stromal cells to suppress inflammation and osteophyte development

Mice with impaired GR dimerization (GR^{dim}) in STIA were resistant to GC actions with an ongoing inflammation and failure to suppress osteophyte formation. Dexamethasone (DEX) is shown to suppress osteophyte formation in osteoarthritis (OA) by direct actions on chondrocytes (Bajpayee et al., 2017). In contrast, we could show that impaired GR dimerization in radio resistant cells like chondrocytes (wt→GR^{dim}) did not affect DEX-mediated suppression of osteophytes in STIA, while GR dimerization in immune cells is essentially required. Interestingly, development of osteophytes is dependent on synovial macrophages, as clodronate depletion prior to OA-induction prevented osteophytes formation in two different experimental models of OA (Blom et al., 2004; van Lent et al., 2004). Moreover, intra-articular injections of the synthetic GC triamcinolone acetonide reduced osteophyte formation by inducing anti-inflammatory CD163-expressing macrophages (Siebelt et al., 2015). Interestingly, we could show that DEX-treatment induced CD163 solely in wt→wt mice but not in wt→GR^{dim} mice, but that osteophyte development was inhibited independently of GR dimerization. Direct targeting of macrophages with liposomal packed prednisolone equally induced CD163 expression in joints of immune complex-induced arthritis but not in AIA (Hofkens et al., 2013). In this regard we could show, that GR in immune cells is essentially required for osteophyte suppression in STIA, which in line with the literature indicates an important role for GCs on macrophages.

Macrophages are thought to control osteophyte formation through induction of different growth factors like TGFβ, and BMP-2 and -4 (van Lent et al., 2004). Interestingly, DEX treatment was shown to suppress BMP-signaling and instead to induce BMP-antagonists in osteoblast cell lines (Luppen et al., 2003; Hayashi et al., 2009). Moreover, macrophage-specific delivery of liposomal packed prednisolone results in down regulation of TGFβ in AIA and immune complex arthritis (Hofkens et al., 2013). In our wt→GR^{dim} mice, GR-dimerization is not impaired in immune cells including macrophages, and DEX treatment could possibly directly affect macrophages to regulate BMP- and TGFβ-signaling in

osteoblast or periosteal cells, resulting in the suppression of osteophyte formation. Further, TGFβ and BMP-2 expression is important in STIA-induced osteophyte formation and blocking the hedgehog-signaling pathway prevented the induction of TGFβ and BMP-2 in ankle mRNA and total serum as well as osteophyte formation without affecting the inflammatory score in STIA (Ruiz-Heiland et al., 2012). In DEX-treated wt→GR^{dim} mice a similar suppression of osteophytes without affected inflammatory score was detected, suggesting an independent mechanisms for osteophyte prevention and suppression of inflammation in STIA. Nevertheless, in OA, depletion of synovial macrophages by intra-articular injection of chlodronate also resulted in osteophyte suppression and was accompanied by a 50% reduction of infiltrating cells into knee joints (Blom et al., 2004). In our study, suppression of osteophytes was accompanied with suppression of Il-1β, TNFα and IFNγ but independent of the ongoing inflammation, implying a potential role for cytokine suppression in the process of osteophyte reduction. However, patients with psoriatic arthritis that also develop osteophytes, lack any improvement in osteophyte appearance after administration of TNFα inhibitors (Finzel et al., 2013). Although other cytokines could be involved, suppression of cytokines by DEX might not be a likely target to suppress osteophyte formation and the regulation might be independent of the inflammatory status of the joint. It rather involves the regulation of TGFβ and BMP by immune cells, presumably macrophages.

4.2. Cytokine suppression is not sufficient to suppress STIA

We and others showed that cytokine suppression is one of the hallmarks of GC treatment (Lee et al., 1988; Yang-Yen et al., 1990; Schüle et al., 1990; Heck et al., 1994; Barnes, 1998; Steer et al., 2000; Baschant et al., 2011; Coutinho and Chapman, 2011; Vettorazzi et al., 2015). Specifically, IL-1β and TNFα are essential for the initiation of STIA (Ji et al., 2002) and their expression correlates with disease severity in patients (Mateen et al., 2017) and mice (Kagari et al., 2002). Inhibition of TNFα or Il-1β by neutralizing antibodies abrogated CIA arthritis completely, although neutralizing antibodies were not administered therapeutically

but prior to CIA induction (Kagari et al., 2002). In the hTNFα arthritis model, therapeutically administration of TNFα inhibitors strongly suppress disease progression through decreased influx and increased apoptosis of classical (Ly6C+) macrophages (Huang et al., 2018). In our experiments, in contrast, DEX-mediated suppression of cytokines did not affect STIA progression in wt→GR^{dim} mice when administered in a therapeutic setting (Koenen et al., 2018). In addition, simultaneous administration of DEX together with induction of STIA sufficiently suppress serum cytokines, yet failed to abrogate disease development but strongly impaired STIA progression in wt mice (Koenen et al., 2018). One explanation might be a different effectiveness in the suppression of cytokines by DEX compared to neutralizing antibodies, as DEX treatment provided a strong suppression but not a complete absence of measurable serum cytokines. In this regard, Ji et al. (2002), failed to suppress STIA by the use of blocking anti-Il-1R antibodies mostly due to inefficient blockage of Il-1 (Ji et al., 2002). This is in agreement with trials in RA patients, where treatment with recombinant Il-1 receptor antagonist showed only weak effects (Burger et al., 2006).

TNFα inhibitors are more promising in RA patients with a clinical response rate of 20% improvement in 46-70% of the patients (defined by the American College of Rheumatology criteria for 20% improvement) (Mikuls and Weaver, 2003). Nevertheless, TNFα-inhibitors failed to exert effective disease remission and 20-40% of patients fail to respond at all to the therapy (Mikuls and Weaver, 2003). In responders, sensitive to TNFα-inhibitors, treatment can improve joint destruction (Smolen et al., 2005; Jung et al., 2014). Interestingly in this regard, Dennis and colleagues (2014) showed a correlation of effectiveness of TNFα-inhibitors with specific synovial phenotypes of patients (Dennis et al., 2014). Patients with a higher expression of myeloid, inflammatory M1 macrophage- and NFκB-associated genes in their synovial tissue responded much better to TNFα-inhibitors then patients with a gene expression pattern dominated by Il-6 and lymphoid genes or with a pauci-immune fibroid synovial phenotype (characterized by a low involvement of immune cells) (Dennis et al., 2014). They conclude, that the simple presence of inflammation does not predict clinical outcome to TNFα-inhibitors. In respect to this, the STIA mouse model is characterized by strong involvement of myeloid cells, although, its development depends on non-classical

Ly6C-negative monocytes and not on classical activated M1 macrophages (Misharin et al., 2014). Flow cytometry analysis of our wt→GR^{dim} mice revealed no changes in classical activated macrophage, indicating another possible explanation why the observed suppression of pro-inflammatory cytokines by DEX is insufficient to suppress STIA. This seems to be the case also in other types of inflammation. A study of acute lung injury (Vettorazzi et al., 2015) revealed that suppression of cytokines was not sufficient to resolve inflammation. Interestingly, suppression of inflammation in acute lung injury also depended on a functional GR dimerization (Vettorazzi et al., 2015). GC-mediated suppression of pro-inflammatory cytokines Il-6, INFγ and IL-17 in antigen-induced arthritis (Baschant et al., 2011) and of INFγ and TNFα in our STIA experiments completely depends on an intact GR dimerization. Comparing complete GR^{dim} mice with our bone marrow chimeric wt→GR^{dim} mice, suggested that cytokine suppression of TNFα and IFNγ was regulated by direct action on immune cells. This is supported by the inability of mice with GR-deficient macrophages to suppress LPS-induced TNFα and Il-6 (Bhattacharyya et al., 2007). Surprisingly, however, interleukin-1β was suppressed independently of GR dimerization in STIA, although, isolated GR^{dim} macrophages stimulated with Lipopolysaccharides (LPS) also fail to suppress interleukin-1β (Tuckermann et al., 2007). We assume that suppression of Il-1β in STIA is regulated by monomeric GR in cells other than macrophages or that the prevalent amount of Il-1β found in STIA might not be produced by macrophages. Thus, cytokine suppression by direct actions of GCs on immune cells is insufficient to suppress STIA; instead, GR actions in stromal cells are essential to initiate DEX-mediated suppression of STIA.

4.3. GR dimer-dependent induction of non-classical macrophages suppresses STIA

GCs suppress antigen-induced arthritis (AIA) by direct effects on immune cells (Baschant et al., 2011; Hofkens et al., 2013). Analysis of conditional GR-deficient

mice revealed that T-cells but not macrophages were indispensable in GC-mediated suppression of AIA (Baschant et al., 2011), although, direct targeting of macrophages with liposomal packed prednisolone decreased AIA (Hofkens et al., 2013), however, the potential leakage of liposomes might have an additional affect on other cells. Direct targeting of macrophages with liposomal packed prednisolone decreased pro-inflammatory macrophages but did not favor anti-inflammatory macrophages in AIA (Hofkens et al., 2013). In STIA, in contrast, we show that GR is dispensable in immune cells but crucial in stromal cells, specifically FLS to mediate the anti-inflammatory effects of GCs (Koenen et al., 2018). Although changes in the amount of classical activated macrophages were missing, we observed an increase of anti-inflammatory macrophages in DEX-treated wt→wt but not wt→GR^{dim} chimeric mice, leading to a shift of the ratio in favor of anti-inflammatory macrophages (Koenen et al., 2018). These anti-inflammatory Ly6C, MHCII double-negative macrophages were shown to be essential for the natural resolution of STIA (Misharin et al., 2014). The failure of GCs to induce these anti-inflammatory macrophages when directly delivered to macrophages by liposomal-packing (Hofkens et al., 2013) supports our finding that a cross talk of macrophages with FLS is required to induce this phenotype. Nevertheless, Hofkens and colleagues (2013) showed that direct targeting of macrophages in immune complex-induced arthritis results in the induction of CD163, but no other anti-inflammatory macrophage marker genes. CD163 is solely expressed on cells of the myeloid lineage (Heuvel et al., 1999) and its major function is the clearance of toxic free hemoglobin in the blood (Kristiansen et al., 2001). Anti-inflammatory macrophages show a strong CD163 expression that was suggested to dampen inflammation by scavenging components generated by damaged cells (Moestrup and Møller, 2004). In addition, as pattern recognition molecule, CD163 is involved in innate host defense against pathogens (Fabriek et al., 2009) and promotes recognition and phagocytosis of bacteria (Kneidl et al., 2012). Moreover, CD163 neutralizing antibody RM3/1 prevents the adhesion of DEX-treated monocytes to activated endothelial cells (Wenzel et al., 1996; Högger et al., 1998), indicating a role of CD163 in transendothelial migration. Several studies support, our finding of GC-mediated induction of CD163 (Wenzel et al., 1996; Varga et al., 2008; Siebelt et al., 2015) and vice versa that pro-inflammatory mediators like IFNγ and TNFα suppress CD163 (Buechler et al., 2000). In

agreement with the finding of Hofkens et al. (2013), we demonstrated that sole induction of CD163 is not sufficient to induce an anti-inflammatory macrophage phenotype, as CD163-deficient mice, similar to control mice, were able to suppress STIA by DEX-treatment. Besides CD163, qRT-PCR revealed that DEX induced the expression of additional genes associated with phagocyting anti-inflammatory macrophages substantially in wt→wt but not wt→GR^{dim} mice (CD36, AnxA1, Axl, MerTK and Tyro3). Induction of phagocytosis of apoptotic cells, a mechanism also called efferocytosis (Elliott et al., 2017), is essential for tissue homeostasis and the lack of proper cell clearance can induce autoimmune reactions (Poon et al., 2014).

Specifically, secondary necrotic neutrophils derived from un-cleared apoptotic neutrophils secrete huge amounts of Interleukin-16C (Roth et al., 2015), which is also enhanced in RA patients and associated with joint destruction (Lard et al., 2004). Serum interleukin-16C measurements of GR^{flox} and $GR^{Col1a2\text{-}ERT}$ mice treated with PBS or DEX revealed a strong trend for increased Il-16C levels in DEX-treated $GR^{Col1a2\text{-}ERT}$ mice compared to DEX-treated GR^{flox} mice (p=0,08 by two-way ANOVA, data not shown). This supports our hypothesis that the lack of non-classical, non-activated macrophages detected by flow cytometry and the lack of increased *mRNA* levels of genes involved in phagocytosis, affects efferocytosis efficiency in $GR^{Col1a2\text{-}ERT}$ mice.

Van Lent et al. (2001) showed that synovial lining macrophages phagocyte apoptotic neutrophils and that induction of this process by injection of apoptotic neutrophils reduced immune complex-induced arthritis by inhibiting neutrophil migration. We found CD36 induced in a GR dimer dependent manner after DEX treatment. Interestingly, CD36 was demonstrated to be required for phagocytosis of apoptotic cells in macrophages and antibody-mediated blockade or silencing of CD36 suppressed efferocytosis (Fadok et al., 1998; Kim et al., 2017). Furthermore, the induction of CD36 was dependent on nuclear factor E2-related factor-2 (Nrf2) and Nrf2-deficient mice fail to mediate efferocytosis (Kim et al., 2017) and display accelerated STIA with increased leukocyte migration and joint destruction (Maicas et al., 2011). Nrf2 target genes are regulated in a GR dependent manner by recruitment of the co-repressor SMART (Ki et al., 2005). Whereas low-dose GC treatment (10-100mM) results in decreased target gene

expression, high dose (1µM) GCs surprisingly results in their induction in liver hepatoma cells (Ki et al., 2005). Translocation and activation of Nrf2 itself, however is not affected by GCs (Alam et al., 2017). Thus, DEX-induction of CD36 might be independent of Nrf2 or regulated by a different mechanism as GC-mediated effects strongly vary between different cell types and their chromatin landscape (Grøntved et al., 2013; Uhlenhaut et al., 2013).

Another gene associated with increased phagocytosis that was up regulated in DEX-treated wt→wt but not DEX-treated wt→GR^{dim} mice was Annexin A1 (AnxA1). In arthritis, AnxA1 is strongly increased in synovial macrophages and neutrophils (Goulding et al., 1995; Perretti and Flower, 1996; Patel et al., 2012). When neutrophils undergo secondary necrosis, AnxA1 is externalized, cleaved and the derived N-terminal peptide acts as a chemo-attractant to recruit macrophages (Blume et al., 2012). Interestingly, AnxA1-deficient mice generate less phagocyting cells (Hannon et al., 2003) with an impaired clearance of apoptotic cells by macrophages (Maderna et al., 2005). In addition, DEX induced efferocytosis in macrophages can be blocked by Anxa1-depletion in vitro (Maderna et al., 2005). In this regard, we could show that DEX-mediated induction of efferocytosis in GR-deficient macrophages is induced by direct contact to wt but not GR^{dim} FLS.

Strikingly, AnxA1 is a classical GR-dimer associated target gene with a classical GRE located in the promoter region (Kovacic et al., 1991) and in an acute model of carrageenan-induced paw edema, AnxA1-deficient mice were partially resistant to DEX treatment, associated with a lack of suppression of neutrophil emigration (Hannon et al., 2003). In contact allergy, impaired recruitment of neutrophils and macrophages in mice with GC-deficient neutrophils and macrophages was dimer dependent and thought to be regulated by impaired suppression of cytokines (IL1β, MCP-1 and Mip-2) (Tuckermann et al., 2007). In addition, Ricci et al. (2017) reported that DEX-mediated neutrophil migration depends on Gilz, a classical GR dimer target gene and its regulation of AnxA1. Implying an important role for DEX-mediated AnxA1 in neutrophil and macrophage recruitment

In arthritis, AnxA1-deficiency was associated with increased levels of IL-1β, TNFα and IL-6 and an accelerated histological score (Yang et al., 2004). Intriguingly,

AnxA1-deficient mice are resistant to GC-treatment in STIA (Patel et al., 2012) and treatment with AnxA1 induces a shift from pro- to anti-inflammatory macrophage phenotype *in vitro* (Li et al., 2011). Interestingly, only cleavage-protected but not full-length AnxA1 could slightly attenuate STIA progression (Patel et al., 2012). AnxA1 treatment however was not as potent as GC treatment in STIA (Patel et al., 2012), implying an additive effect of other DEX-induced efferocytosis-associated genes in the suppression of STIA.

Next to the GR dimer-dependent up regulation of CD163, CD36 and AnxA1, DEX-treated wt→wt also displayed a dimer-dependent increase in the expression of TAM receptors MerTK and Axl and a trend for Tyro3. Triple mutants of TAM receptors develop autoimmunity (Lu and Lemke, 2001), similarly observed in RA patients (Stuart et al., 1984) and MerTK and Axl double-deficient mice display a lack of apoptotic cell clearance, induction of autoimmunity (Seitz et al., 2007) and worsening of STIA (Waterborg et al., 2017). Interestingly, MerTK-deficiency resulted in an accelerated disease development at an early stage (day 2) whereas Axl-deficiency leads to accelerated inflammation at a later stage (day 7) (Waterborg et al., 2017). This is supported by our findings that MerTK was induced only at an early time-point after DEX-treatment (72h), but not after 10 days, while Axl was continuously increased by DEX. In addition, MerTK-deficient mice had up regulated levels of Interleukin-16C (Waterborg et al., 2018), which was similarly up regulated by trend in DEX-treated $GR^{Col1a2\text{-}ERT}$ mice, resistant to GC treatment. Interestingly, although macrophages from mice with a truncated signaling tyrosine kinase domain of MerTK (Mer^{kd}) show impaired efferocytosis efficiency, phagocytosis of bacteria and latex beads was not affected (Scott et al., 2001). This is relevant, for the design of future *in vivo* experiments to functionally validate impaired efferocytosis in wt→GR^{dim} mice resistant to GC treatment. Importantly, we also detected a GR dimer-dependent increased expression of Gas6 in Il-1β- and DEX-treated wt FLS but not GR^{dim} FLS. Gas6 is a ligand of the TAM receptors, with highest affinity to Axl that also bind to phospholipids on apoptotic cells (Lew et al., 2014). Strikingly, systemic and intra-articular overexpression of Gas6 reduces inflammation and joint destruction in CIA mice (van den Brand et al., 2013).

The failure of wt→GR^{dim} mice to increase the expression of these anti-inflammatory macrophage associated genes (CD163, CD36, AnxA1 and TAM receptors), after DEX treatment together with a lack of Gas6 induction in GR^{dim} FLS and slightly increased Il-16C serum levels in GC resistant GR$^{Col1a2\text{-}ERT}$ mice, could point towards an impaired clearance of apoptotic cells after DEX treatment, leading to an ongoing inflammation. Of note, DEX itself can induce apoptosis, resulting in an increased need for apoptotic cell clearance dependent on anti-inflammatory macrophages. This hypothesis is supported by the failure of Mer^{kd} mice to clear a DEX-induced apoptotic cell burden in the thymus (Scott et al., 2001). To test whether GCs induce increased apoptosis in wt→wt / wt→GR^{dim} and GR^{flox} / GR$^{Col1a2\text{-}ERT}$ mice and whether GR mutant mice fail to clear the apoptotic cell burden, needs to be validated in future *in vivo* experiments.

Recently it was shown that induction of anti-inflammatory macrophages by SIRT1-overexpression results in a reduced joint swelling and disease severity in CIA mice (Park et al., 2017). These results support our findings that anti-inflammatory macrophages play a prominent role in the suppression of STIA. As mentioned above and shown by our analysis of bone marrow chimeric mice, direct GC-targeting to immune cells like macrophages is not sufficient to increase the fraction of anti-inflammatory macrophage (Hofkens et al., 2013). In combination with our analysis of GR$^{Col1a2\text{-}ERT}$ mice we characterized FLS as mediators of the GC-induced rise of anti-inflammatory macrophages.

In our experiment, DEX-treated GR^{flox} mice show a robust induction of non-classical and non-activated macrophages compared to PBS-treated GR^{flox} mice, this is however different from DEX-treated GR$^{Col1a2\text{-}ERT}$ mice, showing no induction of non-classical and non-activated macrophages compared to PBS-treated GR$^{Col1a2\text{-}ERT}$ mice. This leads to a change of the ratio of non-activated versus activated macrophages in favor of non-activated macrophages in GR^{flox} mice that is absent in GR$^{Col1a2\text{-}ERT}$ mice, supporting our results from DEX-treated wt→GR^{dim} chimeric mice. However, PBS-treated GR$^{Col1a2\text{-}ERT}$ mice show surprisingly high levels of non-classical and non-activated macrophages, compared to PBS-treated GR^{flox} mice. Inexplicably, GR$^{Col1a2\text{-}ERT}$ mice also displayed a delayed onset of disease that might suggest a protective role of GR-deficiency in FLS. In osteoblasts, suppression of endogenous GC-signaling, through overexpression of

the GC-inactivating enzyme 11β-HSD-2 resulted in an attenuation of swelling and inflammation, indicating an inflammatory role of GC-signaling in osteoblasts (Buttgereit et al., 2009). In contrast, Coutinho et al. (2012) showed that deficiency of 11β-HSD-2 had no effect on STIA while deficiency in 11β-HSD-1, the enzyme that activates endogenous GC-signaling worsens STIA as expected (Coutinho et al., 2012). Interestingly, mice that solely overexpress 11β-HSD-2 in osteoblasts additionally showed an induction of macrophage colony-stimulating factor (M-CSF) in serum at day 7 compared to healthy transgenic mice (Buttgereit et al., 2009). M-CSF is necessary for monocyte differentiation and proliferation and can be suppressed by GC treatment (Ishii et al., 1983; Popova et al., 2011). Interestingly, fibroblasts were shown to produce M-CSF (Fibbe et al., 1988) enabling a potentially increased expression in GR-deficient FLS in our $GR^{Col1a2\text{-}ERT}$ mice compared to GR^{flox} mice. Increased M-CSF could potentially increase the differentiation of Ly6C-negative monocytes to non-classical Ly6C-negative macrophages and thus dampen STIA development. In contrary, injections of M-CSF in CIA mice revealed a pro-inflammatory role of M-CSF (Campbell et al., 2000), however, CIA in contrast to STIA is not characterized by a pivotal role of Ly6C-negative monocytes for disease development (Misharin et al., 2014).

In general, the effects on cell composition in GR^{flox} and $GR^{Col1a2\text{-}ERT}$ mice were less pronounced compared to wt→wt and wt→GR^{dim} mice. This might be due to a lower incidence and reduced severity of STIA, compared to wt→wt and wt→GR^{dim} mice. Interestingly, Ji et al. (2001) reported a variety of responses in different mouse strains, with C57BL/6 mice showing a slower disease development with a peak of ankle thickness around day 10 compared to Balb/c mice showing the peak paw swelling at day 4 (Ji et al., 2001). GR^{flox} and $GR^{Col1a2\text{-}ERT}$ littermates are C57BL/6-derived and revealed delayed and less severe development of STIA with a complete lack or only a low-grade inflammation in half of the mice, resulting in a low number of animals with a full-blown disease for further analysis. This was not observed in Balb/c-derived wt→wt and wt→GR^{dim} littermates. Although, the general percentage of hematopoietic and myeloid infiltrate was not changed in GR^{flox} /$GR^{Col1a2\text{-}ERT}$ mice, neutrophil (Ly6G+) content in PBS-treated mice compared to PBS-treated chimeric mice, was almost doubled, whereas infiltrating (Ly6C+) monocytes were strongly reduced. This is important because neutrophils are the first responders to inflammatory stimuli with macrophages following

recruitment. These differences suggest that the time point for the flow cytometer analysis in GR^{flox} /$GR^{Col1a2\text{-}CreERT}$ mice, resembles an earlier phase in STIA progression, compared to wt→wt / wt→GR^{dim} mice.

Nevertheless, GR^{flox} control mice showed a clear trend towards an induced fraction of non-classical, non-activated macrophages after DEX-treatment, which is supported by the significant shift of the ratio in favor of non-activated macrophages to activated macrophages, absent in $GR^{Col1a2\text{-}CreERT}$ mice. In addition, we also detected an increased induction of efferocytosis in Il-1β- and DEX-treated macrophages co-cultured with wt FLS, which was absent in co-cultures with GR^{dim} FLS indicating an important role for FLS in the induction of anti-inflammatory macrophages. In addition, our finding was underlined by a study on rat AIA showing that direct targeting of FLS by peptide-bound liposomal packed prednisolone also reduces experimental arthritis (Vanniasinghe et al., 2014). In this context, one might speculate that direct targeting of FLS with prednisolone might also affect anti-inflammatory macrophages.

Thus, we can conclude, that GCs directly target FLS, which subsequently induce anti-inflammatory macrophages that show an increased efferocytosis activity and are shown to mediate resolution in STIA (Misharin et al., 2014).

4.4. GR in FLS, but not other non-immune cells, mediate the anti-inflammatory effects in STIA

At present there are only a few studies analyzing the effect of FLS on macrophage. Here we show that DEX-stimulated wt FLS can increase the efferocytosis efficiency of macrophages and demonstrate that the induction is GR dimer-dependent. In a co-culture system of peritoneal macrophages and lung fibroblasts, expression of the cell adhesion molecule-1 (ICAM-1) was shown to mediate the induction of the macrophage-recruiting factor “macrophage inflammatory protein-1α" (Mip-1α) (Steinhauser et al., 1998). Similarly, this was

demonstrated for RA-derived FLS when co-cultured with macrophages and monocytes (Blue et al., 1993; Hanyuda et al., 2003).

Hierarchical clustering analysis of differentially expressed genes from RNA sequencing of wt and GR^{dim} FLS treated with Il-1β alone or in combination with DEX, revealed a clear cluster separation by treatment within the same genotype, suggesting a clear effect of DEX treatment on several genes independent of the genotype. When comparing wt and GR^{dim} FLS treated with Il-1β and DEX we found a clear clustering by genotype, however, many of the effected genes were still regulated in the same direction but less effective. Specifically GR dimer-dependent target genes were often not completely abolished in GR^{dim} FLS but dramatically less induced, indicating a residual GR dimerization ability in these cells. This is supported by several studies showing that GR^{dim} mice only have a strong impairment of GR dimerization but not a complete lack (Jewell et al., 2012; Lim et al., 2015). Nevertheless, this impaired GR dimerization was demonstrated to strongly affect suppression of different inflammatory models by GCs (Baschant et al., 2011; Tuckermann et al., 2007; Vandevyver et al., 2012; Vettorazzi et al., 2015).

Interestingly, RNA sequencing from wt and GR^{dim} FLS treated with Il-1β alone or in combination with DEX revealed increased levels of ICAM-1 in GR^{dim} FLS after Il-1β+DEX treatment, due to the lack of suppression by DEX in GR^{dim} FLS. In addition, GR^{dim} FLS treated with IL-1β and DEX secreted significantly higher amounts of Mip-1α into their supernatant than corresponding wt FLS. Steinhauser et al. (1998) reported that co-cultures of macrophages with FLS deficient for ICAM-1 produce significantly lower amounts of Mip-1α (Steinhauser et al., 1998)and neutralizing ICAM-1 in RA FLS supported this findings (Hanyuda et al., 2003). In contrast to our finding, lung fibroblast and RA-derived FLS cultured alone did not secrete Mip-1α (Hanyuda et al., 2003; Steinhauser et al., 1998). Strikingly, Mip-1α-deficient mice developed milder CIA with a reduced histo-pathological score (Chintalacharuvu et al., 2005), underlining our hypothesis that impaired suppression of Mip-1α is important for ongoing inflammation in DEX-treated wt→GR^{dim} mice. In addition, macrophages were shown to directly interact with ICAM-1 on squamous cell carcinoma cells (Usami et al., 2013), indicating an essential function of ICAM-1 in FLS-macrophage cross talk. Interestingly, mice

with a triple knock-out of the TAM receptors (MerTK, Axl and Tyro3) also show increased expression of ICAM-1 on endothelial cells (Lu and Lemke, 2001), suggesting a feed-back of TAM receptor signaling with other cells, that subsequently induce ICAM-1. Whether TAM-receptor-deficiency also affects ICAM-1 expression on FLS, still needs to be determined, however, the results of TAM-deficient mice reveal a potential interaction of TAM receptors and ICAM-1 expression in mice. In this regard, we observed a significant induction of TAM receptors after DEX treatment in STIA that depends on GR dimerization in FLS. Further, we showed that DEX-treated wt FLS strongly suppress ICAM-1 expression, which is not the case in DEX-treated GR^{dim} FLS. The impaired suppression of ICAM-1 in GR^{dim} FLS, thus, might affect the induction of TAM receptors on macrophages and result in the ongoing inflammation in DEX-treated wt→GR^{dim} mice. Moreover, in agreement with an increased efferocytosis observed in DEX-treated co-cultures of wt FLS with macrophages, which is absent from GR^{dim} FLS, co-cultured with macrophages, we also detected a reduced secretion of Mip-1α in wt FLS compared to GR^{dim} FLS. A potential connection of increased efferocytosis with decreased Mip-1α expression is supported by the suppression of Mip-1α in macrophages after efferocytosis of apoptotic cells (McDonald et al., 1999). The induction of efferocytosis associated genes (TAM receptors, AxA1, CD36) in DEX-treated wt→wt mice might thus be involved in suppression of Mip-1α.

In OA-fibroblasts, expression of ICAM-1 was down regulated by induction of miR146a (Yang et al., 2014). Interestingly in this regard, miR146a-deficiency resulted in an increased STIA development (Saferding, 2015) and increased synovial inflammation in the hTNFa model (Saferding et al., 2017). In addition, RNA sequencing and functional analysis revealed that loss of miR146a led to increased proliferation and elevated metabolic activity of FLS (Saferding et al., 2017). In course of our RNA sequencing analysis, we obtained results indicating a lack of suppression of the pro-proliferative genes, Cdk1 and Cdkn3, in GR^{dim} FLS compared to wt FLS. Moreover, pathway enrichment analysis revealed a strong enrichment for cell cycle and cell adhesion molecules in GR^{dim} FLS.

Taken together, our results suggest a disease-associated pathology for increased proliferation of FLS. It is longstanding knowledge, that the synovium in RA patients

develops hyperplasia, however, it is still unclear whether increased proliferation (Mohr et al., 1975; Qu et al., 1994), reduced apoptosis (Miagkov et al., 1998) or invasion of immune cells into the synovium accounts for these pathological changes.

Our findings indicate an important role for FLS proliferation in arthritis. Saferding et al (2017) suggested a pivotal role of TRAF6 in controlling miR146a dependent FLS proliferation, however, in our experiments TRAF6 was not differentially expressed between wt and GR^{dim} FLS. In addition, compared to wt FLS we detected a strong enrichment for the p53 pathway in GR^{dim} FLS treated with Il-1β and DEX. It should be noted that p53 mutations are associated with increased synovial proliferation, decreased apoptosis and increased invasiveness (Aupperle et al., 1998), however, the impact of GR dimerization on p53 signalling pathway needs to be investigated.

Migration of FLS can be induced also by sphingosine-1-phosphate (S1P) via interaction with its receptor S1P receptor 1 and 3 (S1PR-1 and -3) (Zhao et al., 2008). Interestingly, our RNA sequencing data revealed that S1PR-3 was significantly higher expressed in GR^{dim} FLS than in wt FLS when treated with IL-1β and DEX. Moreover, in acute lung injury induction of S1P levels was dependent on the GR dimer-dependent induction of Sphk-1 resulting in an anti-inflammatory effect (Vettorazzi et al., 2015). In arthritis, however, Sphk-1 has a pro-inflammatory effect and Sphk-1-deficient mice are partially protected against hTNFα arthritis (Baker et al., 2010). In this respect, *in vivo* DEX-treated wt→wt mice show significantly lower Sphk-1 expression then wt→GR^{dim} mice after 24h (data now shown) and our FLS data revealed that GR dimerization is also critical for the regulation of the receptor of S1P in arthritis. In addition, Kitano et al. (2006) showed that S1P increases the proliferation and expression of pro-inflammatory mediators in FLS isolated from RA patients and that S1PR-1 similarly was increased in RA FLS (Kitano et al., 2006). Interestingly, S1P treatment of FLS did not result in secretion of Mip1α or Mip-1β (Zhao et al., 2008), however, it was shown to induce the expression of ICAM-1 and the adhesion of monocytes to alveolar epithelial cells (Lin et al., 2016). Furthermore, the induction of ICAM-1 by S1P is mediated by the p38 MAPK signaling pathway, dependent on S1PR-1 and-3 in alveolar epithelial cells (Lin et al., 2015). In this regard, it was shown that p38

inhibition prevents collagen-induced arthritis, improves bone destruction and suppression was almost comparable to prednisolone treatment (Mihara et al., 2008). In addition, the therapeutic effects of oral p38 inhibitors were examined in clinical trials for RA patients but so far did not succeed, however, these studies revealed a dose-related toxicity (Cohen and Fleischmann, 2010). Recently, Vettorazzi et al. (2015) reported that GR dimer in combination with p38 signaling pathways were necessary to induce the anti-inflammatory response of GCs in acute lung injury. In addition, DEX-treatment of macrophages inhibited p38 MAPK in macrophages (Bhattacharyya et al., 2007). Moreover, p38 inhibition was associated with the induction of Dusp-1 (Bhattacharyya et al., 2007), a classical activated GR dimer-dependent target gene of GCs and Dusp-1-deficiency results in increased severity in CIA (Vattakuzhi et al., 2012). Accordingly, compared to our wt FLS, Dusp-1 was significantly less expressed in GR^{dim} FLS treated with Il-1β and DEX. Similarly, the classical GR dimer target genes Gilz, Mt-1 and Mt-2 were less expressed in GR^{dim} FLS treated with Il-1β and DEX. Despite increased levels of Mt-1 and Mt-2 detected *in vivo* and *in vitro* and anti-inflammatory effects of Metallothionein administration in CIA (YOUN et al., 2002), we could show that deficiency of Mt-1/-2 in mice did not result in resistance to GC treatment in STIA. Gilz on the other hand was shown to affect DEX mediated migration of neutrophils via the control of AnxA1 expression (Ricci et al., 2017) and depletion of endogenous Gilz by siRNA treatment worsened CIA arthritis (Beaulieu et al., 2010). In addition, adenoviral injections of GILZ into knee joints of CIA mice leads to a significant reduced severity of arthritis (Ngo et al., 2013) and Gilz-overexpression was shown to inhibit ICAM-1 and p38 and to increase DUSP-1 expression (Cheng et al., 2013). Thus, the absence of Gilz and Dusp-1 induction in GR^{dim} FLS might result in increased ICAM-1 expression, which consequently prevents Mip-1α suppression and induces adhesion to macrophages.

Taken together, our data imply an important role for GC inhibition of cell adhesion and proliferation in FLS, to regulate the interaction of FLS with macrophages by inhibition of chemokines and cell-cell contact, potentially resulting in the induction of anti-inflammatory macrophages and finally suppression of inflammatory arthritis.

4.5. Working model and relevance for future direction in research and therapy

In the present study we show that non-immune cells, specifically FLS are essentially required for the suppression of STIA. Furthermore, we demonstrate that GR dimer in non-immune cells substantially influence the cross talk of FLS and macrophages, leading to the induction of anti-inflammatory macrophages, and an increased efferocytosis activity. Strikingly, the suppression of cytokines was not essentially involved in this cross talk, as their suppression was insufficient to suppress STIA. RNA sequencing provided several potential target genes that could mediate this interaction instead, namely Mip-1α and -β as well as Icam-1, S1PR3, Gilz and Dusp-1. Their involvement, however, needs to be further validated by protein and functional analysis. Further, we show that the reduction of osteophytes was independent of the ongoing inflammation in the ankles and suppressed by a GR dimer-dependent mechanism in immune cells, presumably macrophages (Figure 4.1).

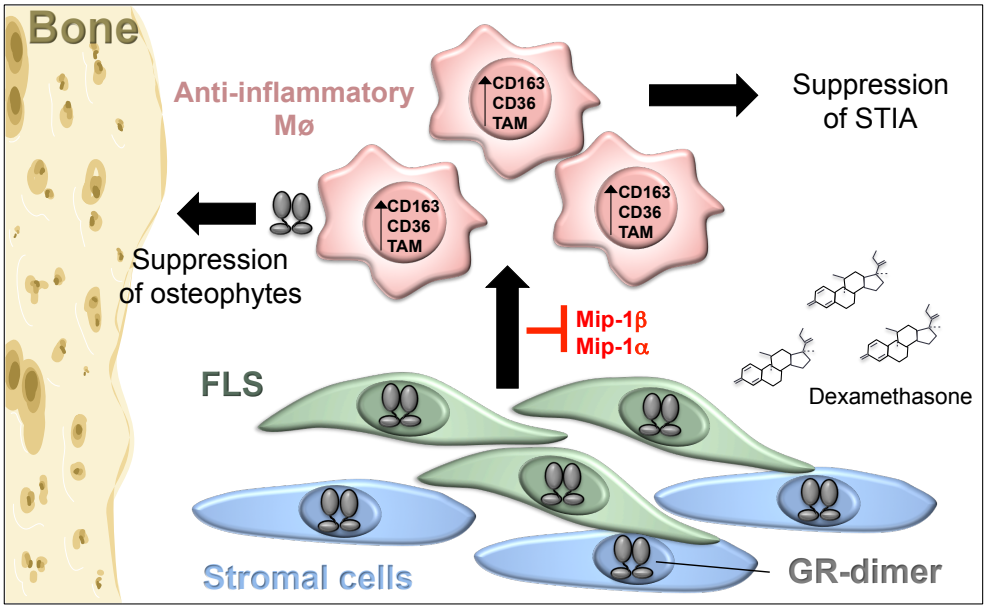

Figure 4.1 Schematic model of the GC-mediated suppression of STIA and osteophyte development

GCs directly act *via* GR dimer in stromal cells, like FLS, to induce anti-inflammatory macrophages that resolve inflammation. The suppression of Mip-1α and -β might be an essential factor in the cross talk of FLS and macrophages in STIA. Osteophyte development, however, is regulated by the GR dimer in immune cells, presumably in macrophages, independent of the ongoing inflammation. GR=glucocorticoid receptor, Mip=macrophage inflammatory protein, FLS=fibroblast-

like synoviocytes. (Parts of this artwork were published in Koenen et al., 2018 under a CC BY-NC 4.0 license, https://creativecommons.org/licenses/by-nc/4.0/deed.de).

These findings are important for the potential development of new treatment strategies in arthritis, because they highlight the importance of non-immune cells, specifically FLS as potential target cells for a cell type-specific GC-delivery. This is underlined by the study of Vanniasinghe et al. (2014) that demonstrated that peptide-coupled liposomal delivery of GCs directed to FLS successfully suppresses AIA (Vanniasinghe et al., 2014). Furthermore, we offer a potential explanation why cytokine-inhibitors are sometimes less successful than expected, which in case of TNFα-Inhibitors was associated with an FLS-driven phenotype in RA patients (Dennis et al., 2014). Our results also provide potential new target genes, which might be used independent of GC therapy, to prevent negative side effects of GC treatment. Hereof, induction of anti-inflammatory macrophage genes (CD163, CD36, AnxA1 and the TAM receptors) offer a potential strategy to suppress arthritis, whereas suppression of Mip-1α and -β and potentially Icam-1 and S1PR3 could be valuable for GC-independent suppression of arthritis. Interestingly, it was shown that apoptotic cells induces efferocytosis (Elliott et al., 2017) and that injection of apoptotic cells suppresses arthritis (Bonnefoy et al., 2016). In addition, the induction of CD163 also might provide favorable aspects for the reduction of osteophytes (Siebelt et al., 2015).

Future research should focus on the exploration of the interplay of FLS with macrophages and the potential impact of the detected target genes in the induction of anti-inflammatory macrophages. Direct targeting of FLS and its impact on anti-inflammatory macrophages by GCs should be tested in the STIA model and rescue experiments of GR^{dim} mice by substitution with apoptotic cells in STIA might offer validation of the role of induced efferocytosis in suppression of STIA.

Taken together, further analysis of the GC-induced anti-inflammatory cross talk between FLS and macrophages will provide novel rationales for therapies with higher efficiency and may avoid side effects of steroid therapy.

5. Summary

Rheumatoid arthritis (RA) is a severe inflammatory autoimmune disease affecting approximately 1% of the world's population and glucocorticoids (GCs) are still among the most frequently prescribed drugs to suppress inflammation in RA. However, GCs are under constant clinical audit due to detrimental side effects on bone homeostasis and metabolism, thus, revealing the necessity to improve treatment strategy. Although many studies have been conducted, the understanding of the critical cell types, especially considering the role of non-immune cells and their cross talk with other cells, a prevalent characteristic of RA, is still surprisingly vague.

The glucocorticoid receptor (GR) is a ligand-induced transcription factor that can act as a monomeric or dimeric molecule. A longstanding view considered repression of cytokines by the GR monomer in immune cells as the pivotal mechanism; however, here we show that cytokine suppression is mostly GR dimer-dependent but insufficient to suppress serum transfer-induced arthritis (STIA). Moreover, we demonstrate that GR dimers instead are crucial to mediate anti-inflammatory effects in non-immune cells, specifically fibroblast-like synoviocytes (FLS), to induce anti-inflammatory macrophages. GC treatment of co-cultures of FLS and macrophages revealed a GR dimer-dependent induction of the ability to clear an apoptotic cell burden, a process called efferocytosis. Strikingly, efferocytosis and anti-inflammatory macrophages are reported to mediate the spontaneous resolution of STIA and thus, GCs might induce the same processes involved in spontaneous resolution of inflammation. Interestingly, we further could show that GCs suppress osteophyte formation in STIA in a GR dimer-dependent mechanism, however, in contrast to inflammation, this process essentially requires GR in immune cells.

Taken together, we identified a major role for GR dimers in FLS to suppress arthritis by GCs through regulating the interplay of these FLS with macrophages. Exploiting the GC-induced anti-inflammatory cross talk between FLS and macrophages will provide novel rationales for therapies with higher efficiency and may avoid adverse side effects of steroid therapy.

6. References

Afridi, H.I., Kazi, T.G., Talpur, F.N., Naher, S., and Brabazon, D. (2014). Relationship between toxic metals exposure via cigarette smoking and rheumatoid arthritis. Clin. Lab. *60*, 1735–1745.

Ai, R., Hammaker, D., Boyle, D.L., Morgan, R., Walsh, A.M., Fan, S., Firestein, G.S., and Wang, W. (2016). Joint-specific DNA methylation and transcriptome signatures in rheumatoid arthritis identify distinct pathogenic processes. Nature Communications *7*, 11849.

Alam, M.M., Okazaki, K., Nguyen, L.T.T., Ota, N., Kitamura, H., Murakami, S., Shima, H., Igarashi, K., Sekine, H., and Motohashi, H. (2017). Glucocorticoid Receptor Signaling Represses the Antioxidant Response by Inhibiting Histone Acetylation Mediated by the Transcriptional Activator NRF2. J. Biol. Chem. jbc.M116.773960.

Annefeld, M. (1992). Changes in rat epiphyseal cartilage after treatment with dexamethasone and glycosaminoglycan-peptide complex. Pathol. Res. Pract. *188*, 649–652.

Aupperle, K.R., Boyle, D.L., Hendrix, M., Seftor, E.A., Zvaifler, N.J., Barbosa, M., and Firestein, G.S. (1998). Regulation of synoviocyte proliferation, apoptosis, and invasion by the p53 tumor suppressor gene. Am. J. Pathol. *152*, 1091–1098.

Bajpayee, A.G., De la Vega, R.E., Scheu, M., Varady, N.H., Yannatos, I.A., Brown, L.A., Krishnan, Y., Fitzsimons, T.J., Bhattacharya, P., Frank, E.H., et al. (2017). Sustained intra-cartilage delivery of low dose dexamethasone using a cationic carrier for treatment of post traumatic osteoarthritis. Eur Cell Mater *34*, 341–364.

Baker, D.A., Barth, J., Chang, R., Obeid, L.M., and Gilkeson, G.S. (2010). Genetic sphingosine kinase 1 deficiency significantly decreases synovial inflammation and joint erosions in murine TNFα-induced arthritis. J Immunol *185*, 2570–2579.

Bakker, M.F., Jacobs, J.W.G., Welsing, P.M.J., Verstappen, S.M.M., Tekstra, J., Ton, E., Geurts, M.A.W., van der Werf, J.H., van Albada-Kuipers, G.A., Jahangier-de Veen, Z.N., et al. (2012). Low-dose prednisone inclusion in a methotrexate-

based, tight control strategy for early rheumatoid arthritis: a randomized trial. Ann. Intern. Med. *156*, 329–339.

Barnes, P.J. (1998). Anti-inflammatory actions of glucocorticoids: molecular mechanisms. Clin. Sci. *94*, 557–572.

Baron, R., and Kneissel, M. (2013). WNT signaling in bone homeostasis and disease: from human mutations to treatments. Nat. Med. *19*, 179–192.

Bartok, B., and Firestein, G.S. (2010). Fibroblast-like synoviocytes: key effector cells in rheumatoid arthritis. Immunol Rev *233*, 233–255.

Baschant, U., Frappart, L., Rauchhaus, U., Bruns, L., Reichardt, H.M., Kamradt, T., Bräuer, R., and Tuckermann, J.P. (2011). Glucocorticoid therapy of antigen-induced arthritis depends on the dimerized glucocorticoid receptor in T cells. Proc. Natl. Acad. Sci. U.S.A. *108*, 19317–19322.

Baschant, U., Lane, N.E., and Tuckermann, J. (2012). The multiple facets of glucocorticoid action in rheumatoid arthritis. Nat Rev Rheumatol *8*, 645–655.

Beato, M. (1989). Gene regulation by steroid hormones. Cell *56*, 335–344.

Beaulieu, E., Ngo, D., Santos, L., Yang, Y.H., Smith, M., Jorgensen, C., Escriou, V., Scherman, D., Courties, G., Apparailly, F., et al. (2010). Glucocorticoid-induced leucine zipper is an endogenous antiinflammatory mediator in arthritis. Arthritis Rheum. *62*, 2651–2661.

Bechtold, S., Dalla Pozza, R., Schwarz, H.P., and Simon, D. (2009). Effects of growth hormone treatment in juvenile idiopathic arthritis: bone and body composition. Horm. Res. *72 Suppl 1*, 60–64.

Bhattacharyya, S., Brown, D.E., Brewer, J.A., Vogt, S.K., and Muglia, L.J. (2007). Macrophage glucocorticoid receptors regulate Toll-like receptor 4-mediated inflammatory responses by selective inhibition of p38 MAP kinase. Blood *109*, 4313–4319.

Bijlsma, J.W.J., and Jacobs, J.W.G. (2014). Glucocorticoids in the treatment of rheumatoid arthritis: still used after 65 years. Ann. N. Y. Acad. Sci. *1318*, 27–31.

Bledsoe, R.K., Montana, V.G., Stanley, T.B., Delves, C.J., Apolito, C.J., McKee, D.D., Consler, T.G., Parks, D.J., Stewart, E.L., Willson, T.M., et al. (2002). Crystal structure of the glucocorticoid receptor ligand binding domain reveals a novel mode of receptor dimerization and coactivator recognition. Cell *110*, 93–105.

Blom, A.B., van Lent, P.L.E.M., Holthuysen, A.E.M., van der Kraan, P.M., Roth, J., van Rooijen, N., and van den Berg, W.B. (2004). Synovial lining macrophages mediate osteophyte formation during experimental osteoarthritis. Osteoarthr. Cartil. *12*, 627–635.

Blue, M.L., Conrad, P., Webb, D.L., Sarr, T., and Macaro, M. (1993). Interacting monocytes and synoviocytes induce adhesion molecules by a cytokine-regulated process. Lymphokine Cytokine Res. *12*, 213–218.

Blume, K.E., Soeroes, S., Keppeler, H., Stevanovic, S., Kretschmer, D., Rautenberg, M., Wesselborg, S., and Lauber, K. (2012). Cleavage of Annexin A1 by ADAM10 during Secondary Necrosis Generates a Monocytic “Find-Me” Signal. The Journal of Immunology *188*, 135–145.

Bombara, M.P., Webb, D.L., Conrad, P., Marlor, C.W., Sarr, T., Ranges, G.E., Aune, T.M., Greve, J.M., and Blue, M.L. (1993). Cell contact between T cells and synovial fibroblasts causes induction of adhesion molecules and cytokines. J. Leukoc. Biol. *54*, 399–406.

Bonnefoy, F., Daoui, A., Valmary-Degano, S., Toussirot, E., Saas, P., and Perruche, S. (2016). Apoptotic cell infusion treats ongoing collagen-induced arthritis, even in the presence of methotrexate, and is synergic with anti-TNF therapy. Arthritis Res Ther *18*.

Bottini, N., and Firestein, G.S. (2013). Duality of fibroblast-like synoviocytes in RA: passive responders and imprinted aggressors. Nat Rev Rheumatol *9*, 24–33.

Brackertz, D., Mitchell, G.F., and Mackay, I.R. (1977). Antigen-induced arthritis in mice. I. Induction of arthritis in various strains of mice. Arthritis Rheum. *20*, 841–850.

van den Brand, B.T., Abdollahi-Roodsaz, S., Vermeij, E.A., Bennink, M.B., Arntz, O.J., Rothlin, C.V., van den Berg, W.B., and van de Loo, F. a. J. (2013).

Therapeutic efficacy of Tyro3, Axl, and Mer tyrosine kinase agonists in collagen-induced arthritis. Arthritis Rheum. *65*, 671–680.

Bruna, A., Nicolàs, M., Muñoz, A., Kyriakis, J.M., and Caelles, C. (2003). Glucocorticoid receptor–JNK interaction mediates inhibition of the JNK pathway by glucocorticoids. EMBO J *22*, 6035–6044.

Buechler, C., Ritter, M., Orsó, E., Langmann, T., Klucken, J., and Schmitz, G. (2000). Regulation of scavenger receptor CD163 expression in human monocytes and macrophages by pro- and antiinflammatory stimuli. Journal of Leukocyte Biology *67*, 97–103.

Burdan, F., Szumiło, J., Korobowicz, A., Farooquee, R., Patel, S., Patel, A., Dave, A., Szumiło, M., Solecki, M., Klepacz, R., et al. (2009). Morphology and physiology of the epiphyseal growth plate. Folia Histochem. Cytobiol. *47*, 5–16.

Burger, D., Dayer, J.-M., Palmer, G., and Gabay, C. (2006). Is IL-1 a good therapeutic target in the treatment of arthritis? Best Pract Res Clin Rheumatol *20*, 879–896.

Butler, J.S., Queally, J.M., Devitt, B.M., Murray, D.W., Doran, P.P., and O'Byrne, J.M. (2010). Silencing Dkk1 expression rescues dexamethasone-induced suppression of primary human osteoblast differentiation. BMC Musculoskelet Disord *11*, 210.

Buttgereit, F., and Bijlsma, J.W. (2017). Glucocorticoids in rheumatoid arthritis: the picture is shaping up. Annals of the Rheumatic Diseases *76*, 1785–1787.

Buttgereit, F., Zhou, H., Kalak, R., Gaber, T., Spies, C.M., Huscher, D., Straub, R.H., Modzelewski, J., Dunstan, C.R., and Seibel, M.J. (2009). Transgenic disruption of glucocorticoid signaling in mature osteoblasts and osteocytes attenuates K/BxN mouse serum-induced arthritis in vivo. Arthritis Rheum. *60*, 1998–2007.

Caelles, C., González-Sancho, J.M., and Muñoz, A. (1997). Nuclear hormone receptor antagonism with AP-1 by inhibition of the JNK pathway. Genes Dev *11*, 3351–3364.

Campbell, I.K., Rich, M.J., Bischof, R.J., and Hamilton, J.A. (2000). The colony-stimulating factors and collagen-induced arthritis: exacerbation of disease by M-CSF and G-CSF and requirement for endogenous M-CSF. J. Leukoc. Biol. *68*, 144–150.

Canalis, E., Mazziotti, G., Giustina, A., and Bilezikian, J.P. (2007). Glucocorticoid-induced osteoporosis: pathophysiology and therapy. Osteoporos Int *18*, 1319–1328.

Chang, J.-K., Li, C.-J., Liao, H.-J., Wang, C.-K., Wang, G.-J., and Ho, M.-L. (2009). Anti-inflammatory drugs suppress proliferation and induce apoptosis through altering expressions of cell cycle regulators and pro-apoptotic factors in cultured human osteoblasts. Toxicology *258*, 148–156.

Cheng, Q., Fan, H., Ngo, D., Beaulieu, E., Leung, P., Lo, C.Y., Burgess, R., Zwan, Y.G. van der, White, S.J., Khachigian, L.M., et al. (2013). GILZ Overexpression Inhibits Endothelial Cell Adhesive Function through Regulation of NF-κB and MAPK Activity. J Immunol *191*, 424–433.

Chintalacharuvu, S.R., Wang, J.X., Giaconia, J.M., and Venkataraman, C. (2005). An essential role for CCL3 in the development of collagen antibody-induced arthritis. Immunol. Lett. *100*, 202–204.

Christensen, A.D., Haase, C., Cook, A.D., and Hamilton, J.A. (2016). K/BxN Serum-Transfer Arthritis as a Model for Human Inflammatory Arthritis. Front Immunol *7*, 213.

Chrysis, D., Ritzen, E.M., and Savendahl, L. (2003). Growth retardation induced by dexamethasone is associated with increased apoptosis of the growth plate chondrocytes. J Endocrinol *176*, 331–337.

Chrysis, D., Zaman, F., Chagin, A.S., Takigawa, M., and Sävendahl, L. (2005). Dexamethasone Induces Apoptosis in Proliferative Chondrocytes through Activation of Caspases and Suppression of the Akt-Phosphatidylinositol 3′-Kinase Signaling Pathway. Endocrinology *146*, 1391–1397.

Clark, A.R., and Lasa, M. (2003). Crosstalk between glucocorticoids and mitogen-activated protein kinase signalling pathways. Current Opinion in Pharmacology *3*, 404–411.

Cohen, S., and Fleischmann, R. (2010). Kinase inhibitors: a new approach to rheumatoid arthritis treatment. Curr Opin Rheumatol *22*, 330–335.

Corr, M., and Crain, B. (2002). The Role of FcγR Signaling in the K/B × N Serum Transfer Model of Arthritis. The Journal of Immunology *169*, 6604–6609.

Coutinho, A.E., and Chapman, K.E. (2011). The anti-inflammatory and immunosuppressive effects of glucocorticoids, recent developments and mechanistic insights. Mol Cell Endocrinol *335*, 2–13.

Coutinho, A.E., Gray, M., Brownstein, D.G., Salter, D.M., Sawatzky, D.A., Clay, S., Gilmour, J.S., Seckl, J.R., Savill, J.S., and Chapman, K.E. (2012). 11β-Hydroxysteroid Dehydrogenase Type 1, But Not Type 2, Deficiency Worsens Acute Inflammation and Experimental Arthritis in Mice. Endocrinology *153*, 234–240.

Danielian, P.S., White, R., Lees, J.A., and Parker, M.G. (1992). Identification of a conserved region required for hormone dependent transcriptional activation by steroid hormone receptors. EMBO J *11*, 1025–1033.

Darimont, B.D., Wagner, R.L., Apriletti, J.W., Stallcup, M.R., Kushner, P.J., Baxter, J.D., Fletterick, R.J., and Yamamoto, K.R. (1998). Structure and specificity of nuclear receptor-coactivator interactions. Genes Dev. *12*, 3343–3356.

Dennis, G., Holweg, C.T.J., Kummerfeld, S.K., Choy, D.F., Setiadi, A.F., Hackney, J.A., Haverty, P.M., Gilbert, H., Lin, W.Y., Diehl, L., et al. (2014). Synovial phenotypes in rheumatoid arthritis correlate with response to biologic therapeutics. Arthritis Res. Ther. *16*, R90.

Dodds, R.A., Merry, K., Littlewood, A., and Gowen, M. (1994). Expression of mRNA for IL1 beta, IL6 and TGF beta 1 in developing human bone and cartilage. J. Histochem. Cytochem. *42*, 733–744.

Dovio, A., Perazzolo, L., Osella, G., Ventura, M., Termine, A., Milano, E., Bertolotto, A., and Angeli, A. (2004). Immediate fall of bone formation and transient increase of bone resorption in the course of high-dose, short-term glucocorticoid therapy in young patients with multiple sclerosis. J. Clin. Endocrinol. Metab. *89*, 4923–4928.

Eastell, R., Reid, D.M., Compston, J., Cooper, C., Fogelman, I., Francis, R.M., Hosking, D.J., Purdie, D.W., Ralston, S.H., Reeve, J., et al. (1998). A UK Consensus Group on management of glucocorticoid-induced osteoporosis: an update. J. Intern. Med. *244*, 271–292.

Elliott, M.R., Koster, K.M., and Murphy, P.S. (2017). Efferocytosis Signaling in the Regulation of Macrophage Inflammatory Responses. The Journal of Immunology *198*, 1387–1394.

Emkey, R.D., Lindsay, R., Lyssy, J., Weisberg, J.S., Dempster, D.W., and Shen, V. (1996). The systemic effect of intraarticular administration of corticosteroid on markers of bone formation and bone resorption in patients with rheumatoid arthritis. Arthritis Rheum. *39*, 277–282.

Erdmann, G., Schütz, G., and Berger, S. (2007). Inducible gene inactivation in neurons of the adult mouse forebrain. BMC Neuroscience *8*, 63.

van Everdingen, A.A., Jacobs, J.W.G., Siewertsz van Reesema, D.R., and Bijlsma, J.W.J. (2002). Low-Dose Prednisone Therapy for Patients with Early Active Rheumatoid Arthritis: Clinical Efficacy, Disease-Modifying Properties, and Side Effects: A Randomized, Double-Blind, Placebo-Controlled Clinical Trial. Ann Intern Med *136*, 1–12.

Fabriek, B.O., Bruggen, R. van, Deng, D.M., Ligtenberg, A.J.M., Nazmi, K., Schornagel, K., Vloet, R.P.M., Dijkstra, C.D., and Berg, T.K. van den (2009). The macrophage scavenger receptor CD163 functions as an innate immune sensor for bacteria. Blood *113*, 887–892.

Fadok, V.A., Warner, M.L., Bratton, D.L., and Henson, P.M. (1998). CD36 is required for phagocytosis of apoptotic cells by human macrophages that use either

a phosphatidylserine receptor or the vitronectin receptor (alpha v beta 3). J. Immunol. *161*, 6250–6257.

Fibbe, W.E., Van Damme, J., Billiau, A., Duinkerken, N., Lurvink, E., Ralph, P., Altrock, B.W., Kaushansky, K., Willemze, R., and Falkenburg, J.H. (1988). Human fibroblasts produce granulocyte-CSF, macrophage-CSF, and granulocyte-macrophage-CSF following stimulation by interleukin-1 and poly(rI).poly(rC). Blood *72*, 860–866.

Finzel, S., Kraus, S., Schmidt, S., Hueber, A., Rech, J., Engelke, K., Englbrecht, M., and Schett, G. (2013). Bone anabolic changes progress in psoriatic arthritis patients despite treatment with methotrexate or tumour necrosis factor inhibitors. Ann. Rheum. Dis. *72*, 1176–1181.

Firestein, G.S., and McInnes, I.B. (2017). Immunopathogenesis of Rheumatoid Arthritis. Immunity *46*, 183–196.

Fonseca, J.E., Cavaleiro, J., Teles, J., Sousa, E., Andreozzi, V.L., Antunes, M., Amaral-Turkman, M.A., Canhão, H., Mourão, A.F., Lopes, J., et al. (2007). Contribution for new genetic markers of rheumatoid arthritis activity and severity: sequencing of the tumor necrosis factor-alpha gene promoter. Arthritis Res. Ther. *9*, R37.

Frego, L., and Davidson, W. (2006). Conformational changes of the glucocorticoid receptor ligand binding domain induced by ligand and cofactor binding, and the location of cofactor binding sites determined by hydrogen/deuterium exchange mass spectrometry. Protein Sci. *15*, 722–730.

van Gaalen, F.A., Toes, R.E.M., Ditzel, H.J., Schaller, M., Breedveld, F.C., Verweij, C.L., and Huizinga, T.W.J. (2004). Association of autoantibodies to glucose-6-phosphate isomerase with extraarticular complications in rheumatoid arthritis. Arthritis Rheum. *50*, 395–399.

Gaujoux-Viala, C., and Gossec, L. (2014). When and for how long should glucocorticoids be used in rheumatoid arthritis? International guidelines and recommendations. Annals of the New York Academy of Sciences *1318*, 32–40.

Goldring, M.B., and Otero, M. (2011). Inflammation in osteoarthritis. Curr Opin Rheumatol *23*, 471–478.

Gossye, V., Elewaut, D., Bougarne, N., Bracke, D., Van Calenbergh, S., Haegeman, G., and De Bosscher, K. (2009). Differential mechanism of NF-κB inhibition by two glucocorticoid receptor modulators in rheumatoid arthritis synovial fibroblasts. Arthritis & Rheumatism *60*, 3241–3250.

Goulding, N.J., Dixey, J., Morand, E.F., Dodds, R.A., Wilkinson, L.S., Pitsillides, A.A., and Edwards, J.C. (1995). Differential distribution of annexins-I, -II, -IV, and -VI in synovium. Ann. Rheum. Dis. *54*, 841–845.

Grøntved, L., John, S., Baek, S., Liu, Y., Buckley, J.R., Vinson, C., Aguilera, G., and Hager, G.L. (2013). C/EBP maintains chromatin accessibility in liver and facilitates glucocorticoid receptor recruitment to steroid response elements. EMBO J. *32*, 1568–1583.

de Hair, M.J.H., van de Sande, M.G.H., Ramwadhdoebe, T.H., Hansson, M., Landewé, R., van der Leij, C., Maas, M., Serre, G., van Schaardenburg, D., Klareskog, L., et al. (2014). Features of the synovium of individuals at risk of developing rheumatoid arthritis: implications for understanding preclinical rheumatoid arthritis. Arthritis & Rheumatology (Hoboken, N.J.) *66*, 513–522.

Hannon, R., Croxtall, J.D., Getting, S.J., Roviezzo, F., Yona, S., Paul-Clark, M.J., Gavins, F.N.E., Perretti, M., Morris, J.F., Buckingham, J.C., et al. (2003). Aberrant inflammation and resistance to glucocorticoids in annexin 1-/- mouse. FASEB J. *17*, 253–255.

Hanyuda, M., Kasama, T., Isozaki, T., Matsunawa, M.M., Yajima, N., Miyaoka, H., Uchida, H., Kameoka, Y., Ide, H., and Adachi, M. (2003). Activated leucocytes express and secrete macrophage inflammatory protein-1α upon interaction with synovial fibroblasts of rheumatoid arthritis via a β2-integrin/ICAM-1 mechanism. Rheumatology (Oxford) *42*, 1390–1397.

Hardy, R.S., Hülso, C., Liu, Y., Gasparini, S.J., Fong-Yee, C., Tu, J., Stoner, S., Stewart, P.M., Raza, K., Cooper, M.S., et al. (2013). Characterisation of fibroblast-

like synoviocytes from a murine model of joint inflammation. Arthritis Res Ther *15*, R24.

Hardy, R.S., Raza, K., and Cooper, M.S. (2014). Glucocorticoid metabolism in rheumatoid arthritis. Ann. N.Y. Acad. Sci. *1318*, 18–26.

Hartmann, K., Koenen, M., Schauer, S., Wittig-Blaich, S., Ahmad, M., Baschant, U., and Tuckermann, J.P. (2016). Molecular Actions of Glucocorticoids in Cartilage and Bone During Health, Disease, and Steroid Therapy. Physiol. Rev. *96*, 409–447.

Hayashi, K., Yamaguchi, T., Yano, S., Kanazawa, I., Yamauchi, M., Yamamoto, M., and Sugimoto, T. (2009). BMP/Wnt antagonists are upregulated by dexamethasone in osteoblasts and reversed by alendronate and PTH: potential therapeutic targets for glucocorticoid-induced osteoporosis. Biochem Biophys Res Commun *379*, 261–266.

Heck, S., Kullmann, M., Gast, A., Ponta, H., Rahmsdorf, H.J., Herrlich, P., and Cato, A.C. (1994). A distinct modulating domain in glucocorticoid receptor monomers in the repression of activity of the transcription factor AP-1. EMBO J *13*, 4087–4095.

Henderson, B., and Pettipher, E.R. (1985). The synovial lining cell: biology and pathobiology. Semin. Arthritis Rheum. *15*, 1–32.

Heuvel, M.M. van den, Tensen, C.P., As, J.H. van, Berg, T.K. van den, Fluitsma, D.M., Dijkstra, C.D., Döpp, E.A., Droste, A., Gaalen, F.A. van, Sorg, C., et al. (1999). Regulation of CD163 on human macrophages: cross-linking of CD163 induces signaling and activation. Journal of Leukocyte Biology *66*, 858–866.

Hill, J.A., Southwood, S., Sette, A., Jevnikar, A.M., Bell, D.A., and Cairns, E. (2003). Cutting edge: the conversion of arginine to citrulline allows for a high-affinity peptide interaction with the rheumatoid arthritis-associated HLA-DRB1*0401 MHC class II molecule. J. Immunol. *171*, 538–541.

Hofbauer, L.C., Zeitz, U., Schoppet, M., Skalicky, M., Schüler, C., Stolina, M., Kostenuik, P.J., and Erben, R.G. (2009). Prevention of glucocorticoid-induced bone loss in mice by inhibition of RANKL. Arthritis Rheum. *60*, 1427–1437.

Hofkens, W., Grevers, L.C., Walgreen, B., de Vries, T.J., Leenen, P.J.M., Everts, V., Storm, G., van den Berg, W.B., and van Lent, P.L. (2011). Intravenously delivered glucocorticoid liposomes inhibit osteoclast activity and bone erosion in murine antigen-induced arthritis. Journal of Controlled Release *152*, 363–369.

Hofkens, W., Schelbergen, R., Storm, G., van den Berg, W.B., and van Lent, P.L. (2013). Liposomal Targeting of Prednisolone Phosphate to Synovial Lining Macrophages during Experimental Arthritis Inhibits M1 Activation but Does Not Favor M2 Differentiation. PLoS One *8*.

Högger, P., Dreier, J., Droste, A., Buck, F., and Sorg, C. (1998). Identification of the integral membrane protein RM3/1 on human monocytes as a glucocorticoid-inducible member of the scavenger receptor cysteine-rich family (CD163). J. Immunol. *161*, 1883–1890.

Hollenberg, S.M., and Evans, R.M. (1988). Multiple and cooperative trans-activation domains of the human glucocorticoid receptor. Cell *55*, 899–906.

Hua, G., Ganti, K.P., and Chambon, P. (2016a). Glucocorticoid-induced tethered transrepression requires SUMOylation of GR and formation of a SUMO-SMRT/NCoR1-HDAC3 repressing complex. PNAS *113*, E635–E643.

Hua, G., Paulen, L., and Chambon, P. (2016b). GR SUMOylation and formation of an SUMO-SMRT/NCoR1-HDAC3 repressing complex is mandatory for GC-induced IR nGRE-mediated transrepression. Proc. Natl. Acad. Sci. U.S.A. *113*, E626-634.

Huang, Q.-Q., Birkett, R., Doyle, R., Shi, B., Roberts, E.L., Mao, Q., and Pope, R.M. (2018). The Role of Macrophages in the Response to TNF Inhibition in Experimental Arthritis. J. Immunol. *200*, 130–138.

Huch, K., Kleffner, S., Stöve, J., Puhl, W., Günther, K.-P., and Brenner, R.E. (2003). PTHrP, PTHr, and FGFR3 are involved in the process of endochondral ossification in human osteophytes. Histochem. Cell Biol. *119*, 281–287.

Ishii, Y., Shinoda, M., and Shikita, M. (1983). Specificity of the suppressive action of glucocorticoids on the proliferation of monocyte/macrophages in the CSF-stimulated cultures of mouse bone marrow. Exp. Hematol. *11*, 178–186.

Jafari, S., Maleki-Dizaji, N., Barar, J., Barzegar-Jalali, M., Rameshrad, M., and Adibkia, K. (2016). Methylprednisolone acetate-loaded hydroxyapatite nanoparticles as a potential drug delivery system for treatment of rheumatoid arthritis: In vitro and in vivo evaluations. European Journal of Pharmaceutical Sciences *91*, 225–235.

Jewell, C.M., Scoltock, A.B., Hamel, B.L., Yudt, M.R., and Cidlowski, J.A. (2012). Complex human glucocorticoid receptor dim mutations define glucocorticoid induced apoptotic resistance in bone cells. Mol. Endocrinol. *26*, 244–256.

Ji, H., Gauguier, D., Ohmura, K., Gonzalez, A., Duchatelle, V., Danoy, P., Garchon, H.-J., Degott, C., Lathrop, M., Benoist, C., et al. (2001). Genetic Influences on the End-Stage Effector Phase of Arthritis. J Exp Med *194*, 321–330.

Ji, H., Pettit, A., Ohmura, K., Ortiz-Lopez, A., Duchatelle, V., Degott, C., Gravallese, E., Mathis, D., and Benoist, C. (2002). Critical Roles for Interleukin 1 and Tumor Necrosis Factor α in Antibody-induced Arthritis. J Exp Med *196*, 77–85.

John, S., Sabo, P.J., Thurman, R.E., Sung, M.-H., Biddie, S.C., Johnson, T.A., Hager, G.L., and Stamatoyannopoulos, J.A. (2011). Chromatin accessibility pre-determines glucocorticoid receptor binding patterns. Nature Genetics *43*, 264–268.

Jung, S.M., Kim, K.W., Yang, C.-W., Park, S.-H., and Ju, J.H. (2014). Cytokine-mediated bone destruction in rheumatoid arthritis. J Immunol Res *2014*, 263625.

Jux, C., Leiber, K., Hügel, U., Blum, W., Ohlsson, C., Klaus, G., and Mehls, O. (1998). Dexamethasone Impairs Growth Hormone (GH)-Stimulated Growth by Suppression of Local Insulin-Like Growth Factor (IGF)-I Production and Expression of GH- and IGF-I-Receptor in Cultured Rat Chondrocytes. Endocrinology *139*, 3296–3305.

Kagari, T., Doi, H., and Shimozato, T. (2002). The Importance of IL-1β and TNF-α, and the Noninvolvement of IL-6, in the Development of Monoclonal Antibody-Induced Arthritis. The Journal of Immunology *169*, 1459–1466.

Karin, M., and Herschman, H.R. (1979). Dexamethasone stimulation of metallothionein synthesis in HeLa cell cultures. Science *204*, 176–177.

Keffer, J., Probert, L., Cazlaris, H., Georgopoulos, S., Kaslaris, E., Kioussis, D., and Kollias, G. (1991). Transgenic mice expressing human tumour necrosis factor: a predictive genetic model of arthritis. EMBO J *10*, 4025–4031.

Ki, S.H., Cho, I.J., Choi, D.W., and Kim, S.G. (2005). Glucocorticoid Receptor (GR)-Associated SMRT Binding to C/EBPβ TAD and Nrf2 Neh4/5: Role of SMRT Recruited to GR in GSTA2 Gene Repression. Mol. Cell. Biol. *25*, 4150–4165.

Kim, W., Lee, H.-N., Jang, J.-H., Kim, S.H., Lee, Y.-H., Hahn, Y.-I., Ngo, H.-K.-C., Choi, Y., Joe, Y., Chung, H.T., et al. (2017). 15-Deoxy-Δ(12,14)-Prostaglandin J2 Exerts Proresolving Effects Through Nuclear Factor E2-Related Factor 2-Induced Expression of CD36 and Heme Oxygenase-1. Antioxid. Redox Signal.

Kitano, M., Hla, T., Sekiguchi, M., Kawahito, Y., Yoshimura, R., Miyazawa, K., Iwasaki, T., Sano, H., Saba, J.D., and Tam, Y.Y. (2006). Sphingosine 1-phosphate/sphingosine 1-phosphate receptor 1 signaling in rheumatoid synovium: regulation of synovial proliferation and inflammatory gene expression. Arthritis Rheum. *54*, 742–753.

Kneidl, J., Löffler, B., Erat, M.C., Kalinka, J., Peters, G., Roth, J., and Barczyk, K. (2012). Soluble CD163 promotes recognition, phagocytosis and killing of Staphylococcus aureus via binding of specific fibronectin peptides. Cell. Microbiol. *14*, 914–936.

Koenen M., Culemann S., Vettorazzi S., Caratti G., Frappart L., Baum W., Krönke G., Baschant U., Tuckermann J.P. (2018). The glucocorticoid receptor in stromal cells is essential for glucocorticoid-mediated resolution of inflammation in arthritis. *Ann. Rheum. Dis* 77, 1610-1618

Korganow, A.S., Ji, H., Mangialaio, S., Duchatelle, V., Pelanda, R., Martin, T., Degott, C., Kikutani, H., Rajewsky, K., Pasquali, J.L., et al. (1999). From systemic T cell self-reactivity to organ-specific autoimmune disease via immunoglobulins. Immunity *10*, 451–461.

Kouskoff, V., Korganow, A.S., Duchatelle, V., Degott, C., Benoist, C., and Mathis, D. (1996). Organ-specific disease provoked by systemic autoimmunity. Cell *87*, 811–822.

Kovacic, R.T., Tizard, R., Cate, R.L., Frey, A.Z., and Wallner, B.P. (1991). Correlation of gene and protein structure of rat and human lipocortin I. Biochemistry *30*, 9015–9021.

van der Kraan, P.M., and van den Berg, W.B. (2007). Osteophytes: relevance and biology. Osteoarthritis and Cartilage *15*, 237–244.

Kristiansen, M., Graversen, J.H., Jacobsen, C., Sonne, O., Hoffman, H.-J., Law, S.K.A., and Moestrup, S.K. (2001). Identification of the haemoglobin scavenger receptor. Nature *409*, 198–201.

Kucera, T., Waltner-Law, M., Scott, D.K., Prasad, R., and Granner, D.K. (2002). A Point Mutation of the AF2 Transactivation Domain of the Glucocorticoid Receptor Disrupts Its Interaction with Steroid Receptor Coactivator 1. J. Biol. Chem. *277*, 26098–26102.

Kuhn, K.A., Kulik, L., Tomooka, B., Braschler, K.J., Arend, W.P., Robinson, W.H., and Holers, V.M. (2006). Antibodies against citrullinated proteins enhance tissue injury in experimental autoimmune arthritis. J Clin Invest *116*, 961–973.

Kyburz, D., Carson, D.A., and Corr, M. (2000). The role of CD40 ligand and tumor necrosis factor alpha signaling in the transgenic K/BxN mouse model of rheumatoid arthritis. Arthritis Rheum. *43*, 2571–2577.

Lagha, A., Zidi, S., Stayoussef, M., Gazouani, E., Kochkar, R., Kochbati, S., Almawi, W.Y., and Yacoubi-Loueslati, B. (2015). Interleukin-1β, Interleukin1-Ra, Interleukin-10, and tumor necrosis factor-α polymorphisms in Tunisian patients with rheumatoid arthritis. Pathol. Biol. *63*, 179–184.

Lapponi, M.J., Carestia, A., Landoni, V.I., Rivadeneyra, L., Etulain, J., Negrotto, S., Pozner, R.G., and Schattner, M. (2013). Regulation of neutrophil extracellular trap formation by anti-inflammatory drugs. J. Pharmacol. Exp. Ther. *345*, 430–437.

Lard, L.R., Roep, B.O., Toes, R.E.M., and Huizinga, T.W.J. (2004). Enhanced concentrations of interleukin 16 are associated with joint destruction in patients with rheumatoid arthritis. J. Rheumatol. *31*, 35–39.

Lee, D.M., Friend, D.S., Gurish, M.F., Benoist, C., Mathis, D., and Brenner, M.B. (2002). Mast cells: a cellular link between autoantibodies and inflammatory arthritis. Science *297*, 1689–1692.

Lee, D.M., Kiener, H.P., Agarwal, S.K., Noss, E.H., Watts, G.F.M., Chisaka, O., Takeichi, M., and Brenner, M.B. (2007). Cadherin-11 in synovial lining formation and pathology in arthritis. Science *315*, 1006–1010.

Lee, S.W., Tsou, A.P., Chan, H., Thomas, J., Petrie, K., Eugui, E.M., and Allison, A.C. (1988). Glucocorticoids selectively inhibit the transcription of the interleukin 1 beta gene and decrease the stability of interleukin 1 beta mRNA. Proc Natl Acad Sci U S A *85*, 1204–1208.

van Lent, P.L.E.M., Blom, A.B., van der Kraan, P., Holthuysen, A.E.M., Vitters, E., van Rooijen, N., Smeets, R.L., Nabbe, K.C. a. M., and van den Berg, W.B. (2004). Crucial role of synovial lining macrophages in the promotion of transforming growth factor beta-mediated osteophyte formation. Arthritis Rheum. *50*, 103–111.

Lew, E.D., Oh, J., Burrola, P.G., Lax, I., Zagórska, A., Través, P.G., Schlessinger, J., and Lemke, G. (2014). Differential TAM receptor–ligand–phospholipid interactions delimit differential TAM bioactivities. ELife Sciences *3*, e03385.

Li, P., and Schwarz, E.M. (2003). The TNF-α transgenic mouse model of inflammatory arthritis. Springer Semin Immunopathol *25*, 19–33.

Li, Y., Cai, L., Wang, H., Wu, P., Gu, W., Chen, Y., Hao, H., Tang, K., Yi, P., Liu, M., et al. (2011). Pleiotropic regulation of macrophage polarization and tumorigenesis by formyl peptide receptor-2. Oncogene *30*, 3887–3899.

Lim, H.-W., Uhlenhaut, N.H., Rauch, A., Weiner, J., Hübner, S., Hübner, N., Won, K.-J., Lazar, M.A., Tuckermann, J., and Steger, D.J. (2015). Genomic redistribution of GR monomers and dimers mediates transcriptional response to exogenous glucocorticoid in vivo. Genome Res. *25*, 836–844.

Limbourg, F.P., Huang, Z., Plumier, J.-C., Simoncini, T., Fujioka, M., Tuckermann, J., Schütz, G., Moskowitz, M.A., and Liao, J.K. (2002). Rapid nontranscriptional activation of endothelial nitric oxide synthase mediates increased cerebral blood flow and stroke protection by corticosteroids. J. Clin. Invest. *110*, 1729–1738.

Lin, C.-C., Lee, I.-T., Hsu, C.-H., Hsu, C.-K., Chi, P.-L., Hsiao, L.-D., and Yang, C.-M. (2015). Sphingosine-1-phosphate mediates ICAM-1-dependent monocyte adhesion through p38 MAPK and p42/p44 MAPK-dependent Akt activation. PLoS ONE *10*, e0118473.

Lin, C.-C., Yang, C.-C., Cho, R.-L., Wang, C.-Y., Hsiao, L.-D., and Yang, C.-M. (2016). Sphingosine 1-Phosphate-Induced ICAM-1 Expression via NADPH Oxidase/ROS-Dependent NF-κB Cascade on Human Pulmonary Alveolar Epithelial Cells. Front Pharmacol *7*.

Liu, X., Zou, Q., Zeng, B., Fang, Y., and Wei, H. (2013). Analysis of Fecal Lactobacillus Community Structure in Patients with Early Rheumatoid Arthritis. Curr Microbiol *67*, 170–176.

Liu, X., Zeng, B., Zhang, J., Li, W., Mou, F., Wang, H., Zou, Q., Zhong, B., Wu, L., Wei, H., et al. (2016). Role of the Gut Microbiome in Modulating Arthritis Progression in Mice. Sci Rep *6*.

Löwenberg, M., Tuynman, J., Bilderbeek, J., Gaber, T., Buttgereit, F., Deventer, S. van, Peppelenbosch, M., and Hommes, D. (2005). Rapid immunosuppressive effects of glucocorticoids mediated through Lck and Fyn. Blood *106*, 1703–1710.

Lu, Q., and Lemke, G. (2001). Homeostatic Regulation of the Immune System by Receptor Tyrosine Kinases of the Tyro 3 Family. Science *293*, 306–311.

Lühder, F., and Reichardt, H.M. (2017). Novel Drug Delivery Systems Tailored for Improved Administration of Glucocorticoids. Int J Mol Sci *18*.

Luppen, C.A., Smith, E., Spevak, L., Boskey, A.L., and Frenkel, B. (2003). Bone morphogenetic protein-2 restores mineralization in glucocorticoid-inhibited MC3T3-E1 osteoblast cultures. J. Bone Miner. Res. *18*, 1186–1197.

Maccioni, M., Zeder-Lutz, G., Huang, H., Ebel, C., Gerber, P., Hergueux, J., Marchal, P., Duchatelle, V., Degott, C., van Regenmortel, M., et al. (2002). Arthritogenic monoclonal antibodies from K/BxN mice. J. Exp. Med. *195*, 1071–1077.

Maderna, P., Yona, S., Perretti, M., and Godson, C. (2005). Modulation of Phagocytosis of Apoptotic Neutrophils by Supernatant from Dexamethasone-Treated Macrophages and Annexin-Derived Peptide Ac2–26. The Journal of Immunology *174*, 3727–3733.

Maicas, N., Ferrándiz, M.L., Brines, R., Ibáñez, L., Cuadrado, A., Koenders, M.I., van den Berg, W.B., and Alcaraz, M.J. (2011). Deficiency of Nrf2 accelerates the effector phase of arthritis and aggravates joint disease. Antioxid. Redox Signal. *15*, 889–901.

Makrygiannakis, D., Revu, S., Neregård, P., af Klint, E., Snir, O., Grundtman, C., and Catrina, A.I. (2008). Monocytes are essential for inhibition of synovial T-cell glucocorticoid-mediated apoptosis in rheumatoid arthritis. Arthritis Res Ther *10*, R147.

Mateen, S., Moin, S., Shahzad, S., and Khan, A.Q. (2017). Level of inflammatory cytokines in rheumatoid arthritis patients: Correlation with 25-hydroxy vitamin D and reactive oxygen species. PLoS One *12*.

Matsumoto, I., Maccioni, M., Lee, D.M., Maurice, M., Simmons, B., Brenner, M., Mathis, D., and Benoist, C. (2002). How antibodies to a ubiquitous cytoplasmic enzyme may provoke joint-specific autoimmune disease. Nat. Immunol. *3*, 360–365.

McDonald, P.P., Fadok, V.A., Bratton, D., and Henson, P.M. (1999). Transcriptional and translational regulation of inflammatory mediator production by endogenous TGF-beta in macrophages that have ingested apoptotic cells. J. Immunol. *163*, 6164–6172.

McInnes, I.B., and Schett, G. (2007). Cytokines in the pathogenesis of rheumatoid arthritis. Nature Reviews Immunology *7*, 429–442.

McInnes, I.B., and Schett, G. (2011). The pathogenesis of rheumatoid arthritis. N. Engl. J. Med. *365*, 2205–2219.

Miagkov, A.V., Kovalenko, D.V., Brown, C.E., Didsbury, J.R., Cogswell, J.P., Stimpson, S.A., Baldwin, A.S., and Makarov, S.S. (1998). NF-kappaB activation

provides the potential link between inflammation and hyperplasia in the arthritic joint. Proc. Natl. Acad. Sci. U.S.A. *95*, 13859–13864.

Miesel, R., and Zuber, M. (1993). Copper-dependent antioxidase defenses in inflammatory and autoimmune rheumatic diseases. Inflammation *17*, 283–294.

Mihara, K., Almansa, C., Smeets, R.L., Loomans, E.E.M.G., Dulos, J., Vink, P.M.F., Rooseboom, M., Kreutzer, H., Cavalcanti, F., Boots, A.M., et al. (2008). A potent and selective p38 inhibitor protects against bone damage in murine collagen-induced arthritis: a comparison with neutralization of mouse TNFα. Br J Pharmacol *154*, 153–164.

Mikuls, T.R., and Weaver, A.L. (2003). Lessons learned in the use of tumor necrosis factor-alpha inhibitors in the treatment of rheumatoid arthritis. Curr Rheumatol Rep *5*, 270–277.

Misharin, A.V., Cuda, C.M., Saber, R., Turner, J.D., Gierut, A.K., Haines, G.K., Berdnikovs, S., Filer, A., Clark, A.R., Buckley, C.D., et al. (2014). Nonclassical Ly6C(-) monocytes drive the development of inflammatory arthritis in mice. Cell Rep *9*, 591–604.

Moestrup, S., and Møller, H. (2004). CD163: a regulated hemoglobin scavenger receptor with a role in the anti-inflammatory response. Annals of Medicine *36*, 347–354.

Mohr, W., Beneke, G., and Mohing, W. (1975). Proliferation of synovial lining cells and fibroblasts. Annals of the Rheumatic Diseases *34*, 219–224.

Monach, P.A., Verschoor, A., Jacobs, J.P., Carroll, M.C., Wagers, A.J., Benoist, C., and Mathis, D. (2007). Circulating C3 is necessary and sufficient for induction of autoantibody-mediated arthritis in a mouse model. Arthritis Rheum *56*, 2968–2974.

Monach, P.A., Mathis, D., and Benoist, C. (2008). The K/BxN arthritis model. Curr Protoc Immunol *Chapter 15*, Unit 15.22.

Monach, P.A., Nigrovic, P.A., Chen, M., Hock, H., Lee, D.M., Benoist, C., and Mathis, D. (2010). Neutrophils in autoantibody-mediated arthritis: critical producers of FcRγ , the receptor for C5a, and LFA-1. Arthritis Rheum *62*, 753–764.

Murray, P.J. (2017). Macrophage Polarization. Annu. Rev. Physiol. *79*, 541–566.

Nagy, L., Kao, H.Y., Love, J.D., Li, C., Banayo, E., Gooch, J.T., Krishna, V., Chatterjee, K., Evans, R.M., and Schwabe, J.W. (1999). Mechanism of corepressor binding and release from nuclear hormone receptors. Genes Dev. *13*, 3209–3216.

Nakano, K., Whitaker, J.W., Boyle, D.L., Wang, W., and Firestein, G.S. (2013). DNA methylome signature in rheumatoid arthritis. Annals of the Rheumatic Diseases *72*, 110–117.

Nepom, G.T., Byers, P., Seyfried, C., Healey, L.A., Wilske, K.R., Stage, D., and Nepom, B.S. (1989). HLA genes associated with rheumatoid arthritis. Identification of susceptibility alleles using specific oligonucleotide probes. Arthritis Rheum. *32*, 15–21.

Ngo, D., Beaulieu, E., Gu, R., Leaney, A., Santos, L., Fan, H., Yang, Y., Kao, W., Xu, J., Escriou, V., et al. (2013). Divergent effects of endogenous and exogenous glucocorticoid-induced leucine zipper in animal models of inflammation and arthritis. Arthritis Rheum. *65*, 1203–1212.

Nigrovic, P.A., Binstadt, B.A., Monach, P.A., Johnsen, A., Gurish, M., Iwakura, Y., Benoist, C., Mathis, D., and Lee, D.M. (2007). Mast cells contribute to initiation of autoantibody-mediated arthritis via IL-1. PNAS *104*, 2325–2330.

Noss, E.H., and Brenner, M.B. (2008). The role and therapeutic implications of fibroblast-like synoviocytes in inflammation and cartilage erosion in rheumatoid arthritis. Immunological Reviews *223*, 252–270.

O'Brien, C.A., Jia, D., Plotkin, L.I., Bellido, T., Powers, C.C., Stewart, S.A., Manolagas, S.C., and Weinstein, R.S. (2004). Glucocorticoids act directly on osteoblasts and osteocytes to induce their apoptosis and reduce bone formation and strength. Endocrinology *145*, 1835–1841.

Ogawa, A., Johnson, J.H., Ohneda, M., McAllister, C.T., Inman, L., Alam, T., and Unger, R.H. (1992). Roles of insulin resistance and beta-cell dysfunction in dexamethasone-induced diabetes. J. Clin. Invest. *90*, 497–504.

Oñate, S.A., Tsai, S.Y., Tsai, M.-J., and O'Malley, B.W. (1995). Sequence and Characterization of a Coactivator for the Steroid Hormone Receptor Superfamily. Science *270*, 1354–1357.

Pan, M., Kang, I., Craft, J., and Yin, Z. (2004). Resistance to development of collagen-induced arthritis in C57BL/6 mice is due to a defect in secondary, but not in primary, immune response. J. Clin. Immunol. *24*, 481–491.

Papadimitriou, A., and Priftis, K.N. (2009). Regulation of the hypothalamic-pituitary-adrenal axis. Neuroimmunomodulation *16*, 265–271.

Park, S.Y., Lee, S.W., Lee, S.Y., Hong, K.W., Bae, S.S., Kim, K., and Kim, C.D. (2017). SIRT1/Adenosine Monophosphate-Activated Protein Kinase α Signaling Enhances Macrophage Polarization to an Anti-inflammatory Phenotype in Rheumatoid Arthritis. Front Immunol *8*.

Parlato, R., Otto, C., Tuckermann, J., Stotz, S., Kaden, S., Gröne, H.-J., Unsicker, K., and Schütz, G. (2009). Conditional inactivation of glucocorticoid receptor gene in dopamine-beta-hydroxylase cells impairs chromaffin cell survival. Endocrinology *150*, 1775–1781.

Patel, H.B., Kornerup, K.N., Sampaio, A.L.F., D'Acquisto, F., Seed, M.P., Girol, A.P., Gray, M., Pitzalis, C., Oliani, S.M., and Perretti, M. (2012). The impact of endogenous annexin A1 on glucocorticoid control of inflammatory arthritis. Ann. Rheum. Dis. *71*, 1872–1880.

Payvar, F., Wrange, O., Carlstedt-Duke, J., Okret, S., Gustafsson, J.A., and Yamamoto, K.R. (1981). Purified glucocorticoid receptors bind selectively in vitro to a cloned DNA fragment whose transcription is regulated by glucocorticoids in vivo. Proc Natl Acad Sci U S A *78*, 6628–6632.

Perretti, M., and Flower, R.J. (1996). Measurement of lipocortin 1 levels in murine peripheral blood leukocytes by flow cytometry: modulation by glucocorticoids and inflammation. Br. J. Pharmacol. *118*, 605–610.

Philip S. Hench (1950). The reversibility of certain rheumatic and non-rheumatic conditions by the use of cortisone or of the pituitary adrenocorticotropic hormone.

Plotkin, L.I., Manolagas, S.C., and Bellido, T. (2007). Glucocorticoids induce osteocyte apoptosis by blocking focal adhesion kinase-mediated survival. Evidence for inside-out signaling leading to anoikis. J. Biol. Chem. *282*, 24120–24130.

Poon, I.K.H., Lucas, C.D., Rossi, A.G., and Ravichandran, K.S. (2014). Apoptotic cell clearance: basic biology and therapeutic potential. Nat. Rev. Immunol. *14*, 166–180.

Popova, A., Kzhyshkowska, J., Nurgazieva, D., Goerdt, S., and Gratchev, A. (2011). Pro- and anti-inflammatory control of M-CSF-mediated macrophage differentiation. Immunobiology *216*, 164–172.

Presman, D.M., Ganguly, S., Schiltz, R.L., Johnson, T.A., Karpova, T.S., and Hager, G.L. (2016). DNA binding triggers tetramerization of the glucocorticoid receptor in live cells. Proc. Natl. Acad. Sci. U.S.A. *113*, 8236–8241.

Qu, Z., Garcia, C.H., O'Rourke, L.M., Planck, S.R., Kohli, M., and Rosenbaum, J.T. (1994). Local Proliferation of Fibroblast-Like Synoviocytes Contributes to Synovial Hyperplasia. Arthritis & Rheumatism *37*, 212–220.

Quan, L., Zhang, Y., Dusad, A., Ren, K., Purdue, P.E., Goldring, S.R., and Wang, D. (2016). The Evaluation of the Therapeutic Efficacy and Side Effects of a Macromolecular Dexamethasone Prodrug in the Collagen-Induced Arthritis Mouse Model. Pharm Res *33*, 186–193.

Rauch, A., Seitz, S., Baschant, U., Schilling, A.F., Illing, A., Stride, B., Kirilov, M., Mandic, V., Takacz, A., Schmidt-Ullrich, R., et al. (2010). Glucocorticoids suppress bone formation by attenuating osteoblast differentiation via the monomeric glucocorticoid receptor. Cell Metab. *11*, 517–531.

Reichardt, H.M., Kaestner, K.H., Tuckermann, J., Kretz, O., Wessely, O., Bock, R., Gass, P., Schmid, W., Herrlich, P., Angel, P., et al. (1998). DNA Binding of the Glucocorticoid Receptor Is Not Essential for Survival. Cell *93*, 531–541.

Ricci, E., Ronchetti, S., Pericolini, E., Gabrielli, E., Cari, L., Gentili, M., Roselletti, E., Migliorati, G., Vecchiarelli, A., and Riccardi, C. (2017). Role of the glucocorticoid-induced leucine zipper gene in dexamethasone-induced inhibition of mouse neutrophil migration via control of annexin A1 expression. FASEB J. *31*, 3054–3065.

Rose, B.J., and Kooyman, D.L. (2016). A Tale of Two Joints: The Role of Matrix Metalloproteases in Cartilage Biology. Dis Markers *2016*.

Rose, H.M., Ragan, C., Pearce, E., and Lipman, M.O. (1948). Differential Agglutination of Normal and Sensitized Sheep Erythrocytes by Sera of Patients with Rheumatoid Arthritis. Proceedings of the Society for Experimental Biology and Medicine *68*, 1–6.

Roth, S., Agthe, M., Eickhoff, S., Möller, S., Karsten, C.M., Borregaard, N., Solbach, W., and Laskay, T. (2015). Secondary necrotic neutrophils release interleukin-16C and macrophage migration inhibitory factor from stores in the cytosol. Cell Death Discovery *1*, 15056.

Ruiz-Heiland, G., Horn, A., Zerr, P., Hofstetter, W., Baum, W., Stock, M., Distler, J.H., Nimmerjahn, F., Schett, G., and Zwerina, J. (2012). Blockade of the hedgehog pathway inhibits osteophyte formation in arthritis. Ann. Rheum. Dis. *71*, 400–407.

Saferding, V. (2015). Important Role of microRNA-146a in Inflammatory Arthritis By Controlling Local Bone Destruction.

Saferding, V., Puchner, A., Goncalves-Alves, E., Hofmann, M., Bonelli, M., Brunner, J.S., Sahin, E., Niederreiter, B., Hayer, S., Kiener, H.P., et al. (2017). MicroRNA-146a governs fibroblast activation and joint pathology in arthritis. J. Autoimmun. *82*, 74–84.

Sandell, L.J., and Aigner, T. (2001). Articular cartilage and changes in Arthritis: Cell biology of osteoarthritis. Arthritis Research & Therapy *3*, 107.

Schäcke, H., Berger, M., Rehwinkel, H., and Asadullah, K. (2007). Selective glucocorticoid receptor agonists (SEGRAs): novel ligands with an improved therapeutic index. Mol. Cell. Endocrinol. *275*, 109–117.

Scharstuhl, A., Glansbeek, H.L., van Beuningen, H.M., Vitters, E.L., van der Kraan, P.M., and van den Berg, W.B. (2002). Inhibition of endogenous TGF-beta during experimental osteoarthritis prevents osteophyte formation and impairs cartilage repair. J. Immunol. *169*, 507–514.

Schiller, B.J., Chodankar, R., Watson, L.C., Stallcup, M.R., and Yamamoto, K.R. (2014). Glucocorticoid receptor binds half sites as a monomer and regulates specific target genes. Genome Biology *15*, 418.

Schrier, L., Ferns, S.P., Barnes, K.M., Emons, J.A.M., Newman, E.I., Nilsson, O., and Baron, J. (2006). Depletion of resting zone chondrocytes during growth plate senescence. J Endocrinol *189*, 27–36.

Schubert, D., Maier, B., Morawietz, L., Krenn, V., and Kamradt, T. (2004). Immunization with Glucose-6-Phosphate Isomerase Induces T Cell-Dependent Peripheral Polyarthritis in Genetically Unaltered Mice. The Journal of Immunology *172*, 4503–4509.

Schüle, R., Rangarajan, P., Kliewer, S., Ransone, L.J., Bolado, J., Yang, N., Verma, I.M., and Evans, R.M. (1990). Functional antagonism between oncoprotein c-Jun and the glucocorticoid receptor. Cell *62*, 1217–1226.

Schulz, M., Eggert, M., Baniahmad, A., Dostert, A., Heinzel, T., and Renkawitz, R. (2002). RU486-induced glucocorticoid receptor agonism is controlled by the receptor N terminus and by corepressor binding. J. Biol. Chem. *277*, 26238–26243.

Scott, R.S., McMahon, E.J., Pop, S.M., Reap, E.A., Caricchio, R., Cohen, P.L., Earp, H.S., and Matsushima, G.K. (2001). Phagocytosis and clearance of apoptotic cells is mediated by MER. Nature *411*, 207–211.

Seitz, H.M., Camenisch, T.D., Lemke, G., Earp, H.S., and Matsushima, G.K. (2007). Macrophages and dendritic cells use different Axl/Mertk/Tyro3 receptors in clearance of apoptotic cells. J. Immunol. *178*, 5635–5642.

Shaw, A.T., and Gravallese, E.M. (2016). Mediators of inflammation and bone remodeling in rheumatic disease. Semin Cell Dev Biol *49*, 2–10.

Siebelt, M., Korthagen, N., Wei, W., Groen, H., Bastiaansen-Jenniskens, Y., Müller, C., Waarsing, J.H., de Jong, M., and Weinans, H. (2015). Triamcinolone acetonide activates an anti-inflammatory and folate receptor-positive macrophage that prevents osteophytosis in vivo. Arthritis Res. Ther. *17*, 352.

Šimelyte, E., Rimpiläinen, M., Zhang, X., and Toivanen, P. (2003). Role of peptidoglycan subtypes in the pathogenesis of bacterial cell wall arthritis. Annals of the Rheumatic Diseases *62*, 976–982.

Singh, K., Maity, P., Krug, L., Meyer, P., Treiber, N., Lucas, T., Basu, A., Kochanek, S., Wlaschek, M., Geiger, H., et al. (2015). Superoxide anion radicals induce IGF-1 resistance through concomitant activation of PTP1B and PTEN. EMBO Mol Med *7*, 59–77.

Sionov, R.V., Cohen, O., Kfir, S., Zilberman, Y., and Yefenof, E. (2006). Role of mitochondrial glucocorticoid receptor in glucocorticoid-induced apoptosis. J Exp Med *203*, 189–201.

Smolen, J.S., Han, C., Bala, M., Maini, R.N., Kalden, J.R., van der Heijde, D., Breedveld, F.C., Furst, D.E., Lipsky, P.E., and ATTRACT Study Group (2005). Evidence of radiographic benefit of treatment with infliximab plus methotrexate in rheumatoid arthritis patients who had no clinical improvement: a detailed subanalysis of data from the anti-tumor necrosis factor trial in rheumatoid arthritis with concomitant therapy study. Arthritis Rheum. *52*, 1020–1030.

Solomon, S., Rajasekaran, N., Jeisy-Walder, E., Snapper, S.B., and Illges, H. (2005). A crucial role for macrophages in the pathology of K/B × N serum-induced arthritis. Eur. J. Immunol. *35*, 3064–3073.

Stahl, E.A., Raychaudhuri, S., Remmers, E.F., Xie, G., Eyre, S., Thomson, B.P., Li, Y., Kurreeman, F.A.S., Zhernakova, A., Hinks, A., et al. (2010). Genome-wide association study meta-analysis identifies seven new rheumatoid arthritis risk loci. Nature Genetics *42*, 508–514.

Stangenberg, L., Burzyn, D., Binstadt, B.A., Weissleder, R., Mahmood, U., Benoist, C., and Mathis, D. (2014). Denervation protects limbs from inflammatory

arthritis via an impact on the microvasculature. Proc. Natl. Acad. Sci. U.S.A. *111*, 11419–11424.

Steer, J.H., Kroeger, K.M., Abraham, L.J., and Joyce, D.A. (2000). Glucocorticoids suppress tumor necrosis factor-alpha expression by human monocytic THP-1 cells by suppressing transactivation through adjacent NF-kappa B and c-Jun-activating transcription factor-2 binding sites in the promoter. J. Biol. Chem. *275*, 18432–18440.

Steinhauser, M.L., Kunkel, S.L., Hogaboam, C.M., Evanoff, H., Strieter, R.M., and Lukacs, N.W. (1998). Macrophage/fibroblast coculture induces macrophage inflammatory protein-1alpha production mediated by intercellular adhesion molecule-1 and oxygen radicals. J. Leukoc. Biol. *64*, 636–641.

Strähle, U., Klock, G., and Schütz, G. (1987). A DNA sequence of 15 base pairs is sufficient to mediate both glucocorticoid and progesterone induction of gene expression. PNAS *84*, 7871–7875.

Strehl, C., Gaber, T., Löwenberg, M., Hommes, D.W., Verhaar, A.P., Schellmann, S., Hahne, M., Fangradt, M., Wagegg, M., Hoff, P., et al. (2011). Origin and functional activity of the membrane-bound glucocorticoid receptor. Arthritis & Rheumatism *63*, 3779–3788.

Stuart, J.M., Townes, A.S., and Kang, A.H. (1984). Collagen Autoimmune Arthritis. Annual Review of Immunology *2*, 199–218.

Surjit, M., Ganti, K.P., Mukherji, A., Ye, T., Hua, G., Metzger, D., Li, M., and Chambon, P. (2011). Widespread Negative Response Elements Mediate Direct Repression by Agonist- Liganded Glucocorticoid Receptor. Cell *145*, 224–241.

Swinstead, E.E., Miranda, T.B., Paakinaho, V., Baek, S., Goldstein, I., Hawkins, M., Karpova, T.S., Ball, D., Mazza, D., Lavis, L.D., et al. (2016). Steroid Receptors Reprogram FoxA1 Occupancy Through Dynamic Chromatin Transitions. Cell *165*, 593–605.

Symmons, D.P., Bankhead, C.R., Harrison, B.J., Brennan, P., Barrett, E.M., Scott, D.G., and Silman, A.J. (1997). Blood transfusion, smoking, and obesity as risk factors for the development of rheumatoid arthritis: results from a primary care-

based incident case-control study in Norfolk, England. Arthritis Rheum. *40*, 1955–1961.

Trentham, D.E., Townes, A.S., and Kang, A.H. (1977). Autoimmunity to type II collagen an experimental model of arthritis. J Exp Med *146*, 857–868.

Tronche, F., Kellendonk, C., Kretz, O., Gass, P., Anlag, K., Orban, P.C., Bock, R., Klein, R., and Schütz, G. (1999). Disruption of the glucocorticoid receptor gene in the nervous system results in reduced anxiety. Nat. Genet. *23*, 99–103.

Tu, J., Stoner, S., Fromm, P.D., Wang, T., Chen, D., Tuckermann, J., Cooper, M.S., Seibel, M.J., and Zhou, H. (2018). Endogenous glucocorticoid signaling in chondrocytes attenuates joint inflammation and damage. FASEB J. *32*, 478–487.

Tuckermann, J.P., Kleiman, A., Moriggl, R., Spanbroek, R., Neumann, A., Illing, A., Clausen, B.E., Stride, B., Förster, I., Habenicht, A.J.R., et al. (2007). Macrophages and neutrophils are the targets for immune suppression by glucocorticoids in contact allergy. J Clin Invest *117*, 1381–1390.

Uhlenhaut, N.H., Barish, G.D., Yu, R.T., Downes, M., Karunasiri, M., Liddle, C., Schwalie, P., Hübner, N., and Evans, R.M. (2013). Insights into negative regulation by the glucocorticoid receptor from genome-wide profiling of inflammatory cistromes. Mol. Cell *49*, 158–171.

Usami, Y., Ishida, K., Sato, S., Kishino, M., Kiryu, M., Ogawa, Y., Okura, M., Fukuda, Y., and Toyosawa, S. (2013). Intercellular adhesion molecule-1 (ICAM-1) expression correlates with oral cancer progression and induces macrophage/cancer cell adhesion. Int. J. Cancer *133*, 568–578.

Vandevyver, S., Dejager, L., Van Bogaert, T., Kleyman, A., Liu, Y., Tuckermann, J., and Libert, C. (2012). Glucocorticoid receptor dimerization induces MKP1 to protect against TNF-induced inflammation. J Clin Invest *122*, 2130–2140.

Vanniasinghe, A.S., Manolios, N., Schibeci, S., Lakhiani, C., Kamali-Sarvestani, E., Sharma, R., Kumar, V., Moghaddam, M., Ali, M., and Bender, V. (2014). Targeting fibroblast-like synovial cells at sites of inflammation with peptide targeted liposomes results in inhibition of experimental arthritis. Clinical Immunology *151*, 43–54.

Varga, G., Ehrchen, J., Tsianakas, A., Tenbrock, K., Rattenholl, A., Seeliger, S., Mack, M., Roth, J., and Sunderkoetter, C. (2008). Glucocorticoids induce an activated, anti-inflammatory monocyte subset in mice that resembles myeloid-derived suppressor cells. J. Leukoc. Biol. *84*, 644–650.

Vattakuzhi, Y., Abraham, S.M., Freidin, A., Clark, A.R., and Horwood, N.J. (2012). Dual-specificity phosphatase 1-null mice exhibit spontaneous osteolytic disease and enhanced inflammatory osteolysis in experimental arthritis. Arthritis Rheum. *64*, 2201–2210.

Vettorazzi, S., Bode, C., Dejager, L., Frappart, L., Shelest, E., Klaßen, C., Tasdogan, A., Reichardt, H.M., Libert, C., Schneider, M., et al. (2015). Glucocorticoids limit acute lung inflammation in concert with inflammatory stimuli by induction of SphK1. Nat Commun *6*, 7796.

Wan, T., Zhao, Y., Fan, F., Hu, R., and Jin, X. (2017). Dexamethasone Inhibits S. aureus-Induced Neutrophil Extracellular Pathogen-Killing Mechanism, Possibly through Toll-Like Receptor Regulation. Front Immunol *8*.

Wang, J.-X., Bair, A.M., King, S.L., Shnayder, R., Huang, Y.-F., Shieh, C.-C., Soberman, R.J., Fuhlbrigge, R.C., and Nigrovic, P.A. (2012). Ly6G ligation blocks recruitment of neutrophils via a β2-integrin-dependent mechanism. Blood *120*, 1489–1498.

Wang, L., Benedito, R., Bixel, M.G., Zeuschner, D., Stehling, M., Sävendahl, L., Haigh, J.J., Snippert, H., Clevers, H., Breier, G., et al. (2013). Identification of a clonally expanding haematopoietic compartment in bone marrow. EMBO J. *32*, 219–230.

Wang, Y., Nakayama, M., Pitulescu, M.E., Schmidt, T.S., Bochenek, M.L., Sakakibara, A., Adams, S., Davy, A., Deutsch, U., Lüthi, U., et al. (2010). Ephrin-B2 controls VEGF-induced angiogenesis and lymphangiogenesis. Nature *465*, 483–486.

Wassenberg, S., Rau, R., Steinfeld, P., and Zeidler, H. (2005). Very low-dose prednisolone in early rheumatoid arthritis retards radiographic progression over

two years: a multicenter, double-blind, placebo-controlled trial. Arthritis Rheum. *52*, 3371–3380.

Waterborg, C.E.J., Través, P.G., Beermann, S., Koenders, M.I., Lemke, G., and Loo, F.A.J. van de (2017). 03.05 The tam receptors axl and mer play a protective role in a temporal and spatial manner in inflammatory arthritis. Annals of the Rheumatic Diseases *76*, A31–A31.

Waterborg, C.E.J., Beermann, S., Broeren, M.G.A., Bennink, M.B., Koenders, M.I., Lent, V., M, P.L.E., Berg, V.D., B, W., Kraan, V.D., et al. (2018). Protective Role of the MER Tyrosine Kinase via Efferocytosis in Rheumatoid Arthritis Models. Front. Immunol. *9*.

Weikum, E.R., de Vera, I.M.S., Nwachukwu, J.C., Hudson, W.H., Nettles, K.W., Kojetin, D.J., and Ortlund, E.A. (2017). Tethering not required: the glucocorticoid receptor binds directly to activator protein-1 recognition motifs to repress inflammatory genes. Nucleic Acids Res. *45*, 8596–8608.

Weinstein, R.S. (2012). Glucocorticoid-induced osteonecrosis. Endocrine *41*, 183–190.

Weitoft, T., Larsson, A., Saxne, T., and Rönnblom, L. (2005). Changes of cartilage and bone markers after intra-articular glucocorticoid treatment with and without postinjection rest in patients with rheumatoid arthritis. Ann Rheum Dis *64*, 1750–1753.

Wenzel, I., Roth, J., and Sorg, C. (1996). Identification of a novel surface molecule, RM3/1, that contributes to the adhesion of glucocorticoid-induced human monocytes to endothelial cells. Eur. J. Immunol. *26*, 2758–2763.

Weyand, C.M., Hicok, K.C., Conn, D.L., and Goronzy, J.J. (1992). The influence of HLA-DRB1 genes on disease severity in rheumatoid arthritis. Ann. Intern. Med. *117*, 801–806.

Wilson, J.C., Sarsour, K., Gale, S., Pethö-Schramm, A., Jick, S.S., and Meier, C.R. (2018). Incidence and risk of glucocorticoid-associated adverse effects in patients with rheumatoid arthritis. Arthritis Care Res (Hoboken).

Wipke, B.T., and Allen, P.M. (2001). Essential role of neutrophils in the initiation and progression of a murine model of rheumatoid arthritis. J. Immunol. *167*, 1601–1608.

Wipke, B.T., Wang, Z., Kim, J., McCarthy, T.J., and Allen, P.M. (2002). Dynamic visualization of a joint-specific autoimmune response through positron emission tomography. Nat. Immunol. *3*, 366–372.

Wipke, B.T., Wang, Z., Nagengast, W., Reichert, D.E., and Allen, P.M. (2004). Staging the initiation of autoantibody-induced arthritis: a critical role for immune complexes. J. Immunol. *172*, 7694–7702.

Wooley, P.H., Whalen, J.D., Chapman, D.L., Berger, A.E., Richard, K.A., Aspar, D.G., and Staite, N.D. (1993). The effect of an interleukin-1 receptor antagonist protein on type II collagen-induced arthritis and antigen-induced arthritis in mice. Arthritis Rheum. *36*, 1305–1314.

Yang, C.-R., Shih, K.-S., Liou, J.-P., Wu, Y.-W., Hsieh, I.-N., Lee, H.-Y., Lin, T.-C., and Wang, J.-H. (2014). Denbinobin upregulates miR-146a expression and attenuates IL-1β-induced upregulation of ICAM-1 and VCAM-1 expressions in osteoarthritis fibroblast-like synoviocytes. J. Mol. Med. *92*, 1147–1158.

Yang, Y.H., Hutchinson, P., Santos, L.L., and Morand, E.F. (1998). Glucocorticoid inhibition of adjuvant arthritis synovial macrophage nitric oxide production: role of lipocortin 1. Clin Exp Immunol *111*, 117–122.

Yang, Y.H., Morand, E.F., Getting, S.J., Paul-Clark, M., Liu, D.L., Yona, S., Hannon, R., Buckingham, J.C., Perretti, M., and Flower, R.J. (2004). Modulation of inflammation and response to dexamethasone by Annexin 1 in antigen-induced arthritis. Arthritis Rheum. *50*, 976–984.

Yang-Yen, H.-F., Chambard, J.-C., Sun, Y.-L., Smeal, T., Schmidt, T.J., Drouin, J., and Karin, M. (1990). Transcriptional interference between c-Jun and the glucocorticoid receptor: Mutual inhibition of DNA binding due to direct protein-protein interaction. Cell *62*, 1205–1215.

YOUN, J., HWANG, S.-H., RYOO, Z.-Y., LYNES, M.A., PAIK, D.-J., CHUNG, H.-S., and KIM, H.-Y. (2002). Metallothionein suppresses collagen-induced arthritis

via induction of TGF-β and down-regulation of proinflammatory mediators. Clin Exp Immunol *129*, 232–239.

Yuan, H., Yang, P., Zhou, D., Gao, W., Qiu, Z., Fang, F., Ding, S., and Xiao, W. (2014). Knockdown of sphingosine kinase 1 inhibits the migration and invasion of human rheumatoid arthritis fibroblast-like synoviocytes by down-regulating the PI3K/AKT activation and MMP-2/9 production in vitro. Mol. Biol. Rep. *41*, 5157–5165.

Zhao, C., Fernandes, M.J., Turgeon, M., Tancrède, S., Battista, J.D., Poubelle, P.E., and Bourgoin, S.G. (2008). Specific and overlapping sphingosine-1-phosphate receptor functions in human synoviocytes: impact of TNF-α. J. Lipid Res. *49*, 2323–2337.

Zong, M., Lu, T., Fan, S., Zhang, H., Gong, R., Sun, L., Fu, Z., and Fan, L. (2015). Glucose-6-phosphate isomerase promotes the proliferation and inhibits the apoptosis in fibroblast-like synoviocytes in rheumatoid arthritis. Arthritis Research & Therapy *17*, 100.

Zwadlo-Klarwasser, G., Bent, S., Haubeck, H.-D., Sorg, C., and Schmutzler, W. (1990). Glucocorticoid-Induced Appearance of the Macrophage Subtype RM 3/1 in Peripheral Blood of Man. IAA *91*, 175–180.

(2000). Principles of Molecular Rheumatology (Humana Press).

7. List of publications

Koenen M., Culemann S., Vettorazzi S., Caratti G., Frappart L., Baum W., Krönke G., Baschant U.†, Tuckermann J.P.† (2018) The glucocorticoid receptor in stromal cells is essential for glucocorticoid-mediated resolution of inflammation in arthritis ***Accepted*** *in Ann. Rheum. Dis* * UB and JT contribute equally

Rapp A.*, Hachemi Y.*, Kemmler J., **Koenen M.**, Tuckermann J.†, Ignatius A.† (2018). Induced global deletion of glucocorticoid receptor impaires fracture healing. FASEB J. 32(4): 2235-2245 * AR and YH contribute equally to this work and †JP and AI contributed equally to this work

Hartmann K.*, **Koenen M.***, Schauen S.*, Wittig-Blaich S., Ahmad M., Baschant U.†, Tuckermann J.P.† (2016). Molecular Actions of Glucocorticoids in Cartilage and Bone During Health, Disease, and Steroid Therapy. *Physiol. Rev. 96, 409-47* *KH, MK and SS contribute equally and †UB and JPT contribute equally

Koenen M., Baschant U., Culemann S., Kockmann T., Kaltenbach H.M., Vettorazzi S., Nanni P., Roschitzki B., Auf dem Keller U., Tuckermann JP. (2016). Glucocorticoid receptor dimerization in stromal cells modulates macrophage polarization during serum transfer-induced arthritis. [**Abstract**] *Arthritis Rheumatism online supplement 10*

Glantschnig C., **Koenen M.**, Lozano M.G., Karbiener M., Pickrahn I., Williams-Dautovich J., Patel R., Cummins C., Hartleben G., Blüher M., Tuckermann J., Herzig S., Scheideler M (**under revision**) *FASEB*